Full Duplex Systems: Multi-objective Optimization Designs for 5G and Beyond

Mahmoud Tukur Kabir

A thesis submitted in partial fulfillment

of the requirements for the degree of

Doctor of Philosophy

in

Department of Electronic and Electrical Engineering

University College London

July 30, 2019

To my entire family, for everything

I, Mahmoud Tukur Kabir , confirm that the work presented in this thesis is my own. Where information has been derived from other sources, I confirm that this has been indicated in the work.

Abstract

Full duplex (FD) communication is widely recognized as one of the key technologies for the fifth generation (5G) of wireless communication systems. By allowing simultaneous transmission and reception, FD has the potential to drastically improve the spectral efficiency of the half-duplex (HD) communication networks. Moreover, the 5G communication network holds the promise of supporting a wide range of services with different strict communication requirements such as latency, reliability and data rate, that aim at improving capacity, reliability, and energy efficiency, while reducing latency and massively increasing connection density. For this reason, in this thesis we study novel designs for different promising 5G technologies in multi-user FD communication scenarios.

This thesis firstly extends the concept of interference exploitation to multi-user FD systems, where existing works have focused on suppressing interference. In this regard, we propose a multi-objective optimization problem (MOOP) to study the tradeoff between the total downlink and uplink transmit powers. The MOOP approach allows for the power saved to be traded off for both uplink and downlink power savings, leading to an overall energy efficiency improvement in the wireless link. In addition, this thesis explore robust designs in a multiuser FD system with simultaneous wireless information and power transfer (SWIPT). In particular, we propose MOOP designs to jointly minimize the total uplink and downlink transmit power, and maximize the total harvested energy in a FD system with imperfect channel state information for both interference suppression and constructive interference. Furthermore, we investigate the offloading energy and latency trade-off in a multiuser FD mobile-edge-computing (MEC) system that performs both data

transmission and MEC through MOOP designs. Subsequently, we study the optimal beamforming and resource allocation problem in a multiuser FD system, where we design a power efficient algorithm to minimize the long-term sum transmit power under delay constraints.

Comprehensive simulation results and analysis show the improved performance of the introduced techniques compared to the state-of-the-art techniques, which validates the effectiveness of these techniques.

Impact Statement

The incessant evolution and growth of the wireless communication system has brought the need for constant development and design of new enhanced, efficient and cost effective algorithms to address the ever-increasing challenges faced in wireless communication networks. For this reason and motivated by the ongoing research for the materialisation of the 5G network, this thesis presents new and efficient design strategies in the design of the wireless communication networks. These state-of-the-art design strategies address some of the main issues and challenges encountered by the wireless communication systems both inside and outside academia.

This thesis addresses the issue of the limited radio spectrum by employing FD in efficient and practical communication system scenarios. Another important issue addressed by this thesis is the battery life of wireless devices. Replacing and charging the battery of devices has always been a problem and in some instances impossible, hence, by wirelessly transmitting power to devices through energy harvesting, devices can charge their batteries conveniently. Also, with the popularity of smart phones and devices increasing everyday caused by the advancement of the Internet of Things, the use of computational intensive applications has increased drastically. The FD MEC, in this thesis, presents a solution to enable devices offload their intensive and latency-critical computation tasks to nearby server for execution. Furthermore, the issue of packet drop and delay in transmission is also addressed in the thesis. Overall, the findings presented in this thesis provides insights and solutions to the main challenges in the wireless communication network, bringing us a step closer to the realisation of the 5G networks and even beyond.

Acknowledgements

ALHAMDULILLAH!!!
Above all, glory be to God the Almighty.

There are a number of remarkable individuals that I would like to show my appreciation to, who have contributed from the beginning of my PhD to the writing of this thesis.

First, I would like to give my sincere gratitude to my supervisor Dr. Christos Masouros for everything he has done for me through out my study at UCL. From the PhD entry interview he granted me, agreeing to be my PhD supervisor, advising and guiding me through challenging and difficult research decisions and his attitude and support towards me during difficult times throughout my PhD study at UCL. I am deeply thankful for all his corrections, priceless ideas and revisions he has given me in every paper we have produced together. I am forever indebted by his personal and professional support through out my research years.

I would like thank Dr. Muhammad Ruhul Amin Khandaker, a true friend and co-researcher, who was there when ever I needed support and advice, thank you very much. I would thank my fellow research colleagues Dr. Fan Lui, Dr. Arman, Dr. Abdelhamid Salem, Temitope Odedeyi and Abdullahi Mohammad for their support and encouragement during the entire period of my study.

A special thank you to my parents Mr. and Mrs. Kabir Tukur Birchi for their priceless support, financially and emotionally, throughout my stay in the UK. I would like to give a special appreciation to the love of my life, Afrah, for the countless support and encouragement and in particular, for everything she had to put up with, thanks and I love you and our baby. I would also like to thank my

entire extended family for their support, without them this journey would not have been possible.

Finally, I would like to thank the Federal Republic of Nigeria and the Petroleum Technology Development Fund (PTDF) for funding my PhD.

Contents

List of Figures

List of Tables

List of Abbreviations

1G	First generation
4G	Fourth generation
5G	Fifth generation
AP	Access point
AWGN	Additive white Gaussian noise
BER	Bit error rate
BS	Base station
CCI	Co-channel interference
CI	Constructive interference
CPU	Central processing unit
CR	Correlation rotation
CSI	Channel state information
D2D	Device-to-device
DL	Downlink
DPC	Dirty paper coding
EE	Energy efficiency
EH	Energy harvesting
FD	Full-duplex

HD	Half-duplex
IA	Interference alignment
ICI	Inter-channel interference
ID	Information decoding
IE	Interference exploitation
IoT	Internet-of-things
IS	Interference suppression
LTE	Long term evolution
MD	Mobile device
MEC	Mobile-Edge-Computing
MIMO	Multiple-input multiple-output
MMSE	Minimum mean squared error
MOO	Multi-objective optimisation
MOOP	Multi-objective optimisation problem
MSE	Mean square error
MU	Multi-user
MUI	Multi-user interference
OFDMA	Orthogonal frequency-division multiple access
PS	Power splitting
PSK	Phase shift keying
QAM	Quadrature amplitude modulation
QoS	Quality-of-service
RCI	Regularised channel inversion

RF	Radio frequency
RSCI	Regularized selective channel inversion
SCI	Selective channel inversion
SE	Spectral efficiency
SER	symbol error rate
SI	Self-Interference
SINR	Signal-to-interference plus noise ratio
SNR	Signal-to-noise ratio
SWIPT	Simultaneous wireless information and power transfer
TDMA	Time-devision multiple access
THP	Tomlinson-Harashima precoding
TS	Time switching
UE	User equipment
UL	Uplink
URLLC	Ultra-reliable-low-latency communication
VP	Vector perturbation
WPCN	Wireless powered communication network
WPT	Wireless power transfer
ZF	Zero-forcing

List of Notations

a	Scalar
$\mathbf{a}$	Vector
$\mathbf{A}$	Matrix
j	Imaginary unit
$\mathbb{C}^{m\times n}$	A $m \times n$ matrix in the complex set
$\mathbf{A} \succeq 0$	Matrix A is postive semi-definite
$\mathscr{CN}(\alpha,\beta)$	Complex normal distribution
$\mathbb{E}\{\cdot\}$	Expectation of a random variable
$\Re(\cdot)$	Real part of a complex scalar, vector or matrix
$\Im(\cdot)$	Imaginary part of a complex scalar, vector or matrix
$(\cdot)^T$	Transpose
$(\cdot)^H$	Conjugate transpose
$(\cdot)^{-1}$	Inverse of a square matrix
$(\cdot)^\dagger$	Moore-Penrose inverse
$\mathrm{tr}\{\cdot\}$	Trace of a matrix
$diag(\mathbf{a})$	Transformation of the vector $\mathbf{a}$ into a diagonal matrix
$\mathrm{vec}(\cdot)$	Vectorisation operation
$\det\{\cdot\}$	The determinant of a square matrix

$conj(\cdot)$	Conjugate or element-wise conjugate
$\lvert\cdot\rvert$	Absolute value or modulus
$\lVert\cdot\rVert_1$	1-norm
$\lVert\cdot\rVert_F$	Frobenius norm
$(a)^+$	$\max(a,0)$
$\mathcal{O}(\cdot)$	Order of numerical operations

Chapter 1

Introduction

The rapid growth of wireless communication network has caused the need for more power efficient and reliable high data rate communication systems. This has sparked considerable research interests in recent years. Multi-input multi-output (MIMO) system is one of the breakthrough techniques to tackle these needs, as it provides more degree of freedom for efficient resource allocation. However, the efficient resource utilization for MIMO systems come at the cost of high computational complexity at the receivers. Multi-user (MU)-MIMO experiences a reduced complexity at the receivers by employing beamforming at the base station (BS) for the downlink transmission. Even with the MU-MIMO, higher spectral efficient resource allocation can be gained by switching from the conventional half-duplex (HD) mode i.e when only reception or transmission is performed at a time, to a full-duplex (FD) mode where simultaneous reception and transmission is performed at the same time and frequency.

FD communications is widely recognized as one of the key technologies for 5G wireless communication systems [2]. FD has the potential to drastically improve or even double the spectral efficiency of HD systems since it allows the downlink and uplink transmission to function at the same frequency and time. Although, the benefits of FD systems are somewhat intuitive, the practical implementation of such systems have proven to be very challenging which poses a lot of technical problems. As a result, for a long time, there was a general assumption that it is not possible for a radio to simultaneously transmit and receive at the same frequency [3]. One major

challenge of the implementation of FD systems is the self-interference (SI) signal from the transmit antenna to the receive antenna of the wireless transceiver. Specifically, the transmitted signal by the transceiver in the downlink channel interferes with its receive signal from the uplink channel. This interference raises the noise floor and becomes the dominant factor in the performance of the FD system. Therefore, the performance of the FD system depends on the ability of the transceiver to sufficiently suppress or cancel the SI signal.

Fortunately, major breakthroughs have been recorded in practical FD system setups [4,5] that show that the SI can be partially cancelled to within a few dB of the noise floor. Over the years, several self-interference cancellation techniques have been proposed in the literature [4–8]. [9] presented an experiment-based characterization of passive suppression and active SI cancellation mechanisms in FD systems. The authors characterization of total and individual cancellation mechanisms, based on extensive experimentation shows that a total average cancellation of 74dB can be achieved. In [10], a digital SI cancellation technique was proposed that could mitigate the SI to about 3dB higher than the receiver noise floor, which results in up to 76% rate improvement compared to conventional half-duplex systems at 20dBm transmit power values. Overall, with the above mentioned literature, we can observe that the SI cannot be completely cancelled in FD systems but reduced to a negligible level [6, 10].

Following the breakthroughs with regards to SI suppression and cancellation, recent studies have focused on other FD implementation issues, such as protocol and resource allocation algorithm design, in variety of contexts. Accordingly, with the aim of accelerating the further development and implementation of FD applications in practical wireless systems, this thesis focuses on designs of different schemes and strategies for the realisation of FD in MU-MIMO scenarios.

1.1 Aim and Motivation

Due to the rapid growth of high data rate services, it has become important to design power efficient wireless communication systems in order to reduce the amount

of greenhouse gases emission and operational expenses of communication systems. Thanks to the development of various SI cancellation and suppression techniques, FD is now closer to reality than ever. In the design of the traditional power efficient HD system, the main goal is to minimize the system power consumption while satisfying some quality of service (QoS) constraints [11–13]. Although, many of the FD beamforming and resource allocation solutions build upon the existing HD solutions in the literature, however, the obtained HD results cannot be applicable to FD systems. This is because FD brings a number unique challenges and opportunities to explore with respect to HD systems:

- The simultaneous transmission in the uplink and downlink results in the dependency of optimization variables. In particular, the uplink and downlink transmit powers, in that, increasing the downlink transmit power to satisfy the QoS constraints increases the SI power, which hinders the reception of uplink signals. At the same time, if the uplink transmit power is increased in order to satisfy the QoS constraints, co-channel interference (CCI) is increased at the downlink.

- The existence of SI introduces new constraints in the optimization problem, that change the uplink and downlink power trade-offs involved.

- The coexistence of uplink and downlink users in MU scenarios is further complicated by CCI caused by the uplink transmission to the downlink transmission.

These challenges do not exist in HD systems since the downlink and uplink transmission are separated either in the time domain or in the frequency domain. While FD systems have been widely studied in the literature, there still exist numbers of unresolved areas and applications that require further investigations, especially with regards to the trade-off involved introduced by the dependency and coexistence of the uplink and downlink variables in MU-MIMO scenarios, where existing methods either suffers from performance loss or deviation of the assumptions and models employed from practical scenarios or computational expensive and inefficient

algorithms. Thus, this calls for new and innovative methods to further improve the performance and efficiency of existing techniques.

1.2 Main Contributions

In this thesis, we consider MU-MIMO FD wireless communication systems. In particular, we exploit the dependency of the optimization variables i.e., the uplink transmit power and downlink beamforming vectors, to study the trade-offs between conflicting but important objectives with respect to both the system operators and users. It is these trade-offs that necessitate the study of different multi-objective optimization problems (MOOPs), where intricate trade-off designs have not been sufficiently studied in the literature in FD communication systems. Against the state-of-the-art, the main contributions of this thesis are summarised below:

- Extension of the concept of MU interference (MUI) exploitation in FD communication systems (Chapter 4). By exploiting the useful signal power from interference, in the downlink channel for both phase-shift keying (PSK) and quadrature amplitude modulation (QAM), a power efficient resource allocation is provided for FD MU-MIMO systems. Through the proposed MOOPs, it is shown that FD offers the unique opportunity to trade-off the interference power saved for both uplink and downlink power savings.

- Exploration of robust designs to jointly minimise the total uplink and downlink transmit power and maximise the total harvested energy with imperfect channel state information (CSI) in a FD communication system (Chapter 5). By exploring some convex relaxations to tackle the highly non-convex MOOPs, simulation results show the effectiveness of interference exploitation compared with interference suppression in terms of both power consumption and energy transfer as well as the superiority of FD transmission with respect to HD.

- Design of a low-complexity and efficient algorithm to investigate the offloading energy and offloading latency trade-off in a MU FD communication system with mobile edge computing (Chapter 6). The proposed MOOPs, for

both perfect and imperfect CSI designs, allow for a scalable tradeoff between the two important objectives via the Lagrangian method. Simulation results show greatly improved performance of the proposed FD schemes, for both interference suppression and interference exploitation, compared with the existing baseline HD schemes.

- Design of an optimal beamforming and resource allocation algorithm for power efficient MU FD communication systems based on stochastic optimisation that takes into account the system delays with respect to data queues (Chapter 7). Due to the stochastic nature of the problem, the classic drift-plus-penalty function is exploited and subsequently, the proposed MOOP was simplified into a difference of convex functions. Simulation results show the significant gains achieved by the proposed FD schemes compared with the baseline HD schemes.

1.3 Thesis Organization

Subsequent to this introductory Chapter, this thesis is organised as described below:

Chapter 2 gives a review of different 5G and beyond technologies. Specifically, this chapter presents an overview of full duplex systems, which constitutes the basis of this thesis, with emphasis on existing SI cancellation techniques. Also, the energy harvesting technology, mobile edge computing (MEC), and delay and reliability for the 5G wireless networks are discussed.

Chapter 3 provides a review of MIMO systems. Specifically, this chapter discusses the different precoding techniques in wireless communication systems. In addition, this chapter gives an overview of optimization based beamforming in terms of conventional schemes and constructive interference based beamforming schemes. This chapter also gives detailed review of the existing precoding schemes including simulation results comparing them and showing their advantages and disadvantages. Furthermore, the chapter discusses multi-objective optimisation (MOO) including the 3 categories of the different MOO methods based on the decision maker's preference of the objectives.

Chapter 4 introduces the proposed power efficient FD communication system. In particular, this chapter presents the proposed multi-objective optimisation problem (MOOP) designs in FD systems with interference exploitation for both generic phase shift keying (PSK) modulated signals and quadrature amplitude modulated (QAM) signals. The proposed MOOP designs offer the opportunity to trade the saved downlink interference power for both uplink and downlink power savings. The chapter also presents robust designs for the proposed MOOP designs with imperfect channel state information (CSI). In extension, an iterative algorithm is further proposed to jointly optimise the uplink transmit power, the downlink and uplink beamforming vectors, respectively.

Chapter 5 extends the proposed multi-objective optimisation (MOO) designs in FD systems to energy harvesting scenario. The proposed approach explore robust designs to jointly minimize the total uplink and downlink transmit power and maximize the total harvested energy in a full duplex system with imperfect CSI. First, a formulation, where multiuser interference (MUI) is suppressed is proposed. Then, a second formulation, where the MUI is rather exploited, is proposed, both as useful energy and information power, for guaranteeing quality of service and energy harvesting constraints.

Chapter 6 investigates the offloading energy and latency trade-off in a MU FD mobile edge computing (MEC) system. Specifically, the FD system consists of a FD base station (BS), equipped with a MEC server, which carries out data transmission in the downlink, while at the same time receiving computational tasks from mobile devices in the uplink. Two weighted MOOPs are proposed, one, where the multi-user interference (MUI) is suppressed and the other, where MUI is rather exploited. As a result, the proposed MOOPs allow for a scalable tradeoff between the offloading energy and latency. The robust designs for imperfect CSI are also included.

Chapter 7 studies the beamforming and resource allocation problem in a MU FD system. The chapter presents the design of a power efficient algorithm that minimizes the average long-term sum transmit power under long-term stability con-

straints on the queue buffers for the downlink and uplink users. The proposed design exploits the classic drift-plus-penalty function and subsequently simplify the problem into a difference of convex functions. Building upon the proposed algorithm, an optimisation problem based on delay fairness is also presented.

Chapter 8 concludes the thesis by summarising the entire thesis and then, presenting the possible extensions for future research within the frame of this thesis.

1.4 Publications

The above contributions in this thesis have led to the following peer-reviewed publications:

Journal Papers:

[J1] M. T. Kabir and C. Masouros, "Delay-Constrained Beamforming and Resource Allocation in Full Duplex Systems," *IEEE Transactions on Vehicular Technology, revised (major),* July 2019.

[J2] M. T. Kabir and C. Masouros, "A Scalable Energy vs Latency Trade-off in Full Duplex Mobile Edge Computing Systems," *IEEE Transactions on Communications, accepted*, March 2019.

[J3] M. T. Kabir, M. R. Khandaker, and C. Masouros, "Interference exploitation in full-duplex communications: Trading interference power for both uplink and downlink power savings," *IEEE Transactions on Wireless Communications,* vol. 17, no. 12, pp. 8314-8329, 2018.

[J4] M. T. Kabir, M. R. Khandaker, and C. Masouros, "Robust energy harvesting FD transmission: Interference suppression vs exploitation," *IEEE Communications Letters,* vol. 22, no. 9, pp. 1866-1869, 2018.

Conference Papers:

[C1] M. T. Kabir, M. R. A. Khandaker, and C. Masouros, "Minimizing Energy and Latency in FD MEC Through Multi-objective Optimization," *IEEE Wireless Communications and Networking Conference (WCNC),* pp. 1-6, March 2019.

[C2] M. T. Kabir, M. R. A. Khandaker, and C. Masouros, "A Scalable Performance-Complexity Trade-off for Full Duplex Beamforming," *IEEE Wireless Communications and Networking Conference (WCNC),* pp. 1-6, March 2019.

[C3] M. T. Kabir, M. R. A. Khandaker, and C. Masouros, "Reducing selfinterference in full duplex transmission by interference exploitation," *IEEE Global Communications Conference,* pp. 1-6, December 2017.

Chapter 2

5G Technologies and Beyond

2.1 Introduction

Over the past few years, the wireless communication network has continuously evolved in order to meet the unprecedented demands and growth for wireless communication systems. Moving from the first generation (1G) of cellular communication, which was analog and mainly used for voice calls only, to the recent long term evolution LTE/4G network that provides high data transmission rate, increased capacity and provides multimedia support. Despite the unprecedented high transmission rates, high QoS and other benefits provided by these networks, the ever-growing user demands is beginning to exceed their capabilities. For example, the rapid growth of smartphones and devices have caused an increase mobile data traffic. It has been reported that compared to 2010, the current estimates of mobile data traffic in the years to come foresee a 1,000 times increase by 2020 [14]. The existing networks are not designed to sustain this increase in number of connected devices. Also, the development of new applications such as tactile Internet, high resolution video streaming, tele-medicine, tele-surgery, vehicular communications, and real-time control have set new requirements for throughput, latency, reliability and robustness of the network. As such, researchers and standards development organisations have set out to develop the next generation 5G network in order to continue to tackle these emerging challenges. Some of the expected requirements of the next generation 5G networks are listed in Table 2.1. Therefore, in the

Table 2.1: Requirements for 5G communication systems [2]

Figure of merit	5G requirement	compared with 4G
Peak data rate	10 Gbps	100 times higher
Guranteed data rate	50 Mbps	-
End-to-end latency	less than 1ms	25 times lower
Number of devices	1 M/km^2	1000 times higher
Reliability	99.9999%	99.9999%
Energy consumption	-	90% less
Peak mobility support	$\geq$500 kmph	-

quest to meet these challenging requirements, variety of new technologies such as full-duplex (FD), energy harvesting (EH), massive-MIMO, mobile-edge computing (MEC), millimeter wave (mmWave) communications, non-orthogonal multiple access (NOMA), device-to-device (D2D) communications and visible light communication have emerged as promising techniques and are considered as the key technologies for the next generation 5G network.

In this chapter, we provide an overview of some new promising technologies that are expected to be employed in 5G systems and even beyond, which are considered in this thesis in subsequent chapters.

2.2 Full Duplex Communication System

FD is basically when the transmission and reception of signals is performed at the same time and frequency. The ever-increasing need for improved spectrum-efficiency in wireless communication links has brought FD at the forefront of research attention. To appreciate the gains from the application of FD, we consider a simple multiuser communication system as shown in Fig. 2.1. The system consists of a BS serving a downlink (DL) user and an uplink (UL) user. Therefore, if the BS operates in HD, then the BS can only communicate with either the downlink user or the uplink user in one time slot. However, if the BS operates in FD, then the BS can simultaneously communicate with both downlink and uplink users thereby doubling the spectral efficiency relative to HD operation [15]. Thus, Full duplex communications is widely recognized as one of the key technologies for 5G wireless communication systems [2].

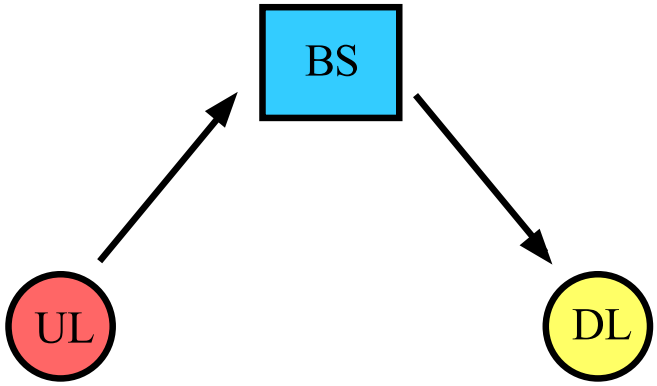

Figure 2.1: A simple communication system

In theory, since FD allows simultaneous transmission and reception of signals, then, it has the potential to double the spectral efficiency of the HD communication systems [4, 5]. However, for many years the implementation of FD systems has been considered impractical due to one major hurdle known as self-interference (SI). The SI is the leakage signal from the transmit antennas to the receive antennas of the FD system that raises the noise floor and becomes a dominant factor in the system making it very difficult to extract the desired received signal. Therefore, to achieve FD the SI, which can be up to 100 dB stronger than the desired received signal, must be completely or partially cancelled. Thus, over the years, major efforts and breakthroughs have been made in order the reduce the effect of SI, even though the SI cannot be completely cancelled in FD systems due to limited dynamic range at the receiver [6].

2.3 Self-interference Cancellation Techniques

Considerable efforts have been made to mitigate the SI signal, this has led to the development of several SI cancellation techniques in the literature. These techniques are classified into: passive suppression and active cancellation.

2.3.1 Passive suppression techniques

In passive suppression techniques, the suppression usually takes place as the signal propagates from the transmit antenna to the receive antenna and majority of the cancellation is due to the isolation between the antennas [5, 16–18]. In [5], an antenna

cancellation technique was proposed in practical FD setup comprising of a single channel FD transceiver. To achieve FD in this scenario, which uses 0dBm of transmit power, the power of the signal from the transmit antenna at the receive antenna placed 6 inches away is approximately -40dBm and with approximately -100dBm of noise floor, then at least 60dB of SI power must be cancelled. Therefore, it was shown that by combining the antenna cancellation technique, which provides up to 30dB cancellation, with digital interference cancellation, up to 60dB interference cancellation could be achieved to enable FD communication in the system. The main principle of antenna cancellation is to use two transmit antennas and one receive antenna, where the two antennas are placed half a wavelength apart thereby causing their signals to add destructively and cancel one another. In [16], the authors used directional antennas to achieve passive suppression in a FD scenario that can exploit directional diversity. The performance analysis shows that gains as high as 90% at a distance of 10m can be achieved compared to HD operation.

2.3.2 Active cancellation techniques

Active cancellation techniques [4,7,9,10,19–21] are techniques that involve any additional signal processing carried out on the received signal to mitigate the SI signal like subtracting a processed copy of the transmitted signal from the received signal. Active cancellation techniques can be divided into analogue and digital techniques: analogue techniques achieve cancellation by sending a cancelling signal through another radio chain and then adding it to the signal at the receiving antenna, while digital techniques use the knowledge of the transmit signal to perform cancellation. The first practical in-band FD WiFi radios was designed and implemented in [4] where the system uses a single antenna for both transmission and reception. To achieve FD, the system makes use of a dynamic algorithm to estimate the amount of SI experienced by the received signal, then cancels it to within few dB of the noise floor of the receiver using analogue and digital cancellation techniques. In [10], a digital SI cancellation technique was proposed that could mitigate the SI to 3dB higher than the receiver noise floor by using an auxiliary receiver chain to obtain a digital copy of the transmitted SI signal. With the copy of the SI signal, the SI signal

and the associated transmitter impairments can be cancelled out, which results in up to 76% rate improvement compared to conventional half-duplex systems at 20dBm transmit power values.

Typically, FD systems employ both passive and active cancellation techniques to help mitigate the SI signal significantly because no single technique is sufficient to bring down the SI signal to the noise floor [10, 19].

2.4 Energy Harvesting

The battery life of wireless devices has always been a very important part to consider in the design of wireless communication networks. Constantly replacing batteries is often costly, inconvenient, hazardous and sometimes even impossible. Energy harvesting (EH) is a promising technique that provides solution for prolonging the lifetime of wireless communications networks such as sensor networks [22–25]. Energy can be harvested from a number of sources like sunlight, wind, vibrations, hydroelectric, and wireless radio frequency (RF) signals, as such, EH has gained a lot of attention from both academia and industry. In the literature, EH systems can be divided into three main transmit schemes; The wireless power transfer (WPT) scheme, where a power bank transfers energy to EH receivers to charge their batteries [26, 27]. The wireless powered communication network (WPCN) scheme, where the energy harvester uses the energy received to transmit information to other receivers [28–31]. The simultaneous wireless information and power transfer (SWIPT) scheme, where the transmitter transfers both information and power signals using the same waveform to various EH and information detectors [32–36].

In addition, the receiver architecture of EH networks is usually of two types, either collocated receivers or separated receivers. In collocated receivers, the receiver can do both EH and information decoding (ID). In this case, the receiver coordinates how the two processes occur: The receiver could employ power splitting (PS) [32], where the received signal power is divided between EH and ID by a specified ratio; Time switching (TS) could be adopted [32], where the receiver shares the receiving time by a factor for both EH and ID; Another method is through antenna switch-

ing, where the receiver employs multiple antennas and dedicates some for EH and others for ID, respectively. While in separated receiver architecture, which is less challenging than the collocated receivers, the receivers can only do either EH or ID.

Most state-of-the-art works on EH networks combine the above transmitter and receiver architectures. In [28], a "harvest then transmit" protocol for WCPN was proposed where an access point (AP) supplies power to all users through their downlink and the users transmit information in the uplink by time-division-multiple-access (TDMA). The authors studied the sum-throughput maximization by optimizing the time allocation downlink EH and uplink information transfer. Likewise, [30] employed space-division multiple-access techniques to maximize the sum rate while jointly optimizing the downlink energy precoding matrices, the uplink information precoding matrices, and time allocation between the downlink and the uplink phases. SWIPT was studied in [32], where one receiver harvests energy and another receiver decodes information separately from the signals sent by a common transmitter. The authors exploited scenarios where the EH receiver and ID receiver are separated and collocated. In the case of collocated receivers, PS and TS were both examined. Also, [36] considered SWIPT in an orthogonal frequency-division multiplexing (OFDM) relaying system, where a PS relay protocol is proposed for a source that transfer information and a fraction of power to a relay nodes which uses the harvested power to transmit information to a destination node. While WCPN was considered in [31] to maximize the energy efficiency (EE) of the network via joint time allocation and power control protocols.

2.5 Mobile Edge Computing

The popularity of mobile devices and other wearable devices, and the unprecedented growth of mobile data traffic have caused tremendous advancement in wireless communication and Internet of Things (IoT). It is estimated that around 50 billion devices will be connected to the IoT by 2020. This calls for a significant increase in the wireless network capacity. Furthermore, the data traffic growth, which is often from our everyday lifestyle of running variety of applications on mobile devices,

smartphones, laptops, e.t.c., for entertainment, healthcare, businesses, networking and so on, is not matched by improvement on devices in terms of battery life, efficiency and data storage capabilities. This widens the gap between the capabilities required to run these applications and capabilities available on the devices. A promising solution to these problems is to enable devices offload their intensive and latency-critical computation tasks to nearby servers for execution through mobile edge computing (MEC). In this way, the battery life, data storage capabilities, latency, efficiency and reliability of the devices are relaxed [14, 37], tackling the key challenges for materializing the 5G vision. In particular, MEC pushes mobile computing, network control and storage to the network edges such as base stations and access points.

In MEC, computation task offloading does not necessarily mean offloading all the tasks for execution at the servers. Whether or not the entire computation task is to be offloaded depends on the system parameters such as the computational intensity of each task, the size of the task to be offloaded, the battery life of the device, the delay constraints and the channel state. Usually, a computation task is often divided into parts, where some are run by the devices while other parts are to be offloaded and executed by the servers. As such, offloading can either be static of dynamic. Static offloading is when the partitioning is done before execution and the decision on what part to be executed locally is taken at the beginning of execution [38–41]. While dynamic offloading is when the decision on whether and what to offload is taken at the run time based on the system current situation [42,43].

Increasing number of applications now benefit from MEC by offloading all or part its tasks to the MEC server for execution. A simple example is the face recognition application on our mobile phones, which can be subdivided into five computation tasks: image acquisition, face detection, pre-processing, feature extraction, and classification [44]. The image acquisition task needs to be locally executed at the mobile phone while the other fours tasks could be offloaded to the MEC server for execution since they involve complex signal processing and machine learning (ML) algorithms. Many of such applications exist and are already part of our day-to-day

life. One of the main MEC research motives is to merge the wireless communication and wireless computing disciplines. This has resulted in a wide range of new design ideas, from different computational offloading techniques/policies to different network architecture.

In the literature, many of the MEC research focus on resource management for both single and multi-user MEC systems. There are three commonly used task models: the deterministic task model with binary offloading, deterministic task model with partial offloading, and stochastic task model. Binary offloading model involves tasks that are relatively small or highly integrated that can only be executed as a whole either locally or offloaded to the server [45, 46]. [45] proposed a local policy that optimizes local computing and offloading by controlling the central processing unit (CPU) frequency and transmission rate for energy minimization. Similarly, [46] proposed a framework to optimize local computing and offloading. The partial offloading task model involves sophisticated tasks that can be subdivided into several tasks that could be executed individually locally or offloaded to the server [47, 48]. In [47], the concept of wireless aware joint scheduling and computation offloading was introduced where the authors jointly optimize the offloading ratio, transmission power and CPU cycle frequency using a variable substitution technique. [48] proposed a joint scheduling and computation offloading algorithm by parallel processing of appropriate modules in the device and server. Stochastic task models are task models that are characterized by random task arrivals, where the arrived but not yet executed tasks join the queues in task buffers. In such models, the long-term average energy consumption or long-term average latency is considered for the system design [49, 50].

2.6 Delay and Reliability

One of the main aims of the next generation 5G network is to support ultra-reliable and low-latency communications (URLLC). Latency is the time it takes to successfully deliver a message or packet from the application layer to the protocol layer through the radio interface in both uplink and downlink without any disruption in

the reception from either the device or BS. The URLLC requirement for latency is set at 1 ms [51]. Reliability is defined as the probability of successfully transmitting a given packet (in bytes) within a given latency/delay given a certain channel quality. For 5G communication networks, the requirement for reliability of transmission of a 32 byte packet is at least 99.999% [51]. This strict level of latency and reliability have given way to various new application such as the following [51]:

- Self-driving [52]: cars that can automatically drive itself by detecting its surroundings without being operated by anyone.
- Tactile internet [53]: internet network that ensures tactile connectivity with the support of short transmit, low latency, high reliability and availability, and high security communications.
- Vehicle-to-vehicle (V2V) [54, 55]: a wireless network that supports communications between vehicles or vehicles-to-everything (V2X).
- Industrial and Process automation [56]: automated industry and processes with unmanned machines that automatically monitor all processes, control the systems and make decision for industrial components such as mixing, heating and pumping.
- E-health [57, 58]: a health care system with the support of information and communication technology (ICT).

These have sparked a lot of research interests in the industry and academia. For example, [59] considered a two-hop FD relay system and proposed three buffer-aided relaying schemes with adaptive reception transmission at the FD relay for the cases when the source and the relay both perform continuous rate transmission with adaptive-power allocation, continuous rate transmission with fixed-power allocation, and discrete-rate transmission, respectively. The buffer aided relaying enables the FD relay to selectively choose either to receive, transmit or simultaneously do both at a given time slot. In [60], the problem of uplink and downlink resource optimization, mode selection and power allocation is studied with stability

constraints in FD systems operating with non-orthogonal multiple access (NOMA). The authors formulated the problem as a network utility maximization for which the Lyapunov framework was employed to solve the problem. In [61], studied a device-to-device (D2D) communication network, where energy efficiency (EE) and delay trade-off was investigated. The authors formulated a stochastic optimization problem that maximizes the EE with average power, interference control, and network stability constraints. While [62] addressed EE-guaranteed throughput-delay trade-off in an interference-free wireless network. The authors formulated two stochastic optimization problems aiming at throughput maximization and rate minimization subject to EE, stability, admission control, and transmit power constraints.

Accordingly, motivated by the ongoing research for URLLC for the realization of the 5G networks, in Chapter 7 we propose a delay-constrained beamforming and resource allocation algorithms in FD systems.

2.7 Summary

This chapter has provided an overview of some of the new and promising technologies that are being considered for the next generation wireless communication systems. These include FD, which allows simultaneous transmission and reception, then, the EH technology that involves transmitting and receiving energy signals in order to prolong the battery life of wireless devices. In addition, this chapter also reviews the MEC technology that allows devices to offload their latency-critical and intensive tasks to MEC servers for execution. Finally, the chapter presents an overview of the technologies that support and provide URLLC.

Chapter 3

MIMO Communication System

3.1 Introduction

Multiple-input multiple-output (MIMO) refers to the method of employing multiple antennas at both the transmitter and receiver of wireless communication systems. Over the years, the use of MIMO has become an essential part of the standards of most wireless communication systems. It is well known that MIMO communication systems provide a number of benefits over the traditional single-input single-output (SISO) communication systems, these include [63]:

- Array gain: This is simply the average power gain of the transmitted signals. By the application of multiple antenna at the transmitter or/and receiver, the average received signal-to-noise (SNR) ratio is increased due to coherent combining effect. The array gain depends on the number of antennas at the transmitter or/and receiver and requires the knowledge of the channel.

- Diversity gain: This is the increase in reliability of the transmission link. As the signal power randomly fluctuates in the wireless channel (channel fading), multiple antenna systems provide a means to diversify the transmitted signal path. Therefore, if the link between the transmitter and receiver fade independently, the receiver can reconstruct the transmitted signal by combining the arriving signals from the multiple antennas, such that the resultant signal is an improved version of the signal from a SISO link.

- Spatial multiplexing gain: With MIMO, there is extra spatial dimension for

communication that is created which can be exploited by simultaneously transmitting independent signals from the individual antennas. This offers a linear increase in capacity and this gain is referred to as spatial multiplexing gain.

- Interference Management: The use of multiple antenna system gives rise to MUI due to simultaneous communication between the users since the same time and frequency resources are being used. The differentiation between the spatial dimension of the desired signal and co-channel can be exploited to reduce the interference by precoding at the transmitter or equalization at the receiver. By reducing the interference energy sent to the co-channel users when transmitting to the desired user, the multi-cell capacity is increased.

We note that, since it is difficult to simultaneously exploit all the advantages of MIMO systems, this thesis focus on exploiting the spatial multiplexing gain by employing multiple antenna multiuser systems, and interference management via precoding techniques.

3.2 Precoding

Over the years, with the deployment of multiple antenna systems, the power consumption and the computational complexity of the receiver based techniques that have been traditionally applied to tackle the impediments of MIMO systems has become a very challenging problem in the design of user equipment (UE) in downlink communications [64–67]. This brought the need to shift the complicated and power consuming signal processing at the UE to the base station in order to maintain a simple and cost-effective UE. As a result, various precoding techniques have been proposed in the literature for downlink transmission, moving from the sophisticated but high performance achieving non-linear precoding techniques [68–75] to the less complex linear precoding techniques [1,76–78]. Several optimization based precoder have also been proposed [13, 79–81] as will be shown in the following.

For notational convenience, here, we assume a forward link multiuser system scenario with a half-duplex base station (BS) having N transmit antennas serving K

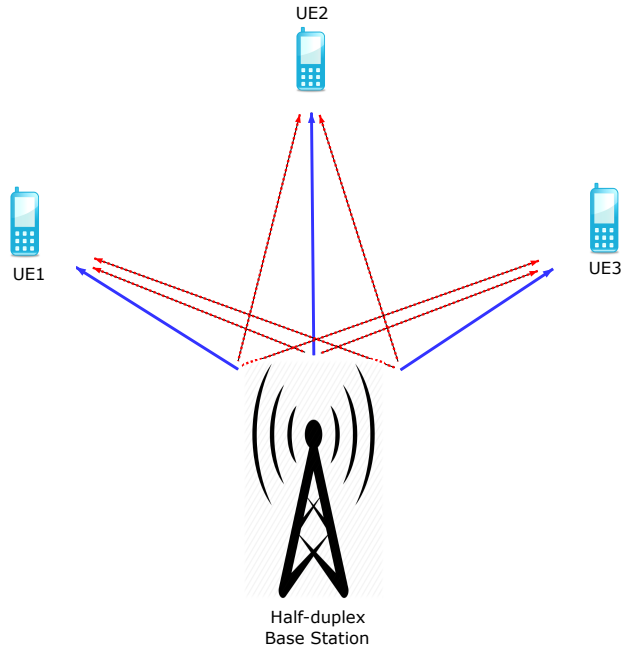

Figure 3.1: Simple broadcast system model

single-antenna users, as shown in Fig. 3.1. We note that, the K receive antennas can also belong to one user without any impact on the processing introduced. The solid lines and dotted lines in Fig. 3.1 represent the desired signals and MUI signal for each user, respectively. The transmitted signal for the k-th user can be expressed as

$$\mathbf{x}_k = \mathbf{t}_k d_k, \tag{3.1}$$

where, $\mathbf{t}_k$ and d_k denote the precoding vector and the unit data symbol for the k-th user, respectively. The received signal at the k-th user is expressed as

$$y_k = \underbrace{\mathbf{h}_k^H \mathbf{x}_k}_{\text{desired signal}} + \underbrace{\sum_{i \neq k}^{K} \mathbf{h}_k^H \mathbf{x}_i}_{\text{multi-user interference}} + n_k, \tag{3.2}$$

where n_k represents the additive white Gaussian noise AWGN at the k-th user and $\mathbf{h}_k$ is the channel vector between the BS and the k-th user. The first term in (3.2) represents the desired signal while the second term is the multi-user interference (MUI) signal from other users.

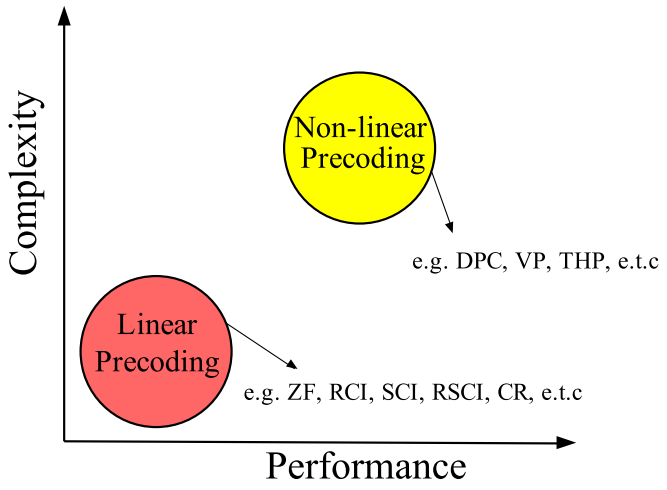

Figure 3.2: Complexity versus performance for linear and non-linear precoding

3.2.1 Linear Precoding

Linear precoding techniques offer less complexity but at the expense of low performance compared to their non-linear counterparts as shown in Fig. 3.2. Channel inversion (also known as zero-forcing (ZF)) which was proposed in [82] offers the least complexity. This technique basically multiplies the vector signal to be transmitted with the inverse of the channel matrix, as a result MUI is completely eliminated. The transmitted signal is expressed as

$$\mathbf{x}^{ZF} = f^{ZF} \cdot \mathbf{H}^{H} \left(\mathbf{H}\mathbf{H}^{H}\right)^{-1} \cdot \mathbf{d}, \tag{3.3}$$

where $\mathbf{H}$ is the $K \times N$ channel matrix between the BS and the users with the *(k,n)*-th element $h_{k,n}$ being the complex-Gaussian channel between the n-th transmit antenna and the k-th receive antenna, $\mathbf{d} \in \mathbf{C}^{N\times 1}$ is the data symbol vector and f^{ZF} is the scaling factor that ensures the average normalization of the transmitted signal power and is given as

$$f^{ZF} = \sqrt{\frac{1}{\mathrm{tr}\left[\left(\mathbf{H}\mathbf{H}^{H}\right)^{-1}\right]}}, \tag{3.4}$$

and the received signal can be written as

$$\mathbf{y}^{ZF} = f^{ZF} \cdot \mathbf{H}\mathbf{H}^{H} \left(\mathbf{H}\mathbf{H}^{H}\right)^{-1} \cdot \mathbf{d} + \mathbf{n} = f^{ZF} \cdot \mathbf{d} + \mathbf{n}, \tag{3.5}$$

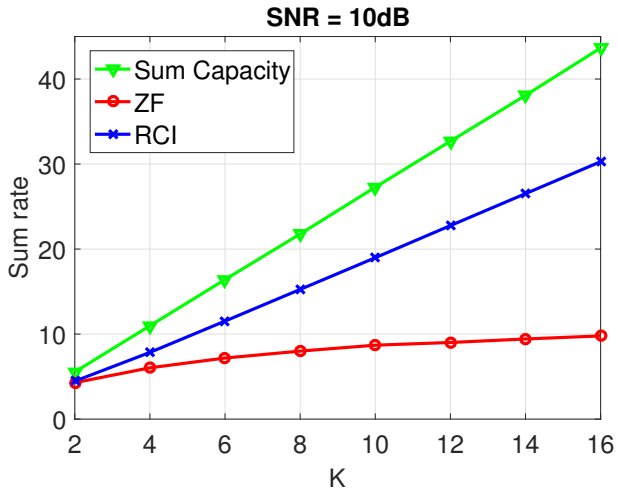

Figure 3.3: Sum rate comparison for channel inversion (ZF) and regularized channel inversion (RCI) where $N = K$ and SNR=10dB [1]

where $\mathbf{n} \in \mathbf{C}^{N\times 1}$ is the additive white Gaussian noise vector of the K receive antennas.

However, it was shown in [1] that channel inversion in its plain form is poor, the sum rate for $K = N$ users is constant as a function of K and does not improve with the increase in the number of antennas i.e. as $K \to \infty$, as can be seen in Fig. 3.3. This poor capacity was explained by looking at the distribution of the eigenvalues of $\left(\mathbf{H}\mathbf{H}^H\right)^{-1}$. Therefore, in [1] a regularized form of channel inversion was developed that improves the performance especially at low SNRs. They proposed to use a regularization parameter to maximize the signal-to-interference-plus-noise ratio (SINR) at each receiver. To regularize the inverse, they simply added a multiple of identity matrix before inverting as in

$$\mathbf{x}^{RZF} = f^{RZF} \cdot \mathbf{H}^H \left(\mathbf{H}\mathbf{H}^H + \alpha\mathbf{I}\right)^{-1} \cdot \mathbf{d}, \tag{3.6}$$

where $(\mathbf{I})$ is the identity matrix and the corresponding scaling factor is given as

$$f^{ZF} = \sqrt{\frac{1}{\mathrm{tr}\left[\frac{\Lambda}{\Lambda+\alpha\mathbf{I}} \cdot \mathbf{Q}^H\mathbf{d}\mathbf{d}^H\mathbf{Q}\right]}}, \tag{3.7}$$

where Λ is the eigenvalue matrix and $\mathbf{Q}$ is the unitary eigenvector matrix of the decomposition $\mathbf{H}\mathbf{H}^H = \mathbf{Q}\cdot\Lambda\cdot\mathbf{Q}^H$. As a result, the received signal (3.8) is no longer

simply a scaled version of **d** but also contains a certain amount of interference from the other users.

$$\mathbf{y}^{RZF} = f^{RZF} \cdot \mathbf{H}\mathbf{H}^H \left(\mathbf{H}\mathbf{H}^H + \alpha\mathbf{I}\right)^{-1} \cdot \mathbf{d} + \mathbf{n}. \tag{3.8}$$

It was shown in [1] that the amount of interference is determined by the regularization factor $\alpha > 0$ and the amount of interference increases with α. So, the best metric to choose the value of α is to maximize the SINR of (3.8), which is when $\alpha = N\sigma^2$, where σ^2 is the noise variance at the receiver. Furthermore, it was shown that with the regularized inversion symbol-error rate (SER) performance improves slightly with K unlike with the channel inversion where SER worsens with K and also the sum rate has a linear growth with K. Even though simulation results show a big improvement over the plain inversion technique, there is still a big gap to capacity that still remains to be exploited.

In quest to develop improved performance precoders, in [76], it was shown that unlike the common practise where the knowledge of the interference is used to eliminate it, this knowledge can be used to acquire benefits from the interference. In some instances where the instantaneous data is such that the interference is constructive, then eliminating it becomes inefficient. Interference is said to be constructive if it pushes the symbol further into the detection region of the constellation. Therefore, by exploiting this constructive part of inter-channel interference (ICI) and eliminating the destructive part, the overall performance is enhanced. This is achieved by selectively applying channel inversion such that the ICI that is beneficial to the instantaneous desired symbols is preserved. It should be noted that this idea is based on the concept of PSK modulation and it is performed on symbol-by-symbol basis. As a result, the average received SINR is improved without increasing the transmitted power per symbol.

The concept of exploiting the interference was taken further in [77], where correlation rotation (CR) precoding was proposed. With CR precoding, on an instantaneous basis, the phase of the symbol of the interfering signal is aligned to the phase of the symbol of the signal of interest at each receive antenna. As a result,

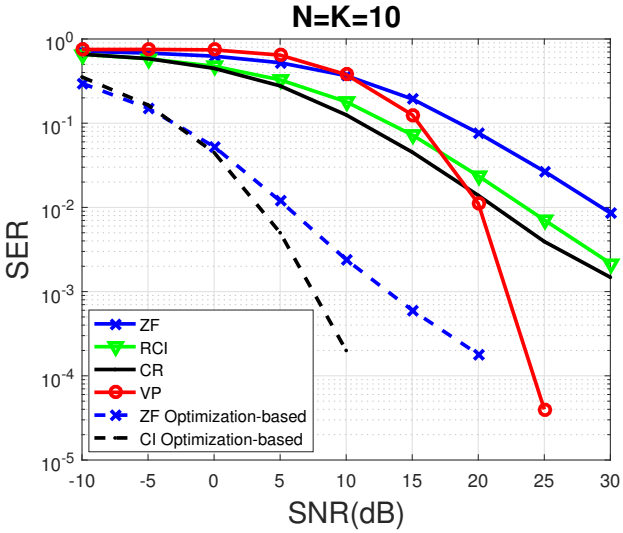

Figure 3.4: Symbol error rate comparison for channel inversion (ZF), regularized channel inversion (RCI), correlation rotation (CR), vector perturbation (VP), conventional SINR-balancing (ZF optimization-based) and constructive interference SINR-balancing (CI optimization-based) where $N = K = 10$

the MUI is always constructive and therefore, the SINR at the receiver is enhanced without increasing the power per transmitted symbol at the BS. To facilitate the alignment of the resulting symbol to the signal of interest after precoding, the phase of the transmitted symbols is corrected and the angle of correlation between them is rotated by constructing a phase-corrected correlation matrix as expressed below

$$\mathbf{R}_{\phi} = \mathbf{R} \circ \Phi, \tag{3.9}$$

where $\mathbf{R} = \mathbf{H}\mathbf{H}^{H}$ is the cross-correlation matrix, $(\circ)$ denotes element-wise matrix multiplication and Φ is the phase rotation matrix with each of its element expressed as

$$\Phi_{k,n} = \mathbf{d}_n \cdot \frac{\text{conj}\left(\mathbf{d}_k \cdot \mathbf{R}_{k,n}\right)}{\left|\mathbf{R}_{k,n}\right|}. \tag{3.10}$$

Therefore, the transmitted signal is expressed as

$$\mathbf{x}^{CR} = f^{CR} \cdot \mathbf{H}^{H}\left(\mathbf{H}\mathbf{H}^{H}\right)^{-1} \cdot \mathbf{R}_{\phi} \cdot \mathbf{d}, \tag{3.11}$$

where

$$f^{CR} = \sqrt{\frac{1}{\text{tr}\left[\mathbf{R}_{\phi}^{H}\left(\mathbf{H}\mathbf{H}^{H}\right)^{-1}\mathbf{R}_{\phi}\right]}}, \tag{3.12}$$

and the received signal is given as

$$\mathbf{y}^{CR} = f^{CR} \cdot \mathbf{R}_{\phi} \cdot \mathbf{d} + \mathbf{n}. \tag{3.13}$$

It is clear from (3.13) that the transmit signal power of CR is enhanced by the correlation matrix $\mathbf{R}_{\phi}$ and therefore improves the performance of the system. We show in Fig. 3.4 the symbol error rate (SER) performance comparison between the linear precoding techniques discussed. It can be seen that the least SER is achieved by exploiting interference with CR precoding followed by RCI and the channel inversion (ZF), respectively.

3.2.2 Non-linear Precoding

Even with the performance offered by the linear precoding techniques, the gap to reaching the theoretical capacity still exist. In order to further decrease this gap, several non-linear precoding techniques have been proposed. Following the initial theoretical analysis in [68], dirty paper coding (DPC) techniques have been proposed [69, 70, 72, 83]. Although, these techniques achieve significant performance benefits compared to linear precoding techniques, however, they involve sophisticated signal processing at the transmitter for example the sphere-encoder algorithm used in [71]. In [71], a vector-perturbation (VP) technique was proposed that is used in conjunction with the regularized channel inversion precoding to achieve better performance. It was shown in [1] that the problem with ZF is due to the large singular values associated with the inverse of the channel matrix ($\mathbf{H}^{-1}$). The VP technique uses a complex sphere encoder to perturb the data so that the resultant data vector is somewhat orthogonal to the singular vectors associated with the large singular values, thereby reducing the energy of the transmitted signal, hence, achieving improved performance especially at high SNRs. This was basically done by forming a vector $\widetilde{\mathbf{d}}$ from the data vector $\mathbf{d}$ such that the norm of $H^{-1}\widetilde{\mathbf{d}}$ is much

smaller than $H^{-1}\mathbf{d}$. Therefore, the transmitted signal is expressed as

$$\mathbf{x} = \frac{1}{\sqrt{\gamma}} H^{-1}\widetilde{\mathbf{d}} = \frac{1}{\sqrt{\gamma}} H^{-1}(\mathbf{d} + \tau\mathbf{l}), \tag{3.14}$$

where, $\gamma = \left\| H^{-1}\widetilde{\mathbf{d}} \right\|^2$, $\tau = 2(|c|_{\max} + \Delta/2)$ (where $|c|_{\max}$ is the absolute value of the constellation symbol with largest magnitude and Δ is the spacing between the constellation points) and $\mathbf{l}$ is the complex perturbation vector which is chosen at the transmitter to minimize γ

$$\mathbf{l} = \arg\min_{\mathbf{l}^*} (\mathbf{d} + \tau\mathbf{l}^*)^H \left(HH^H\right)^{-1} (\mathbf{d} + \tau\mathbf{l}^*). \tag{3.15}$$

Simulation results in Fig. 3.4 show the effectiveness of the VP precoding, where, the average SER performance is shown compared to other linear precoding techniques.

3.3 Optimization Based Techniques

In recent years, more focus has been given to optimization based techniques, where different strategies and algorithms are designed in order to achieve optimum solutions. The main strategy here is based on the system operator's perspective, which is to provide to all users an acceptable quality of service (QoS) as cheaply as possible and at the same time serving as many users as possible. The QoS is usually expressed in terms of the received signal to interference plus noise ratio (SINR). In the following, we use the terms beamforming and precoding interchangeably, in-line with the most relevant literature.

To facilitate beamforming optimization designs, it has been demonstrated that convex optimization [84] provides a variety of tools that allow for rigorous formulations and solutions to ever-existing and emerging beamforming design problems. The main advantage of convex optimization theory is that it allows for complex design formulations to be recast into convex forms which can be solved efficiently using interior point methods or other appropriate numerical techniques.

As a result, several optimization based beamforming schemes have been proposed in the literature which we categorize into two: Conventional optimization

based beamforming and Constructive interference optimization based beamforming.

3.3.1 Conventional Optimization based Techniques

This category of optimization based beamforming is based on the traditional approach, that treats interference as a detrimental phenomenon. Several beamforming schemes that follow this concept have been proposed in the literature, for both perfect channel state information (CSI) cases [79, 80, 85–87] where full knowledge of the channel is known and imperfect CSI cases [88–91]. These schemes adopt different beamforming design strategies based on the desired system performance metric. We summarize the most common beamforming design strategies in the following based on the system model in Fig. 3.1.

- Power minimization problem: This optimization problem is formulated to directly minimize the total transmit power subject to QoS constraints of the users which is typically expressed as [79]

$$\begin{aligned} \underset{\mathbf{t}_k}{\text{minimize}} \quad & \sum_{k=1}^{K} \|\mathbf{t}_k\|^2 \\ \text{subject to.} \quad & \frac{\mathbf{h}_k^H \mathbf{t}_k}{\sum_{i\neq k}^{K} \mathbf{h}_k^H \mathbf{t}_i + \sigma_k^2} \geq \text{minimum required QoS}(\gamma_k), \forall k. \end{aligned} \tag{3.16}$$

  This formulation is based on the conventional precoders that treat all interference as harmful signals. In particular, it gives the precoding vectors that generates the minimum transmit power for the minimum required QoS.

- SINR-balancing problem: This optimization problem aims to maximize the minimum required QoS (γ_t) subject to the total transmit power as shown be-

low [92]

$$\begin{aligned} \underset{\mathbf{t}_k,\gamma_t}{\text{maximize}} \quad & \gamma_t \\ \text{subject to.} \quad & \frac{\mathbf{h}_k^H \mathbf{t}_k}{\sum_{i\neq k}^{K} \mathbf{h}_k^H \mathbf{t}_i + \sigma_k^2} \geq \gamma_t, \forall k, \\ & \sum_{k=1}^{K} \|\mathbf{t}_k\|^2 \leq P_{total}, \end{aligned} \tag{3.17}$$

where P_{total} is the total transmit power budget. Here, the minimum QoS is maximized which in essence minimizes the interference within the power budget.

- Sum-rate maximization: this optimization problem aims to maximize the sum rate of the considered system. The solution to this problem is the precoding vectors that give the maximum sum rate of the system. The sum-rate maximization problem is typically expressed as [93, 94]

$$\begin{aligned} \underset{\mathbf{t}_k}{\text{maximize}} \quad & \sum_{k=1}^{K} \log\left(1 + \frac{\mathbf{h}_k^H \mathbf{t}_k}{\sum_{i\neq k}^{K} \mathbf{h}_k^H \mathbf{t}_i + \sigma_k^2}\right) \\ \text{subject to.} \quad & \sum_{k=1}^{K} \|\mathbf{t}_k\|^2 \leq P_{total}. \end{aligned} \tag{3.18}$$

Many other optimization problems with different objectives have also been proposed like the minimization of the weighted mean-square error (MSE) in [95], the minimization of signal and interference leakage in [96, 97], e.t.c.

3.3.2 Constructive Interference Optimization based Techniques

This category of optimization based beamforming is based on the beamforming schemes that exploit interference rather than suppress it.

In [98] and [13], a symbol-level data-aided transmit beamforming optimization scheme was proposed, based on the initial closed-form precoding in [76, 77] that the interference can contribute constructively in the detection of the desired signal. It was shown that with the knowledge of both the data symbols and the CSI at the transmitter, the SINR constraints in (3.16) and (3.17) can be modified to ac-

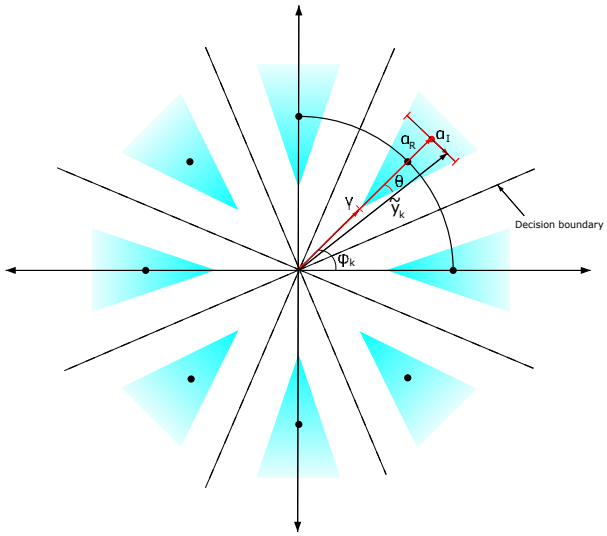

Figure 3.5: Constructive interference area for 8PSK constellation points

commodate for constructive interference for generic PSK modulated signals. This concept is illustrated in Fig. 3.5, which shows the constructive interference area for 8PSK constellation points. The shaded area is the constructive interference region of the constellation points, where γ is the decision threshold i.e. the distance to the decision variable of the constellation point, α_I and α_R are the imaginary and real components $\widetilde{y_k} = \mathbf{h}_k \sum_{k=1}^{K} \mathbf{t}_k e^{j(\phi_i - \phi_k)}$ ignoring the noise, which is phase shifted by the phase of the desired symbol (ϕ_k), respectively. The angle $\theta = \pm\frac{\pi}{M}$ determines the maximum angle shift of the constructive interference area for a modulation order M. Accordingly, if the received signal falls within this area, then interference is said to be exploited constructively. Therefore, by applying basic geometry, from Fig. 3.5 it can be seen that for the received signal to fall in the constructive region of the constellation, we need to have $\alpha_I \leq (\alpha_R - \gamma)\tan\theta$. Hence, by adopting this as the QoS constraint, constructive interference is guaranteed for each user. Therefore, the optimization problem in (3.16) and (3.17) based on CI are given by [13]

- Power minimization problem

$$\begin{aligned} \underset{\mathbf{t}_k}{\text{minimize}} \quad & \sum_{k=1}^{K} \|\mathbf{t}_k d_k\|^2 \\ \text{subject to.} \quad & \alpha_I \leq (\alpha_R - \gamma)\tan\theta, \forall k. \end{aligned} \tag{3.19}$$

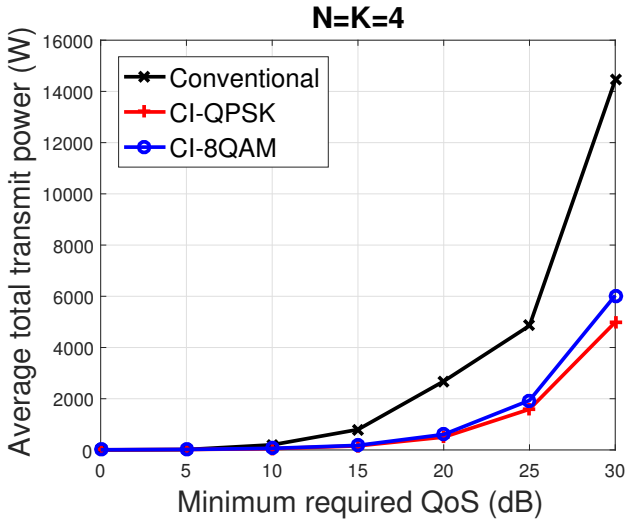

Figure 3.6: Average total transmit power versus the minimum required QoS for conventional (ZF), QPSK and 8QAM when $N = K = 4$

- SINR-balancing problem

$$\begin{aligned} \underset{\mathbf{t}_k,\gamma_t}{\text{maximize}} \quad & \gamma_t \\ \text{subject to.} \quad & \alpha_I \leq (\alpha_R - \gamma_t)\tan\theta, \forall k, \\ & \sum_{k=1}^{K} \|\mathbf{t}_k d_k\|^2 \leq P_{total}. \end{aligned} \tag{3.20}$$

Note that the formulations in (3.16) and (3.17) are data dependent, hence, the optimization is performed on a symbol-by-symbol basis.

As a result, it can be seen in Fig. 3.6 that the same QoS is achieved with lower transmit power as compared to the conventional approaches (3.16) where interference is rather suppressed. Also, in Fig. 3.4 we show the SER of the SINR-balancing problem for both conventional (ZF) approach (3.17) and the CI based approach (3.20). It can be seen that significant error rate savings is achieved with the optimization based approaches compared to the closed-form precoders and in addition, CI provides even better performance compared to the conventional approach.

Similar findings were shown in [81], where the same concept of CI was applied to quadrature amplitude modulated (QAM) signals. To illustrate the concept of constructive interference for QAM modulation we provide a schematic representation

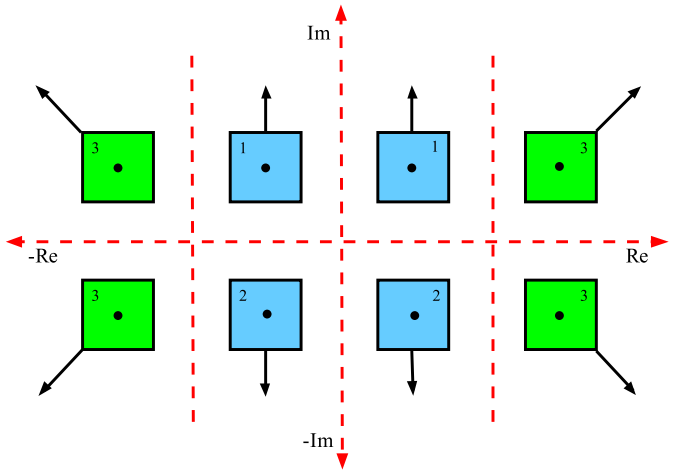

Figure 3.7: Constructive interference region for 8QAM constellation points

of 8QAM constellation points in Fig. 3.7. Based on [81], to guarantee constructive interference for the constellation points, we modify the QoS constraints for each user to exploit the specific detection regions for each group of constellation points separately as detailed below:

- For the group of constellation points labelled "1" and "2" in 3.7, the constraints should guarantee that the received symbol $\widetilde{y_k} = \mathbf{h}_k \sum_{k=1}^{K} \mathbf{t}_k d_k$ ignoring noise, fall in the detection region away from the decision boundaries (dotted lines), which is the real axis. The constraints are

$$\Re(\widetilde{y_k}) = \gamma \cdot \Re(d_k),$$

$$\Im(\widetilde{y_k}) \gtreqless \gamma \cdot \Im(d_k),$$

  where $\Re$ and $\Im$ are the real and imaginary parts.

- For the group of constellation points labelled "3" in 3.7, the constraints should guarantee that the received symbol $(\widetilde{y_k})$ fall in the detection region away from the decision boundaries (dotted lines). Here, the constellation points are not surrounded by the decision boundaries and therefore have a larger detection

region that extend infinitely. The constraints are

$$\Re(\widetilde{y_k}) \gtreqless \gamma \cdot \Re(d_k),$$

$$\Im(\widetilde{y_k}) \gtreqless \gamma \cdot \Im(d_k).$$

Fig. 3.6 shows the average transmit power versus the QoS requirement for conventional, CI-QPSK and CI-8QAM. It can be seen that for the conventional approach more power is required to achieve the same QoS compared to the CI approaches, which is as a result of exploiting the interference rather that suppressing it.

Further findings in [99–107] show that tremendous gains can be achieved by exploiting interference based on symbol level optimization for both PSK and QAM modulated signals. However, all these findings are based on HD systems. In the following chapters, the concept of interference exploitation will be extended and investigated in FD communication systems which provides us with other unique opportunities to explore against the state-of-the-art approaches.

For completeness, we would like to briefly compare the CI technique with another interference suppression technique known as interference alignment (IA) technique in the literature. IA technique proposed in [108] is also a linear precoding technique that has received a lot of attention over the past decade which is fundamentally different to CI and in fact, CI could potentially be applied onto IA. The main idea of IA is to use the spatial dimension offered by the use of MIMO systems to align the interference signals in time, frequency or space such that the users coordinate their transmission, using linear precoding, so the interference lies in a reduced subspace at the receiver. As a result, each user can receive half of the system capacity which effectively increases the sum throughput as compared to when the each interference signal occupy a portion of the subspace. On the other hand, the key idea of CI technique follows a different direction to suppress interference by exploiting the interfering signals. CI precoding as discussed above, aims at aligning the phase of the interfering signals to that of the desired signal by using the knowledge of the transmit symbols at the transmitter. As a result, the received sig-

nal at each receiver is pushed further into the correct detection region of the desired symbol.

3.4 Beamforming in Full Duplex Systems

With the success in most of the proposed SI mitigation techniques over the years, other issues such as, protocol and resource allocation designs need to be re-investigated with respect to FD transmission [109–114]. Many of the FD solutions build upon the existing beamforming solutions discussed in Sections 3.2 and 3.3, where different beamforming design strategies are adopted based on the desired performance metrics. For example, in [109], a MU-MIMO FD system was considered with multiple HD uplink and downlink users, where ZF beamformer was adopted for the downlink transmission while minimum mean squared error (MMSE) was adopted for the uplink transmission. These beamformers were designed to maximize the gains in the FD system in terms of spectral efficiency (SE) and the energy efficiency (EE). These result in two optimization problem formulations: Spectral efficiency also known as sum rate maximization, which aims to maximize the data rate per bandwidth, and Energy efficiency, which aims to maximize the number of bits transmitted per energy unit, in essence, this optimizes the overall energy consumption of the system, which includes the uplink and downlink circuitry power. Similary, in [110], the authors investigated the spectral efficiency of FD small cell wireless systems by considering a joint beamformer design to maximize the spectral efficiency subject to power constraints. In [111], the authors discussed the resource allocation problems in FD-MIMO, FD-Relay, FD-OFDMA and FD-HetNet systems including power control, interference-aware beamforming, e.t.c. Also, resource allocation and scheduling in FD-MIMO-OFDMA relaying systems was studied in [113]. In [114], the authors used massive arrays at the FD relay station to cancel out loop interference and as a result increase the sum spectral efficiency of the system.

Others focused on beamforming design strategies to increase power efficiency [115–117], where the total transmit power of the FD system is minimized subject

to the SINR constraints of the uplink and downlink users. The authors in [115] investigated the power efficient resource allocation for a MU-MIMO FD system. They proposed a multi-objective optimization problem (MOOP) to study the total uplink and downlink transmit power minimization problems jointly via the weighed Tchebycheff method. They extended their work to a robust and secure FD systems model in the presence of roaming users (eavesdroppers) in [116]. Similarly, in [117] the authors used a similar model to investigate the resource allocation for FD simultaneous wireless information and power transfer (SWIPT) systems. Moreover, these works are all based on the traditional approach, where interference is treated as detrimental phenomena, resource allocation in the considered systems are not fully explored. By exploiting interference constructively, a power efficient resource allocation can be provided.

3.5 Multi-objective Optimization

Multi-objective optimization (MOO) is the process of optimizing a number of different objectives simultaneously. The general form of MOO problem (MOOP) is given by

$$\begin{aligned} \underset{a}{\text{minimize}} \quad & \mathbf{Y}(a) = [Y_1(a), Y_2(a), \ldots, Y_N(a)] \\ \text{subject to} \quad & g_k(a) \leq 0, \quad k = 1,2,3,\ldots,K, \\ & f_j(a) = 0, \quad j = 1,2,3,\ldots,J, \end{aligned} \tag{3.21}$$

where a is the optimization variable, N is the number of objective functions, K is the number of inequality constraints, and J is the number of equality constraints. Here, $\mathbf{Y}(a)$ represents the vector of objective functions, respectively.

Different from single-objective optimization problems (SOOPs), there is no single optimal solution to a MOOP, so, it is often necessary to obtain a set of points or solutions that all satisfy a predetermined definition of the optimum solution. The most common way to determine the optimal solution of MOOPs is via the concept of Pareto optimality. A point is said to be Pareto optimal if there is no other point that improves any of the objectives without decreasing the others [118]. In [118], a

survey of several multi-objective optimization methods and concepts in engineering was presented. Based on the primary goal of MOO, which is to model the relative decision maker's preference of the objectives, these methods were categorized into three:

- Category 1: the methods that involve specifying the preference of each objective, which could be attributed with regards to the importance or goals of the objectives. These methods attach weights that can either be used as the decision-maker preferences or can continuously be altered in an effort to represent the complete Pareto optimal set. Some of the methods include: global criterion method, weighted sum method, weighted min-max method or the weighted Tchebycheff method and weighted product method.

- Category 2: the methods that involve selecting a solution out of a set mathematically equivalent solutions. These methods are usually used when it is difficult for the decision maker to set preference for the objectives, thus, it becomes necessary for the decision-maker to choose from a range of available solutions. These methods include: physical programming method, normal boundary intersection (NBI) method and normal constraint (NC) method.

- Category 3: the methods that do not require any articulation of preference. This happens when the decision-maker cannot properly or adequately define the preferences of the objectives. Thus, most of the methods here are simplifications of those in Category 1 above.

Accordingly, in the following Chapters, we design different MOOPs by employing methods with a priori articulation of preferences as in Category 1, which can achieve the complete Pareto optimal set with lower computational complexity.

3.6 Summary

This chapter has provided detailed overview of MIMO wireless communication systems. The various existing linear and non-linear precoding schemes in the literature were discussed, subsequently, showing their performance through simulation results

which highlight their advantages and disadvantages, respectively. In addition, this chapter reviewed optimization based precoding techniques in the literature, which were categorised into conventional and constructive interference based techniques. In was shown that with constructive interference based techniques significant power can be saved by exploiting the MUI rather than suppressing it as compared to the conventional based techniques.

Chapter 4

Interference Exploitation in Full-Duplex Communications

This chapter is based on our publications in [C2], [C3], [J3].

4.1 Introduction

In this chapter, we extend the concept of interference exploitation introduced in Section 3.3.2 of Chapter 3 to FD communication systems, where a FD radio BS serves multiple single-antenna HD uplink and downlink users simultaneously. Unlike conventional interference mitigation approaches, we propose to use the knowledge of the data symbols and the CSI at the FD radio BS to exploit the multi-user interference constructively rather than to suppress it. We propose a MOOP via the weighted Tchebycheff method to study the trade-off between the two desirable system design objectives namely the total downlink transmit power and the total uplink transmit power at the same time ensuring the required QoS for all users. In the proposed MOOP, we adapt the QoS constraints for the downlink users to accommodate CI for both generic PSK modulated signals as well as for QAM signals. We also extended our work to a robust design to study the system with imperfect uplink and downlink CSI.

In particular, this chapter extends the interference exploitation concept to the FD transmission by employing multi-objective optimization, as most recently studied for FD in [115–117]. The authors in [115] investigated the power efficient re-

source allocation for a MU-MIMO FD system. They proposed a MOOP to study the total uplink and downlink transmit power minimization problems jointly. They extended their work to a robust and secure FD systems model in the presence of roaming users (eavesdroppers) in [116]. Similarly, in [117] the authors used a similar model to investigate the resource allocation for FD simultaneous wireless information and power transfer (SWIPT) systems. Accordingly, in this chapter we aim to further reduce the power consumption in FD MU-MIMO wireless communication systems by adopting the concept of CI in the literature to the downlink channel for both PSK and QAM modulation. By exploiting the useful signal power from interference, we can provide a truly power efficient resource allocation for a FD MU-MIMO system. The interference exploitation concept is yet to be explored in the realm of FD transmission, where FD offers the unique opportunity to trade-off the harvested interference power for both uplink and downlink power savings through the MOOP designs.

We note that with regards to existing works in [13, 81, 102, 105–107, 119–126] on interference exploitation (IE), none of them consider FD transmission, and these works therefore are inapplicable to the scenario of interest. In fact, this is the first time in the area of FD transmission to consider the exploitation of interference, where FD scenario brings unique challenges and opportunities to explore with respect to previous works on IE:

- The existence of SI introduces new constraints to the optimization problems, that change the power trade-offs involved.

- The trade-off between uplink and downlink power necessitates the study of MOOP, which is done for the first time here for IE, where previous works focused on single objective power minimization, SINR maximization etc.

- It is this joint optimization that brings, for the first time in the IE works, the opportunity to utilize constructive interference for uplink power savings. All existing works [13, 81, 102, 105–107, 119–126] exploit interference for downlink power savings only.

- The introduction of the SI and receive beamforming vectors in the optimization problems bring particular challenges to the robust optimization problems as will be shown later, which have resulted in new solutions with respect to both [115–117] and to existing robust solutions for IE [13].

However, with respect to the MOOPs shown in [115, 116], they focus on traditional interference rejection. In contrast, our work provides a step change in the MOOP considered, by introducing the concept of interference exploitation. As will be shown later, there is a clear distinction and particular performance gains with respect to the work in [115, 116].

Against the state-of-the-art, we summarize the contributions of this Chapter below:

1. We first introduce the two FD system design objectives namely the total downlink transmit power and the total uplink transmit power. Then we formulate a MOOP to minimize the two objectives jointly via the weighted Tchebycheff method while exploiting the downlink interference for both uplink and downlink power savings.

2. By use of an auxiliary variable, we transform the proposed MOOP into a convex form, which can be efficiently solved using standard solvers.

3. We further derive robust MOOP for both the conventional and the proposed interference exploitation approach for erroneous uplink, downlink and SI channel CSI, where we consider the worst-case performance based on a deterministic model. We do this by recasting the MOOP into a virtual multicast problem and transforming it into a semidefinite program using slack variables.

4.2 System Model

We consider a FD multiuser communication system as shown in Fig. 4.1. The system consists of a FD radio BS with N antennas serving K HD downlink users and J HD uplink users. Each user is equipped with a single antenna to reduce hardware complexity. Let $\mathbf{h}_i \in \mathbb{C}^{N\times 1}$ be the channel vector between the FD radio

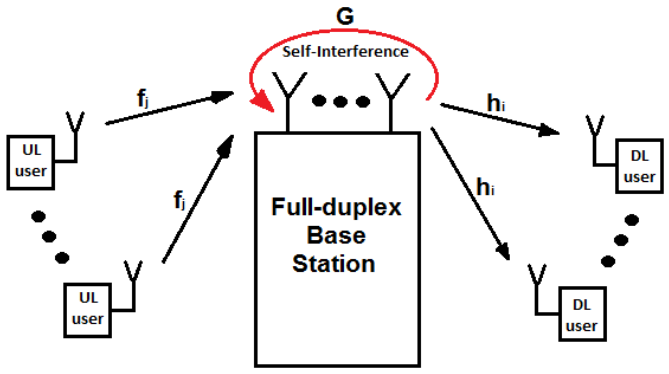

Figure 4.1: System model with a FD radio BS with N antennas, K HD downlink users and J HD uplink users.

BS and the *i-th* downlink user, and $\mathbf{f}_j \in \mathbb{C}^{N\times 1}$ be the channel vector between the FD radio BS and the *j-th* uplink user. We denote the transmit signal vector from the FD radio BS to the *i-th* downlink user as

$$\mathbf{t}_i = \mathbf{w}_i d_i, \tag{4.1}$$

where $\mathbf{w}_i \in \mathbb{C}^{N\times 1}$ and d_i denote the beamforming vector and the unit data symbol for the *i-th* downlink user. The received signal at the *i-th* downlink user is:

$$y_i = \underbrace{\mathbf{h}_i^H \mathbf{t}_i}_{\text{desired signal}} + \underbrace{\sum_{k\neq i}^{K} \mathbf{h}_i^H \mathbf{t}_k + n_i}_{\text{interference plus noise}}, \tag{4.2}$$

where $n_i \sim \mathscr{CN}\left(0, \sigma_i^2\right)$ represents the additive white Gaussian noise AWGN at the *i-th* downlink user. For each time slot the FD radio BS transmits K independent unit data symbols simultaneously at the same frequency to the K downlink users. The first term in (4.2) represents the desired signal while the second term is the multiuser interference signal. For ease of exposition and since the uplink interference cannot be exploited in the style of interference exploitation that we present in this chapter due to the absence of the knowledge of the uplink data at the FD BS, we neglect the uplink-to-downlink interference in our system model. In practice, this may be due to the weak uplink-to-downlink user channels due to physical obstructions and shadowing effects, or due to a dedicated overlaid interference avoidance scheme

such as the one in [127–130]. Accordingly, the explicit interference terms can be avoided for simplicity, or assumed incorporated in the downlink users' noise term. We further note, however, that including the above interference in (4.2), would not change the proposed strategy in which we aim at exploiting the downlink interference power.

The received signal from the J uplink users at the FD radio BS is:

$$\mathbf{y}^{BS} = \sum_{j=1}^{J} \sqrt{P}_j \mathbf{f}_j x_j + \underbrace{\mathbf{G} \sum_{k=1}^{K} \mathbf{t}_k}_{\text{residual self-interference}} + \mathbf{z}, \tag{4.3}$$

where P_j and x_j denotes the uplink transmit power and the data symbol from the *j-th* uplink user respectively. The vector $\mathbf{z} \sim \mathscr{CN}(0, \sigma_N^2)$ represents the additive white Gaussian noise AWGN at the FD radio BS. The matrix $\mathbf{G} \in \mathbb{C}^{N \times N}$ denotes the SI channel. In the literature, different SI mitigation techniques have been proposed [6, 7] to reduce the effect of self-interference. In order to isolate our proposed scheme from the specific implementation of a SI mitigation technique, since the SI cannot be cancelled perfectly in FD systems due to limited dynamic range at the receiver even if the SI channel is known perfectly [6, 116], we consider the worst-case performance based on deterministic model to model the residual-SI channel after cancellation. In essence, we assume the residual-SI channel $\mathbf{G}$ to lie in the neighbourhood of the estimated channel. Hence, the actual channel due to imperfect SI channel estimate is given as

$$\mathbf{G} = \check{\mathbf{G}} + \Delta\mathbf{G}, \tag{4.4}$$

where $\check{\mathbf{G}}$ denotes the SI channel estimate known to the FD BS and $\Delta\mathbf{G}$ represents the SI channel uncertainties, which are assumed to be bounded such that $\|\Delta\mathbf{G}\|^2 \leq \varepsilon_G^2$, for some $\varepsilon_G \geq 0$. We assume the FD BS has no knowledge of $\Delta\mathbf{G}$ only the error bound ε_G.

Accordingly, the first term of (4.3) represents the desired signal from the *j-th* uplink user and the second term represents the residual SI signal. Before we

formulate the problem, we first define the SINR at the *i-th* downlink user and at the FD radio BS respectively as

$$\text{SINR}_i^{DL} = \frac{|\,\mathbf{h}_i^H \mathbf{w}_i\,|^2}{\sum_{k\neq i}^{K} |\,\mathbf{h}_i^H \mathbf{w}_k\,|^2 + \sigma_i^2}, \tag{4.5}$$

$$\text{SINR}_j^{UL} = \frac{P_j\,|\,\mathbf{f}_j^H \mathbf{u}_j\,|^2}{\sum_{n\neq j}^{J} P_n\,|\,\mathbf{f}_n^H \mathbf{u}_j\,|^2 + \sum_{k=1}^{K} |\,\mathbf{u}_j^H(\check{\mathbf{G}} + \Delta\mathbf{G})\mathbf{w}_k\,|^2 + \sigma_N^2 \|\mathbf{u}_j\|^2}, \tag{4.6}$$

where $\mathbf{u}_j \in^{N\times 1}$ is the receive beamforming vector for detecting the received symbol from the *j-th* uplink user. In this chapter, to reduce complexity, we adopt ZF beamforming at the FD BS for the detection of uplink signals. In this context, ZF beamforming is adopted since it provides a good trade-off between complexity and performance [131]. Hence, the receive beamforming vector for the *j-th* uplink user is given as

$$\mathbf{u}_j = (\mathbf{r}_j \mathbf{F}^{\dagger})^H, \tag{4.7}$$

where $\mathbf{r}_j = [\underbrace{0,\ldots,0}_{j-1},1,\underbrace{0,\ldots,0}_{J-j}]$, $\mathbf{F}^{\dagger} = (\mathbf{F}^H\mathbf{F})^{-1}\mathbf{F}^H$,† denotes the pseudo-inverse operation and $\mathbf{F} = [\mathbf{f}_1,\ldots,\mathbf{f}_J]$.

4.3 Conventional Power Minimization Problem

In this section, we introduce the conventional power minimization (PM) problem where all the interference are treated as undesired signals. We first introduce the two system design objectives, then we formulate a MOOP that aims to minimize the two objectives jointly.

In this section, we assume perfect channel state information (CSI) for the uplink and downlink channels. We focus on slow fading channel scenario, where the channels change at the beginning of each frame. Thus, to facilitate the channel real-

ization in practice, handshaking is performed between the FD BS and all users. As the channel changes slowly, pilot signals are usually embedded in the data packets, which allows the FD BS to constantly update the CSI estimation of the transmission links of all users. Later in Section 4.5, we explicitly treat imperfect CSI for designing a robust technique.

The two FD system design objectives are the total downlink transmit power

$$\sum_{i=1}^{K} \|\mathbf{w}_i\|^2, \forall i, \tag{4.8}$$

and the total uplink transmit power

$$\sum_{j=1}^{J} P_j, \forall j. \tag{4.9}$$

These two objectives are very important to both the user and the system operator. In order to study these two objectives jointly, we formulate a MOOP. Multi-objective optimization is employed when there is a need to study jointly the trade-off between two desirable objectives via the concept of Pareto optimality. By using the weighted Tchebycheff method [118], which can achieve the complete Pareto optimal set with lower computational complexity, the MOOP that aims to minimize the total downlink and uplink transmit power jointly for the considered FD system is typically formulated as [115, 116],

$$\begin{aligned} \mathscr{P}4.1: \quad & \min_{\mathbf{w}_i, P_j} \quad \max_{a=1,2} \{\lambda_a (R_a^* - R_a)\} \\ & \text{s.t.} \quad \text{A1}: \frac{|\ \mathbf{h}_i^H \mathbf{w}_i\ |^2}{\sum_{k\neq i}^{K} |\ \mathbf{h}_i^H \mathbf{w}_k\ |^2 + \sigma_i^2} \geq \Gamma_i^{DL}, \forall i, \\ & \qquad \text{A2}: \min_{\Delta\mathbf{G}} \frac{P_j\ |\ \mathbf{f}_j^H \mathbf{u}_j\ |^2}{I_j + \sigma_N^2 \|\mathbf{u}_j\|^2} \geq \Gamma_j^{UL}, \forall j, \end{aligned} \tag{4.10}$$

where, $I_j = \sum_{n\neq j}^{J} P_n\ |\ \mathbf{f}_n^H \mathbf{u}_j\ |^2 + \sum_{k=1}^{K} |\ \mathbf{u}_j^H (\check{\mathbf{G}} + \Delta\mathbf{G}) \mathbf{w}_k\ |^2$. We define Γ_i^{DL} and Γ_j^{UL} as the minimum required SINRs for the *i-th* downlink user and the *j-th* uplink user, respectively. We denote $R_1 = \sum_{i=1}^{K} \|\mathbf{w}_i\|^2$ and $R_2 = \sum_{j=1}^{J} P_j$ as the two system design

objectives, respectively, R_1^* and R_2^* are the optimal values of the two system design objectives in the downlink and uplink, respectively. The variable $\lambda_a \geq 0$, $\sum \lambda_a = 1$, specifies the priority given to the *a-th* objective i.e. for a given $\lambda_1 = 0.8$ means 80% priority is given to R_1 and 20% priority to R_2, respectively. By varying λ_a we can obtain the complete Pareto optimal set. Problem $\mathscr{P}4.1$ is a non-convex problem due to the SINR constraints A1 and A2, and it is commonly solved via semidefinite relaxation as in [115, 116].

4.4 Proposed MOOP based on Constructive Interference

In this section, we study the PM problem based on constructive interference. With prior knowledge of the CSI and users' data symbols for the downlink users, the instantaneous interference can be exploited rather than suppressed [13]. Motivated by this idea, here, we apply this concept to the PM problem in Section 4.3 for both PSK and QAM modulated symbols. We note that constructive interference is only applied to the downlink users and not the uplink users following that only the prior knowledge of the CSI and users' data symbols for the downlink users are available at the BS. Nevertheless, we show in the following that power savings can be obtained for both uplink and downlink transmission, by means of the MOOP design.

4.4.1 Constructive Interference for PSK modulation

To illustrate this concept, we provide a geometric illustration of the constructive interference regions for a QPSK constellation in Fig. 4.2. First, we can define the total downlink transmit signal vector as

$$\sum_{k=1}^{K} \mathbf{w}_k d_k = \sum_{k=1}^{K} \mathbf{w}_k e^{j(\phi_k - \phi_i)} d_i, \tag{4.11}$$

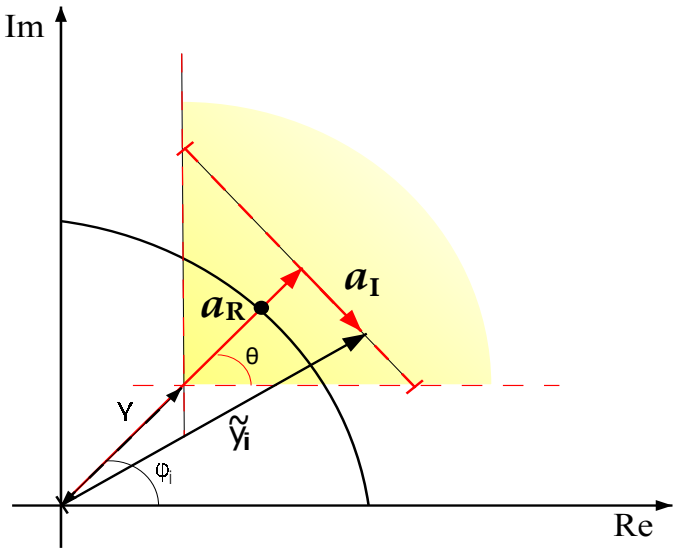

Figure 4.2: Constructive interference region for a QPSK constellation point

where $d_i = de^{\phi_i}$ is the desired symbol for the *i-th* downlink user. Therefore, the received signal (4.2) without noise at the *i-th* downlink user can be defined as

$$\widetilde{y}_i = \mathbf{h}_i^H \sum_{k=1}^{K} \mathbf{w}_k d_k, \tag{4.12}$$

$$= \mathbf{h}_i^H \sum_{k=1}^{K} \mathbf{w}_k e^{j(\phi_k - \phi_i)} d_i, \tag{4.13}$$

Accordingly, since the interference contributes constructively to the received signal, it has been shown in [77] that the downlink SNR at the *i-th* downlink user (4.5) can be rewritten as

$$\mathrm{SNR}_i^{DL} = \frac{\left|\mathbf{h}_i^H \sum_{k=1}^{K} \mathbf{w}_k d_k\right|^2}{\sigma_i^2}. \tag{4.14}$$

Without loss of generality, by taking user 1 as reference the instantaneous downlink transmit power for a unit symbol is

$$\mathrm{P}_{total} = \left\| \sum_{k=1}^{K} \mathbf{w}_k e^{j(\phi_k - \phi_1)} \right\|^2. \tag{4.15}$$

As detailed in [13], the shaded area in Fig. 4.2 is the region of constructive

interference. If the received signal $\widetilde{y}_i$ falls within this region, then interference has been exploited constructively. The angle $\theta = \pm\frac{\pi}{M}$ determines the maximum angle shift of the constructive interference region for a modulation order M, a_I and a_R are the imaginary and real parts of the received signal $\widetilde{y}_i$ without the noise, respectively. The detection threshold is determined by $\gamma = \sqrt{\Gamma_i^{DL}\sigma_i}$.

Therefore, by applying these definitions and basic geometry from Fig. 4.2 it can be seen that for the received signal to fall in the constructive region of the constellation we need to have $a_I \leq (a_R - \gamma)\tan\theta$. Accordingly, we can define the downlink SINR constraint that guarantees constructive interference at the *i-th* downlink user by

$$\left|\mathrm{Im}\left(\mathbf{h}_i^H \sum_{k=1}^{K} \mathbf{w}_k e^{j(\phi_k-\phi_i)}\right)\right| \leq \left(\mathrm{Re}\left(\mathbf{h}_i^H \sum_{k=1}^{K} \mathbf{w}_k e^{j(\phi_k-\phi_i)}\right) - \sqrt{\Gamma_i^{DL}\sigma_i^2}\right)\tan\theta. \tag{4.16}$$

Based on the analysis above, we can modify the SINR constraints for the downlink users in the conventional MOOP to accommodate for CI. Thus, the CI-based MOOP for MPSK modulated symbols is expressed as

$$\begin{aligned}
\mathscr{P}4.2: \min_{\mathbf{w}_i,P_j,t} \quad & t \\
\text{s.t.} \quad & \mathrm{B1}: \left|\mathrm{Im}\left(\mathbf{h}_i^H \sum_{k=1}^{K} \mathbf{w}_k e^{j(\phi_k-\phi_i)}\right)\right| \\
& \leq \left(\mathrm{Re}\left(\mathbf{h}_i^H \sum_{k=1}^{K} \mathbf{w}_k e^{j(\phi_k-\phi_i)}\right) - \sqrt{\Gamma_i^{DL}\sigma_i^2}\right)\tan\theta, \forall i, \\
& \mathrm{B2}: \min_{\Delta\mathbf{G}} \frac{P_j\left|\mathbf{f}_j^H\mathbf{u}_j\right|^2}{I_j^{PSK} + \left|\sum_{k=1}^{K}\mathbf{u}_j^H(\check{\mathbf{G}}+\Delta\mathbf{G})\mathbf{w}_k e^{j(\phi_k-\phi_1)}\right|^2} \geq \Gamma_j^{UL}, \forall j, \\
& \mathrm{B3}: \lambda_a\left(R_a^* - R_a\right) \leq t, \forall a \in \{1,2\},
\end{aligned} \tag{4.17}$$

where, t is an auxiliary variable and $I_j^{PSK} = \sum_{n\neq j}^{J} P_n\left|\mathbf{f}_n^H\mathbf{u}_j\right|^2 + \sigma_N^2\|\mathbf{u}_j\|^2$.

Here $R_1 = \left\|\sum_{k=1}^{K}\mathbf{w}_k e^{j(\phi_k-\phi_1)}\right\|^2$ and $R_2 = \sum_{j=1}^{J} P_j$. Unlike its conventional counterpart, constraint A1, it can be seen that constraint B1 is convex. However, constraint B2 is not convex due to channel uncertainties in the SI term. To transform

B2 into a convex constraint, we rewrite B2 as the following two constraints by introducing a slack variable $S_j^{SI} > 0, \forall j$, respectively,

$$P_j \left|\mathbf{f}_j^H \mathbf{u}_j\right|^2 - \Gamma_j^{UL} \left(\sum_{n \neq j}^{J} P_n \left|\mathbf{f}_n^H \mathbf{u}_j\right|^2 + S_j^{SI} + \sigma_N^2 \|\mathbf{u}_j\|^2 \right) \geq 0, \forall j, \tag{4.18}$$

$$\left| \sum_{k=1}^{K} \mathbf{u}_j^H (\check{\mathbf{G}} + \Delta\mathbf{G}) \mathbf{w}_k e^{j(\phi_k - \phi_1)} \right|^2 - S_j^{SI} \leq 0, \forall \|\Delta\mathbf{G}\|^2 \leq \varepsilon_G^2, \forall j. \tag{4.19}$$

Notice that (4.19) can be guaranteed by the following modified constraint

$$\max_{\|\Delta\mathbf{G}\|^2 \leq \varepsilon_G^2} \left| \sum_{k=1}^{K} \mathbf{u}_j^H (\check{\mathbf{G}} + \Delta\mathbf{G}) \mathbf{w}_k e^{j(\phi_k - \phi_1)} \right|^2 - S_j^{SI} \leq 0, \forall j. \tag{4.20}$$

By using the fact that $\|\mathbf{x}+\mathbf{y}\|^2 \leq (\|\mathbf{x}\| + \|\mathbf{y}\|)^2$, (4.20) can always be guaranteed by the following constraint

$$\max_{\|\Delta\mathbf{G}\|^2 \leq \varepsilon_G^2} \left(\left| \sum_{k=1}^{K} \mathbf{u}_j^H \check{\mathbf{G}} \mathbf{w}_k e^{j(\phi_k - \phi_1)} \right| + \left| \sum_{k=1}^{K} \mathbf{u}_j^H \Delta\mathbf{G} \mathbf{w}_k e^{j(\phi_k - \phi_1)} \right| \right)^2 - S_j^{SI} \leq 0, \forall j, \tag{4.21}$$

whose worst-case formulation is given by

$$\left(\left| \sum_{k=1}^{K} \mathbf{u}_j^H \check{\mathbf{G}} \mathbf{w}_k e^{j(\phi_k - \phi_1)} \right| + \varepsilon_G \left| \sum_{k=1}^{K} \mathbf{u}_j^H \mathbf{w}_k e^{j(\phi_k - \phi_1)} \right| \right)^2 - S_j^{SI} \leq 0, \forall j. \tag{4.22}$$

Therefore, the transformed problem $\mathscr{P}4.2$ is given by

$$
\begin{aligned}
\widetilde{\mathscr{P}4.2}: \min_{\mathbf{w}_i, P_j, t} \quad & t \\
\text{s.t.} \quad & \text{B1}: \left| \text{Im}\left(\mathbf{h}_i^H \sum_{k=1}^{K} \mathbf{w}_k e^{j(\phi_k - \phi_i)} \right) \right| \\
& \qquad \leq \left(\text{Re}\left(\mathbf{h}_i^H \sum_{k=1}^{K} \mathbf{w}_k e^{j(\phi_k - \phi_i)} \right) - \sqrt{\Gamma_i^{DL} \sigma_i^2} \right) \tan\theta, \forall i, \\
& \widetilde{\text{B2a}}: P_j \left| \mathbf{f}_j^H \mathbf{u}_j \right|^2 - \Gamma_j^{UL} \left(\sum_{n \neq j}^{J} P_n \left| \mathbf{f}_n^H \mathbf{u}_j \right|^2 + S_j^{SI} + \sigma_N^2 \|\mathbf{u}_j\|^2 \right) \geq 0, \forall j, \\
& \widetilde{\text{B2b}}: \left(\left| \sum_{k=1}^{K} \mathbf{u}_j^H \check{\mathbf{G}} \mathbf{w}_k e^{j(\phi_k - \phi_1)} \right| + \varepsilon_G \left| \sum_{k=1}^{K} \mathbf{u}_j^H \mathbf{w}_k e^{j(\phi_k - \phi_1)} \right| \right)^2 \leq S_j^{SI}, \forall j, \\
& \text{B3}: \lambda_a \left(R_a^* - R_a \right) \leq t, \forall a \in \{1, 2\}.
\end{aligned}
\tag{4.23}
$$

The problem $\widetilde{\mathscr{P}4.2}$ is now jointly convex with respect to the optimization variables, since constraint B1 is a standard second-order cone constraint, $\widetilde{\text{B2a}}$ is a linear constraint and $\widetilde{\text{B2b}}$ is a quadratic constraint. Hence, $\widetilde{\mathscr{P}4.2}$ can be efficiently solved using standard solvers like CVX [132].

Now we highlight the main advantage of the proposed optimization problem over the conventional optimization problem in Section 4.3. In the optimization problem in Section 4.3, the constraints suppress the interference each user experience, which is equivalent to constraining the interference such that the signal received is just within the nominal constellation point. While in the case of proposed optimization problem $\widetilde{\mathscr{P}4.2}$, constraint B1 relaxes the optimization and allows for a larger detection region as shown in Fig. 4.2. Hence, this translates to a larger feasible solution set thereby leading to reduction in the total transmit power as compared to the conventional optimization problem in Section 4.3, which will be demonstrated later through simulation results.

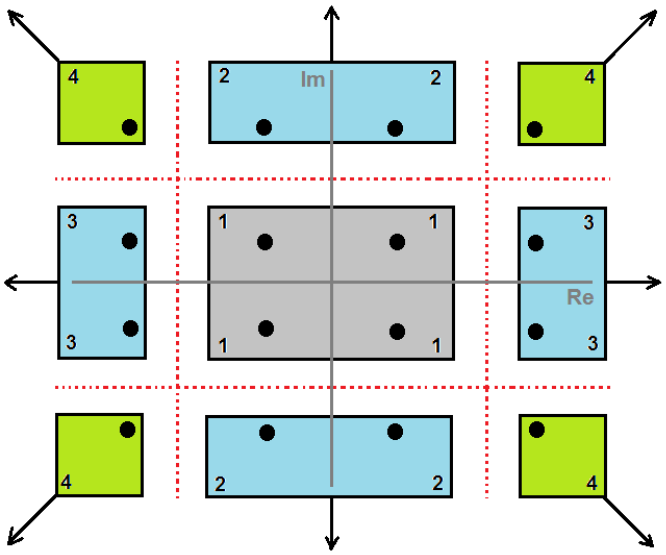

Figure 4.3: Schematic representation of 16QAM constellation points

4.4.2 Constructive Interference for QAM modulation

To illustrate the concept of constructive interference for QAM modulation we provide a schematic representation for 16QAM constellation points in Fig. 4.3. Based on [101], to guarantee constructive interference for the constellation points, we rewrite the SINR constraints for the downlink users to exploit the specific detection regions for each group of constellation points separately as detailed below. First, we redefine the received signal without noise at the *i-th* downlink user as in (4.12) and the instantaneous downlink transmit power (4.15) in terms of amplitude not phase as

$$P_{total} = \left\| \sum_{k=1}^{K} \mathbf{w}_k d_k \right\|^2 . \tag{4.24}$$

From Fig. 4.3, to ensure constructive interference is achieved and the constellation points are received in the correct detection region for the downlink users, the following constraints are adopted. Note that the dotted lines in Fig. 4.3 represent the decision boundaries.

- For the group of constellation points in the box labelled "1" in Fig. 4.3, since they are all surrounded by the decision boundaries, the constraints should guarantee that the received signals achieve the exact constellation point so as

not to exceed the decision boundaries. The constraints are

$$\text{C1} : \text{Re}(\widetilde{y}_i) = \sqrt{\Gamma_i^{DL}}\sigma_i \text{Re}(d_i),$$

$$\text{C2} : \text{Im}(\widetilde{y}_i) = \sqrt{\Gamma_i^{DL}}\sigma_i \text{Im}(d_i).$$

- For the group of constellation points labelled "2" in Fig. 4.3, the constraints should guarantee that the received signals fall in the detection region away from the decision boundaries, which is the real axis. The constraints are

$$\text{C1} : \text{Re}(\widetilde{y}_i) = \sqrt{\Gamma_i^{DL}}\sigma_i \text{Re}(d_i),$$

$$\text{C2} : \text{Im}(\widetilde{y}_i) \gtreqless \sqrt{\Gamma_i^{DL}}\sigma_i \text{Im}(d_i).$$

- For the group of constellation points labelled "3" in Fig. 4.3, the constraints should guarantee that the received signals fall in the detection region away from the decision boundaries, which is the imaginary axis. The constraints are

$$\text{C1} : \text{Re}(\widetilde{y}_i) \gtreqless \sqrt{\Gamma_i^{DL}}\sigma_i \text{Re}(d_i),$$

$$\text{C2} : \text{Im}(\widetilde{y}_i) = \sqrt{\Gamma_i^{DL}}\sigma_i \text{Im}(d_i).$$

- For the group of constellation points labelled "4" in Fig. 4.3, the constraints should guarantee that the received signals fall in the detection region away from the decision boundaries. Here, the constellation points are not surrounded by the decision boundaries and therefore have a larger detection region that extend infinitely. The constraints are

$$\text{C1} : \text{Re}(\widetilde{y}_i) \gtreqless \sqrt{\Gamma_i^{DL}}\sigma_i \text{Re}(d_i),$$

$$\text{C2} : \text{Im}(\widetilde{y}_i) \gtreqless \sqrt{\Gamma_i^{DL}}\sigma_i \text{Im}(d_i).$$

By adopting the required downlink SINR constraints C1 and C2 for the cor-

responding group constellation points, the conventional MOOP can be modified to accommodate for CI. Therefore, the CI-based MOOP for 16QAM modulation can be expressed as

$$\begin{aligned}
\mathscr{P}4.3: \min_{\mathbf{w}_i, P_j, t} \quad & t \\
\text{s.t.} \quad & \text{Constraints C1 and C2}, \forall i, \\
& \text{C3a}: P_j \left|\mathbf{f}_j^H \mathbf{u}_j\right|^2 - \Gamma_j^{UL} \left(\sum_{n \neq j}^{J} P_n \left|\mathbf{f}_n^H \mathbf{u}_j\right|^2 + S_j^{SI} + \sigma_N^2 \|\mathbf{u}_j\|^2 \right) \geq 0, \forall j, \\
& \text{C3b}: \left(\left| \sum_{k=1}^{K} \mathbf{u}_j^H \check{\mathbf{G}} \mathbf{w}_k d_k \right| + \varepsilon_G \left| \sum_{k=1}^{K} \mathbf{u}_j^H \mathbf{w}_k d_k \right| \right)^2 \leq S_j^{SI}, \forall j, \\
& \text{C4}: \lambda_a \left(R_a^* - R_a\right) \leq t, \forall a \in \{1,2\}.
\end{aligned} \tag{4.25}$$

where, $R_1 = \left\| \sum_{k=1}^{K} \mathbf{w}_k d_k \right\|^2$ and $R_2 = \sum_{j=1}^{J} P_j$.

Again, it can be observed that unlike their conventional counterparts, $\mathscr{P}4.3$ above is jointly convex with respect to the optimization variables and can be optimally solved using standard convex solvers like CVX [132].

4.5 Proposed Multi-objective Optimization with Imperfect CSI

4.5.1 Conventional Robust MOOP

In this section we study the robustness of the system when the downlink and the uplink CSI are not perfectly known. There are two approaches frequently used to model or characterize imperfect CSI: the probabilistic approach and the deterministic approach. In probabilistic approach, the error in the CSI knowledge is assumed to have a certain statistical characteristic like the mean or covariance of the channel. In deterministic approach, which is adopted in this Section, the error in the CSI is assumed to belong to a given uncertainty set. The size of the set determines the amount of uncertainty on the channel and the system optimizes the worst-case performance which achieves a guaranteed performance level for any channel realization in the set. Therefore, for convenience and to avoid any statistical assump-

tions on the channel, we adopt the deterministic approach which corresponds well to quantization errors and is also suitable for handling slow-fading channels [89]. Thus, for each user, their actual channel is modeled as

$$\mathbf{h}_i = \check{\mathbf{h}}_i + \Delta\mathbf{h}_i, \forall i, \tag{4.26}$$

$$\mathbf{f}_j = \check{\mathbf{f}}_j + \Delta\mathbf{f}_j, \forall j, \tag{4.27}$$

where $\check{\mathbf{h}}_i$ and $\check{\mathbf{f}}_j$ denote the downlink and the uplink CSI estimates known to the FD BS, respectively. $\Delta\mathbf{h}_i, \forall i$ and $\Delta\mathbf{f}_j, \forall j$ represent the downlink and the uplink CSI uncertainties, respectively, which are assumed to be bounded such that

$$\|\Delta\mathbf{h}_i\|^2 \leq \varepsilon_{h,i}^2, \text{ for some } \varepsilon_{h,i} \geq 0, \tag{4.28}$$

$$\left\|\Delta\mathbf{f}_j\right\|^2 \leq \varepsilon_{f,j}^2, \text{ for some } \varepsilon_{f,j} \geq 0. \tag{4.29}$$

We assume that the FD BS has no knowledge of 9 except for their error bounds, hence, we take the worst-case approach for our problem design. Thus, the MOOP formulation of $\mathscr{P}4.1$ with imperfect CSI is

$$\begin{aligned}
\mathscr{P}4.4: \quad & \min_{\mathbf{w}_i, P_j, t} \quad t \\
\text{s.t.} \quad & \text{D1}: \min_{\Delta\mathbf{h}_i} \frac{\left|\left(\check{\mathbf{h}}_i + \Delta\mathbf{h}_i\right)^H \mathbf{w}_i\right|^2}{\sum_{k\neq i}^{K}\left|\left(\check{\mathbf{h}}_i + \Delta\mathbf{h}_i\right)^H \mathbf{w}_k\right|^2 + \sigma_i^2} \geq \Gamma_i^{DL}, \forall i, \\
& \text{D2}: \min_{\Delta\mathbf{f}_j, \Delta\mathbf{G}} \frac{P_j\left|\left(\check{\mathbf{f}}_j + \Delta\mathbf{f}_j\right)^H \mathbf{u}_j\right|^2}{\sum_{n\neq j}^{J} P_n\left|\left(\check{\mathbf{f}}_n + \Delta\mathbf{f}_n\right)^H \mathbf{u}_j\right|^2 + C_j} \geq \Gamma_j^{UL}, \forall j, \\
& \text{D3}: \lambda_a\left(R_a^* - R_a\right) \leq t, \forall a \in \{1,2\}.
\end{aligned} \tag{4.30}$$

where $C_j = \sum_{k=1}^{K}\left|\mathbf{u}_j^H\left(\check{\mathbf{G}} + \Delta\mathbf{G}\right)\mathbf{w}_k\right|^2 + \sigma_N^2\|\mathbf{u}_j\|^2$

In the downlink and uplink SINR constraints, there are infinitely many inequalities which make the worst-case design particularly challenging. To make $\mathscr{P}4.4$ more tractable, we formulate the problem as a semidefinite program (SDP)

then transform the constraints into linear matrix inequalities (LMI), which can be efficiently solved by existing solvers like CVX [132]. The SDP transformation of problem $\mathscr{P}4.4$ is given by

$$\begin{aligned}
&\min_{\mathbf{W}_i,P_j,t} \quad t \\
\text{s.t.} \quad &\widetilde{\text{D1}}: \min_{\Delta\mathbf{h}_i} \frac{\left(\check{\mathbf{h}}_i+\Delta\mathbf{h}_i\right)^H \mathbf{W}_i \left(\check{\mathbf{h}}_i+\Delta\mathbf{h}_i\right)}{\sum_{k\neq i}^{K}\left((\check{\mathbf{h}}_i+\Delta\mathbf{h}_i)^H\mathbf{W}_k(\check{\mathbf{h}}_i+\Delta\mathbf{h}_i)\right)+\sigma_i^2} \geq \Gamma_i^{DL}, \forall i, \\
&\widetilde{\text{D2}}: \min_{\Delta\mathbf{f}_j,\Delta\mathbf{G}} \frac{P_j\left(\check{\mathbf{f}}_j+\Delta\mathbf{f}_j\right)^H \mathbf{U}_j \left(\check{\mathbf{f}}_j+\Delta\mathbf{f}_j\right)}{\sum_{n\neq j}^{J} P_n\left(\check{\mathbf{f}}_n+\Delta\mathbf{f}_n\right)^H \mathbf{U}_j \left(\check{\mathbf{f}}_n+\Delta\mathbf{f}_n\right)+\widetilde{C}_j} \geq \Gamma_j^{UL}, \forall j, \\
&\widetilde{\text{D3}}: \lambda_a\left(R_a^*-R_a\right) \leq t, \forall a \in \{1,2\}. \\
&\widetilde{\text{D4}}: \mathbf{W}_i \succeq 0, \forall i.
\end{aligned} \tag{4.31}$$

where, $\widetilde{C}_j = \text{Tr}\left\{\left(\check{\mathbf{G}}+\Delta\mathbf{G}\right)\sum_{k=1}^{K}\mathbf{W}_k\left(\check{\mathbf{G}}+\Delta\mathbf{G}\right)^H\mathbf{U}_j\right\}+\sigma_N^2\text{Tr}\left\{\mathbf{U}_j\right\}$ and we define $\mathbf{W}_i=\mathbf{w}_i\mathbf{w}_i^H$ and $\mathbf{U}_j=\mathbf{u}_j\mathbf{u}_j^H$. Next, we can rearrange constraint $\widetilde{\text{D1}}$ into

$$\min_{\Delta\mathbf{h}_i}\left(\check{\mathbf{h}}_i+\Delta\mathbf{h}_i\right)^H\mathbf{Q}_i\left(\check{\mathbf{h}}_i+\Delta\mathbf{h}_i\right)-\Gamma_i^{DL}\sigma_i^2 \geq 0, \forall i. \tag{4.32}$$

where, we introduce

$$\mathbf{Q}_i \triangleq \mathbf{W}_i - \Gamma_i^{DL}\sum_{k\neq i}^{K}\mathbf{W}_k, \forall i$$

and then for constraint $\widetilde{\text{D2}}$, let's define two vectors $\widetilde{\mathbf{f}}$ and $\widetilde{\Delta\mathbf{f}}$ as

$$\widetilde{\mathbf{f}}=\begin{bmatrix}\check{\mathbf{f}}_j\\ \vdots \\ \check{\mathbf{f}}_J\end{bmatrix}\in\mathbb{C}^{NJ\times 1}, \widetilde{\Delta\mathbf{f}}=\begin{bmatrix}\Delta\mathbf{f}_j\\ \vdots \\ \Delta\mathbf{f}_J\end{bmatrix}\in\mathbb{C}^{NJ\times 1}. \tag{4.33}$$

Hence, we can define any $\check{\mathbf{f}}_j=\mathbf{B}_j\widetilde{\mathbf{f}}$ and $\Delta\mathbf{f}_j=\mathbf{B}_j\widetilde{\Delta\mathbf{f}}$, for $j=1,\ldots,J$, with $\mathbf{B}_j\in\mathbb{R}^{N\times NJ}$ defined as $\mathbf{B}_j=\left[\mathbf{B}_{j,1},\ldots,\mathbf{B}_{j,J}\right]$, where $\mathbf{B}_{j,j}=\mathbf{I}_N$ and $\mathbf{B}_{j,n}=\mathbf{0}_N$, for $n=1,\ldots,J, n\neq j$. We have $\mathbf{I}_N$ and $\mathbf{0}_N$ to be an $N\times N$ identity matrix and zero matrix,

respectively. Now constraint $\widetilde{\text{D2}}$ can be rewritten as

$$\min_{\Delta\mathbf{f}_j,\Delta\mathbf{G}} \frac{P_j\left((\mathbf{B}_j\widetilde{\mathbf{f}}+\mathbf{B}_j\widetilde{\Delta\mathbf{f}})^H\mathbf{U}_j(\mathbf{B}_j\widetilde{\mathbf{f}}+\mathbf{B}_j\widetilde{\Delta\mathbf{f}})\right)}{\sum_{n\neq j}^{J}P_n\left((\mathbf{B}_n\widetilde{\mathbf{f}}+\mathbf{B}_n\widetilde{\Delta\mathbf{f}})^H\mathbf{U}_j(\mathbf{B}_n\widetilde{\mathbf{f}}+\mathbf{B}_n\widetilde{\Delta\mathbf{f}})\right)+\widetilde{C}_j} \geq \Gamma_j^{UL},\forall j, \tag{4.34}$$

and can be simplified to give

$$\min_{\Delta\mathbf{f}_j,\Delta\mathbf{G}} \frac{\left(\widetilde{\mathbf{f}}+\widetilde{\Delta\mathbf{f}}\right)^H\mathbf{Z}_j\left(\widetilde{\mathbf{f}}+\widetilde{\Delta\mathbf{f}}\right)}{\text{Tr}\left\{\left(\check{\mathbf{G}}+\Delta\mathbf{G}\right)\sum_{k=1}^{K}\mathbf{W}_k\left(\check{\mathbf{G}}+\Delta\mathbf{G}\right)^H\mathbf{U}_j\right\}+\sigma_N^2\text{Tr}\left\{\mathbf{U}_j\right\}} \geq \Gamma_j^{UL},\forall j, \tag{4.35}$$

where we introduce

$$\mathbf{Z}_j \triangleq P_j\mathbf{B}_j^T\mathbf{U}_j\mathbf{B}_j-\Gamma_j^{UL}\sum_{n\neq j}^{J}P_n\mathbf{B}_n^T\mathbf{U}_j\mathbf{B}_n,\forall j.$$

We further simplify (4.35) by introducing slack variables $s_j>0,\forall j$ [84], such that (4.35) can be written as the following two constraints

$$\min_{\Delta\mathbf{f}_j}\left(\widetilde{\mathbf{f}}+\widetilde{\Delta\mathbf{f}}\right)^H\mathbf{Z}_j\left(\widetilde{\mathbf{f}}+\widetilde{\Delta\mathbf{f}}\right)\geq s_j\Gamma_j^{UL},\forall j, \tag{4.36}$$

$$\max_{\Delta\mathbf{G}}\text{Tr}\left\{\left(\check{\mathbf{G}}+\Delta\mathbf{G}\right)\sum_{k=1}^{K}\mathbf{W}_k\left(\check{\mathbf{G}}+\Delta\mathbf{G}\right)^H\mathbf{U}_j\right\}+\sigma_N^2\text{Tr}\left\{\mathbf{U}_j\right\}\leq s_j,\forall j. \tag{4.37}$$

Next, we review the definitions of the S-procedure for completeness.

Lemma 1. (S-procedure [84]): Let $g_l(\mathbf{x})$, $l=1,2$, be defined as

$$g_l(\mathbf{x})=\mathbf{x}^H\mathbf{A}_l\mathbf{x}+2Re\left\{\mathbf{b}_l^H\mathbf{x}\right\}+c_l,$$

where $\mathbf{A}_l\in\mathbb{C}^{n\times n},\mathbf{b}_l\in\mathbb{C}^n$ and $c_l\in\mathbb{R}$. Then, the implication of $g_1(\mathbf{x})\geq 0\Rightarrow g_2(\mathbf{x})\geq 0$ holds if and only if there exists a $\lambda\geq 0$ such that

$$\lambda\begin{bmatrix}\mathbf{A}_1 & \mathbf{b}_1\\ \mathbf{b}_1^H & c_1\end{bmatrix}-\begin{bmatrix}\mathbf{A}_2 & \mathbf{b}_2\\ \mathbf{b}_2^H & c_2\end{bmatrix}\succeq 0,$$

provided there exists a point $\hat{\mathbf{x}}$ with $g_1(\hat{\mathbf{x}})>0$.

Following Lemma 1 and using the fact that $\mathrm{Tr}\{\mathbf{ABCD}\} = \mathrm{vec}\left(\mathbf{A}^H\right)^H \left(\mathbf{D}^H \otimes \mathbf{B}\right) \mathrm{vec}\left(\mathbf{C}\right)$, constraints (4.32), (4.36) and (4.37) can be expanded as

$$\Delta\mathbf{h}_i^H \mathbf{Q}_i \Delta\mathbf{h}_i + 2Re\left\{\check{\mathbf{h}}_i^H \mathbf{Q}_i \Delta\mathbf{h}_i\right\} + \check{\mathbf{h}}_i^H \mathbf{Q}_i \check{\mathbf{h}}_i - \Gamma_i^{DL}\sigma_i^2 \geq 0, \forall i, \tag{4.38a}$$

$$\Delta\mathbf{h}_i^H \mathbf{I} \Delta\mathbf{h}_i - \varepsilon_{h,i}^2 \leq 0, \forall i, \tag{4.38b}$$

$$\widetilde{\Delta\mathbf{f}}^H \mathbf{Z}_j \widetilde{\Delta\mathbf{f}} + 2Re\left\{\widetilde{\mathbf{f}}^H \mathbf{Z}_j \widetilde{\Delta\mathbf{f}}\right\} + \widetilde{\mathbf{f}}^H \mathbf{Z}_j \widetilde{\mathbf{f}} - s_j \Gamma_j^{UL} \geq 0, \forall j, \tag{4.39a}$$

$$\widetilde{\Delta\mathbf{f}}^H \mathbf{I} \widetilde{\Delta\mathbf{f}} - \varepsilon_f^2 \leq 0, \tag{4.39b}$$

$$\begin{aligned}\Delta\mathbf{g}^H \left(\mathbf{U}_j \otimes \sum_{k=1}^{K} \mathbf{W}_k\right) \Delta\mathbf{g} + 2Re\left\{\check{\mathbf{g}}^H \left(\mathbf{U}_j \otimes \sum_{k=1}^{K} \mathbf{W}_k\right) \Delta\mathbf{g}\right\} \\ + \check{\mathbf{g}}^H \left(\mathbf{U}_j \otimes \sum_{k=1}^{K} \mathbf{W}_k\right) \check{\mathbf{g}} + \sigma_N^2 \mathrm{Tr}\left\{\mathbf{U}_j\right\} - s_j \leq 0, \forall j,\end{aligned} \tag{4.40a}$$

$$\Delta\mathbf{g}^H \mathbf{I} \Delta\mathbf{g} - \varepsilon_G^2 \leq 0. \tag{4.40b}$$

We define $\check{\mathbf{g}} = \mathrm{vec}\left(\check{\mathbf{G}}^H\right)$ and $\Delta\mathbf{g} = \mathrm{vec}\left(\Delta\mathbf{G}^H\right)$ where, $\mathrm{vec}\left(\cdot\right)$ stacks the columns of a matrix into a vector and $\otimes$ stands for Kronecker product.

Hence, according to Lemma 1, (4.38a) and (4.38b) hold if and only if there exist a $\delta_i \geq 0$ such that

$$\begin{bmatrix} \delta_i \mathbf{I} + \mathbf{Q}_i & \mathbf{Q}_i \check{\mathbf{h}}_i \\ \check{\mathbf{h}}_i^H \mathbf{Q}_i & \check{\mathbf{h}}_i^H \mathbf{Q}_i \check{\mathbf{h}}_i - \Gamma_i^{DL}\sigma_i^2 - \delta_i \varepsilon_{h,i}^2 \end{bmatrix} \succeq 0, \forall i.$$

Similar procedure can be applied to constraints (4.39) and (4.40), respectively. Thus, the conventional robust optimization problem $\mathscr{P}4.4$ can be reformulated as

shown in (4.41).

$$
\begin{aligned}
\mathscr{P}4.5: \quad & \min_{\mathbf{W}_i, P_j, t} \quad t \\
\text{s.t.} \quad & \begin{bmatrix} \delta_i \mathbf{I} + \mathbf{Q}_i & \mathbf{Q}_i \check{\mathbf{h}}_i \\ \check{\mathbf{h}}_i^H \mathbf{Q}_i & \check{\mathbf{h}}_i^H \mathbf{Q}_i \check{\mathbf{h}}_i - \Gamma_i^{DL} \sigma_i^2 - \delta_i \varepsilon_{h,i}^2 \end{bmatrix} \succeq 0, \forall i, \\
& \begin{bmatrix} \mu_j \mathbf{I} + \mathbf{Z}_j & \mathbf{Z}_j \widetilde{\mathbf{f}} \\ \widetilde{\mathbf{f}}^H \mathbf{Z}_j & \widetilde{\mathbf{f}}^H \mathbf{Z}_j \widetilde{\mathbf{f}} - s_j \Gamma_j^{UL} - \mu_j \varepsilon_f^2 \end{bmatrix} \succeq 0, \forall j, \\
& \begin{bmatrix} \rho \mathbf{I} - \left(\mathbf{U}_j \otimes \sum_{k=1}^K \mathbf{W}_k\right) & -\left(\mathbf{U}_j \otimes \sum_{k=1}^K \mathbf{W}_k\right) \check{\mathbf{g}} \\ -\check{\mathbf{g}}^H \left(\mathbf{U}_j \otimes \sum_{k=1}^K \mathbf{W}_k\right) & s_j - \check{\mathbf{g}}^H \left(\mathbf{U}_j \otimes \sum_{k=1}^K \mathbf{W}_k\right) \check{\mathbf{g}} - \sigma_N^2 \mathrm{Tr}\left\{\mathbf{U}_j\right\} - \rho \varepsilon_G^2 \end{bmatrix} \succeq 0, \forall j, \\
& \lambda_a \left(R_a^* - R_a\right) \leq t, \forall a \in \{1,2\}, \\
& \mathbf{W}_i \succeq 0, \delta_i \geq 0, \mu_j \geq 0, \rho \geq 0, s_j > 0, \forall i, j.
\end{aligned}
\tag{4.41}
$$

The problem $\mathscr{P}4.5$ is convex, and can be efficiently solved using CVX [132]. The resulting optimal values obtained from $\mathscr{P}4.5$ provide a lower bound for the conventional power minimization problem.

Note that the problem $\mathscr{P}4.5$ is a relaxed form of $\mathscr{P}4$. While it is difficult to prove the rank-one solution of problem $\mathscr{P}4.5$, we have observed over 1000 iterations, problem $\mathscr{P}4.5$ always return rank-one solution $(\mathbf{W}_i, \forall i)$. Although, one could derive a rank-one solution for FD beamforming problem in a similar fashion as in [133]. Still, in the unlikely case of a non rank-one solution the optimal solutions can always be obtained by randomization technique as in [134], such that $\mathbf{W}_i = \mathbf{w}_i \mathbf{w}_i^H, \forall i$.

4.5.2 Constructive Interference MOOP

To study the robustness of the proposed system based on constructive interference, for notational simplicity, we formulate $\widetilde{\mathscr{P}4.2}$ as a virtual multicast problem. The motivation for recasting $\widetilde{\mathscr{P}4.2}$ into a virtual multicast problem is for the ease of transforming the robust CI based MOOP into convex form. As the constraint B1 in the problem $\widetilde{\mathscr{P}4.2}$ involves dealing with real and imaginary parts of the received

signal ($\widetilde{y}_i$) separately, analysis will be easier with real valued numbers, hence, the need for virtual multicast formulation. To facilitate this, we simply incorporate each user's channel with its respective data symbol i.e. $\widetilde{\mathbf{h}}_i = \mathbf{h}_i e^{j(\phi_1-\phi_i)}$ and let $\mathbf{w} = \sum_{k=1}^{K} \mathbf{w}_k e^{j(\phi_k-\phi_1)}$. Following this the multicast formulation of problem $\widetilde{\mathscr{P}4.2}$ can be written as

$$\begin{aligned}
\mathscr{P}4.6: \quad & \min_{\mathbf{w},P_j,t} \quad t \\
\text{s.t.} \quad & \left|\Im\left(\widetilde{\mathbf{h}}_i^H\mathbf{w}\right)\right| \leq \left(\Re\left(\widetilde{\mathbf{h}}_i^H\mathbf{w}\right) - \sqrt{\Gamma_i^{DL}\sigma_i^2}\right)\tan\theta, \forall i, \\
& \frac{P_j\left|\mathbf{f}_j^H\mathbf{u}_j\right|^2}{\sum_{n\neq j}^{J} P_n\left|\mathbf{f}_n^H\mathbf{u}_j\right|^2 + \left|\mathbf{u}_j^H\mathbf{G}\mathbf{w}\right|^2 + \sigma_N^2\|\mathbf{u}_j\|^2} \geq \Gamma_j^{UL}, \forall j, \\
& \lambda_a\left(R_a^* - R_a\right) \leq t, \forall a \in \{1,2\}.
\end{aligned} \tag{4.42}$$

Based on the multicast formulation $\mathscr{P}4.6$, for the worst-case design we model the imperfect CSI as

$$\widetilde{\mathbf{h}}_i = \check{\mathbf{h}}_i + \Delta\widetilde{\mathbf{h}}_i, \forall i, \tag{4.43}$$

where $\check{\mathbf{h}}_i$ denotes the downlink CSI estimate known to the FD BS and $\Delta\widetilde{\mathbf{h}}_i$ is the downlink CSI uncertainty which is bounded such that $\left\|\Delta\widetilde{\mathbf{h}}_i\right\|^2 \leq \varepsilon_{h,i}^2$. Similarly, we model the uplink CSI as in Section 4.5.1. The robust formulation of problem $\mathscr{P}4.6$ is

$$\begin{aligned}
\mathscr{P}4.7: & \min_{\mathbf{w},P_j,t} \quad t \\
\text{s.t.} \quad & \max_{\Delta\mathbf{h}_i} \left|\Im\left((\check{\mathbf{h}}_i + \Delta\widetilde{\mathbf{h}}_i)^H\mathbf{w}\right)\right| \leq \left(\Re\left((\check{\mathbf{h}}_i + \Delta\widetilde{\mathbf{h}}_i)^H\mathbf{w}\right) - \sqrt{\Gamma_i^{DL}\sigma_i^2}\right)\tan\theta, \forall i, \\
& \min_{\Delta\mathbf{f}_j,\Delta\mathbf{G}} \frac{P_j\left|\left(\check{\mathbf{f}}_j + \Delta\mathbf{f}_j\right)^H\mathbf{u}_j\right|^2}{\sum_{n\neq j}^{J} P_n\left|\left(\check{\mathbf{f}}_n + \Delta\mathbf{f}_n\right)^H\mathbf{u}_j\right|^2 + I_j} \geq \Gamma_j^{UL}, \forall j, \\
& \lambda_a\left(R_a^* - R_a\right) \leq t, \forall a \in \{1,2\}.
\end{aligned} \tag{4.44}$$

where $I_j = \left|\mathbf{u}_j^H \left(\check{\mathbf{G}} + \Delta\mathbf{G}\right)\mathbf{w}\right|^2 + \sigma_N^2\|\mathbf{u}_j\|^2$.

First, let's consider the downlink SINR constraint. For convenience we separate the real and imaginary part of the complex notations and represent them as real valued numbers. Let

$$\underline{\mathbf{w}} \triangleq \begin{bmatrix} \Re(\mathbf{w}) \\ \Im(\mathbf{w}) \end{bmatrix}, \tag{4.45}$$

$$\underline{\check{\mathbf{h}}}_i \triangleq \begin{bmatrix} \Im(\check{\mathbf{h}}_i)^H & \Re(\check{\mathbf{h}}_i)^H \end{bmatrix}, \tag{4.46}$$

$$\Delta\underline{\widetilde{\mathbf{h}}}_i \triangleq \begin{bmatrix} \Im(\Delta\widetilde{\mathbf{h}}_i)^H & \Re(\Delta\widetilde{\mathbf{h}}_i)^H \end{bmatrix}, \tag{4.47}$$

$$\Pi \triangleq \begin{bmatrix} \mathbf{0}_N & -\mathbf{I}_N \\ \mathbf{I}_N & \mathbf{0}_N \end{bmatrix}. \tag{4.48}$$

where, $\mathbf{0}_N$ and $\mathbf{I}_N$ denote N x N all-zero matrix and identity matrix, respectively.

With the new notations we can express the real and imaginary terms of downlink SINR constraint in $\mathscr{P}$4.7 as:

$$\Im(\widetilde{\mathbf{h}}_i^H\mathbf{w}) = (\underline{\check{\mathbf{h}}}_i + \Delta\underline{\widetilde{\mathbf{h}}}_i)\underline{\mathbf{w}}, \qquad \Re(\widetilde{\mathbf{h}}_i^H\mathbf{w}) = (\underline{\check{\mathbf{h}}}_i + \Delta\underline{\widetilde{\mathbf{h}}}_i)\Pi\underline{\mathbf{w}}. \tag{4.49}$$

From the definition of the error bound, we have $\left\|\Delta\underline{\widetilde{\mathbf{h}}}_i\right\|^2 \leq \varepsilon_{h,i}^2$, the downlink SINR constraint can be guaranteed by the following constraint

$$\max_{\|\Delta\underline{\widetilde{\mathbf{h}}}_i\|^2 \leq \varepsilon_{h,i}^2} \left|\left(\underline{\check{\mathbf{h}}}_i + \Delta\underline{\widetilde{\mathbf{h}}}_i\right)\underline{\mathbf{w}}\right| - \left(\left(\underline{\check{\mathbf{h}}}_i + \Delta\underline{\widetilde{\mathbf{h}}}_i\right)\Pi\underline{\mathbf{w}} - \sqrt{\Gamma_i^{DL}\sigma_i^2}\right)\tan\theta \leq 0, \forall i. \tag{4.50}$$

Hence, by considering the absolute value term, (4.50) is equivalent to the following two constraints

$$\max_{\|\Delta\underline{\widetilde{\mathbf{h}}}_i\|^2 \leq \varepsilon_{h,i}^2} \underline{\check{\mathbf{h}}}_i\underline{\mathbf{w}} + \Delta\underline{\widetilde{\mathbf{h}}}_i\underline{\mathbf{w}} - \left(\underline{\check{\mathbf{h}}}_i + \Delta\underline{\widetilde{\mathbf{h}}}_i\right)\Pi\underline{\mathbf{w}}\tan\theta + \sqrt{\Gamma_i^{DL}\sigma_i^2}\tan\theta \leq 0, \forall i, \tag{4.51}$$

$$\max_{\|\Delta\underline{\widetilde{\mathbf{h}}}_i\|^2 \leq \varepsilon_{h,i}^2} -\underline{\check{\mathbf{h}}}_i\underline{\mathbf{w}} - \Delta\underline{\widetilde{\mathbf{h}}}_i\underline{\mathbf{w}} - \left(\underline{\check{\mathbf{h}}}_i + \Delta\underline{\widetilde{\mathbf{h}}}_i\right)\Pi\underline{\mathbf{w}}\tan\theta + \sqrt{\Gamma_i^{DL}\sigma_i^2}\tan\theta \leq 0, \forall i, \tag{4.52}$$

whose robust formulations are given by

$$\underline{\check{\mathbf{h}}}_i\underline{\mathbf{w}} - \underline{\check{\mathbf{h}}}_i\Pi\underline{\mathbf{w}}\tan\theta + \varepsilon_{h,i}\left\|\underline{\mathbf{w}} - \Pi\underline{\mathbf{w}}\tan\theta\right\| + \sqrt{\Gamma_i^{DL}\sigma_i^2}\tan\theta \leq 0, \forall i, \tag{4.53}$$

$$-\underline{\check{\mathbf{h}}}_i\underline{\mathbf{w}} - \underline{\check{\mathbf{h}}}_i\Pi\underline{\mathbf{w}}\tan\theta + \varepsilon_{h,i}\left\|-\underline{\mathbf{w}} - \Pi\underline{\mathbf{w}}\tan\theta\right\| + \sqrt{\Gamma_i^{DL}\sigma_i^2}\tan\theta \leq 0, \forall i. \tag{4.54}$$

Next, we consider the uplink SINR constraint in problem $\mathscr{P}4.7$. Following equations (4.33) and (4.34) in Section 4.5.1, the uplink SINR constraint can be rewritten as

$$\min_{\Delta\mathbf{f}_j, \Delta\mathbf{G}} \frac{\left(\widetilde{\mathbf{f}} + \widetilde{\Delta\mathbf{f}}\right)^H \mathbf{Z}_j \left(\widetilde{\mathbf{f}} + \widetilde{\Delta\mathbf{f}}\right)}{\left|\mathbf{u}_j^H\check{\mathbf{G}}\mathbf{w} + \mathbf{u}_j^H\Delta\mathbf{G}\mathbf{w}\right|^2 + \sigma_N^2\|\mathbf{u}_j\|^2} \geq \Gamma_j^{UL}, \forall j. \tag{4.55}$$

We note that (4.55) can be simplified to the following constraints

$$\min_{\Delta\mathbf{f}_j} \left(\widetilde{\mathbf{f}} + \widetilde{\Delta\mathbf{f}}\right)^H \mathbf{Z}_j \left(\widetilde{\mathbf{f}} + \widetilde{\Delta\mathbf{f}}\right) - \Gamma_j^{UL}\left(c_j + \sigma_N^2\|\mathbf{u}_j\|^2\right) \geq 0, \forall j, \tag{4.56}$$

$$\max_{\Delta\mathbf{G}} \left|\mathbf{u}_j^H\check{\mathbf{G}}\mathbf{w} + \mathbf{u}_j^H\Delta\mathbf{G}\mathbf{w}\right|^2 - c_j \leq 0, \forall j, \tag{4.57}$$

where $c_j > 0, \forall j$, are introduced as slack variables [84].

Similar procedure as in Section 4.5.1 can be applied to (4.56). By exploiting the S-procedure in Lemma 1, (4.56) can be expanded and converted into a LMI as shown below

$$\begin{bmatrix} \mu_j\mathbf{I}_N + \mathbf{Z}_j & \mathbf{Z}_j\widetilde{\mathbf{f}} \\ \widetilde{\mathbf{f}}^H\mathbf{Z}_j & \widetilde{\mathbf{f}}^H\mathbf{Z}_j\widetilde{\mathbf{f}} - \Gamma_j^{UL}c_j - \Gamma_j^{UL}\sigma_N^2\mathrm{Tr}(\mathbf{U}_j) - \mu_j\varepsilon_f^2 \end{bmatrix} \succeq 0, \forall j. \tag{4.58}$$

We note that by using the fact that $\|\mathbf{x}+\mathbf{y}\|^2 \leq (\|\mathbf{x}\| + \|\mathbf{y}\|)^2$, (4.57) can always be guaranteed by the following constraint

$$\max_{\|\Delta\mathbf{G}\|^2 \leq \varepsilon_G^2} \left(\left|\mathbf{u}_j^H\check{\mathbf{G}}\mathbf{w}\right| + \left|\mathbf{u}_j^H\Delta\mathbf{G}\mathbf{w}\right|\right)^2 - c_j \leq 0, \forall j, \tag{4.59}$$

whose robust formulation is given by

$$\left(\left|\mathbf{u}_j^H\check{\mathbf{G}}\mathbf{w}\right| + \varepsilon_G\left|\mathbf{u}_j^H\mathbf{w}\right|\right)^2 - c_j \leq 0, \forall j. \tag{4.60}$$

Futhermore, we define $\underline{\mathbf{Y}}_j \triangleq \begin{bmatrix} Re(\mathbf{u}_j^H \check{\mathbf{G}}) & -Im(\mathbf{u}_j^H \check{\mathbf{G}}) \\ Im(\mathbf{u}_j^H \check{\mathbf{G}}) & Re(\mathbf{u}_j^H \check{\mathbf{G}}) \end{bmatrix}$ and $\underline{\mathbf{U}}_j \triangleq \begin{bmatrix} Re(\mathbf{u}_j^H) & -Im(\mathbf{u}_j^H) \\ Im(\mathbf{u}_j^H) & Re(\mathbf{u}_j^H) \end{bmatrix}$, thus, the constraint (4.60) can be written in terms of real valued numbers as

$$\left(\left|\underline{\mathbf{Y}}_j \underline{\mathbf{w}}\right| + \varepsilon_G \left|\underline{\mathbf{U}}_j \underline{\mathbf{w}}\right|\right)^2 \leq c_j, \forall j. \tag{4.61}$$

Therefore, the robust optimization problem based on CI is

$$\begin{aligned} \mathscr{P}4.8: \min_{\underline{\mathbf{w}}, P_j, t} \quad & t \\ \text{s.t.} \quad & \widetilde{\underline{\mathbf{h}}}_i \underline{\mathbf{w}} - \widetilde{\underline{\mathbf{h}}}_i \Pi \underline{\mathbf{w}} \tan\theta + \varepsilon_{h,i} \|\underline{\mathbf{w}} - \Pi \underline{\mathbf{w}} \tan\theta\| \leq \sqrt{\Gamma_i^{DL} \sigma_i^2} \tan\theta, \forall i \\ & -\widetilde{\underline{\mathbf{h}}}_i \underline{\mathbf{w}} - \widetilde{\underline{\mathbf{h}}}_i \Pi \underline{\mathbf{w}} \tan\theta + \varepsilon_{h,i} \|-\underline{\mathbf{w}} - \Pi \underline{\mathbf{w}} \tan\theta\| \leq \sqrt{\Gamma_i^{DL} \sigma_i^2} \tan\theta, \forall i, \\ & \begin{bmatrix} \mu_j \mathbf{I}_N + \mathbf{Z}_j & \mathbf{Z}_j \widetilde{\mathbf{f}} \\ \widetilde{\mathbf{f}}^H \mathbf{Z}_j & \widetilde{\mathbf{f}}^H \mathbf{Z}_j \widetilde{\mathbf{f}} - \Gamma_j^{UL} c_j - \Gamma_j^{UL} \sigma_N^2 \mathrm{Tr}(\mathbf{U}_j) - \mu_j \varepsilon_f^2 \end{bmatrix} \succeq 0, \forall j, \\ & \left(\left|\underline{\mathbf{Y}}_j \underline{\mathbf{w}}\right| + \varepsilon_G \left|\underline{\mathbf{U}}_j \underline{\mathbf{w}}\right|\right)^2 \leq c_j, \forall j, \\ & \lambda_a \left(R_a^* - R_a\right) \leq t, \forall a \in \{1,2\}, \\ & \mu_j \geq 0, c_j > 0, \forall j. \end{aligned} \tag{4.62}$$

Note that problem $\mathscr{P}4.8$ is jointly convex with respect to the optimization variables, thus can be optimally solved using standard convex solvers like CVX [132]. After we obtain the optimal $\underline{\mathbf{w}}^*$ and P_j^*, the complex solution $\mathbf{w}^*$ can be obtained from the relation in (4.45).

4.6 Computational Complexity Analysis

In this Section, we mathematically characterize the computational complexity of the conventional and proposed schemes based on MOOP formulations.

4.6.1 Transmit Complexity

We note that the convex MOOP formulations $\mathscr{P}4.1$, $\widetilde{\mathscr{P}4.2}$, $\mathscr{P}4.5$ and $\mathscr{P}4.8$ involve only LMI and second-order cone (SOC) constraints. As such, the problems can be sovled by a standard interior-point method (IPM) [135]. Therefore we can use the

Table 4.1: Complexity Analysis of the MOOP Formulations

MOOP	Complexity Order
$\mathscr{P}4.1$(SDP)	$\mathscr{O}((KN^2+J)[K(2+N^3)+2J+(KN^2+J)(K(2+N^2)+2J)+KN^2+(KN^2+J)^2])$
$\widetilde{\mathscr{P}4.2}$	$\mathscr{O}((KN+J)[3J(1+(KN+J))+2KN^2+(KN+J)^2])$
$\mathscr{P}4.5$	$\mathscr{O}((KN^2+J)[K(N+1)^2+J(NJ+1)^3+J(N^2+1)^3+J+KN^3+(KN^2+J)(K(N+1)^2+J(NJ+1)^2+J(N^2+1)^2+J+KN^2)+(KN^2+J)(KN^2)+(KN^2+J)^2])$
$\mathscr{P}4.8$	$\mathscr{O}((2N+J)[J(NJ+1)^3+J(N+1)^3+J+(2N+J)(J(NJ+1)^2+J+12N^2)+(2N+J)^2)])$

worst-case runtime to analyse the complexity of the conventional and the proposed CI schemes.

Following [136], the complexity of a generic IPM for solving problems like $\mathscr{P}4.1, \widetilde{\mathscr{P}4.2}, \mathscr{P}4.5$ and $\mathscr{P}4.8$ involve the computation of a per-optimization cost. In each iteration, the computation cost is dominated by (i) the formation of the coefficient matrix of the linear system, and (ii) the factorization of the coefficient matrix. The cost of formation of the coefficient (C_{form}) matrix is on the order of

$$C_{form} = \underbrace{n\sum_{a=1}^{A} k_a^3 + n^2 \sum_{a=1}^{A} k_a^2}_{\text{due to the LMI}} + \underbrace{n\sum_{a=A+1}^{B} k_a^2}_{\text{due to the SOC}},$$

while the cost of factorizing (C_{fact}) is on the order of $C_{fact} = n^3$ ($n =$ number of decision variables). Hence, the total computation cost per optimization is on the order of $C_{form} + C_{fact}$ [136]. We assume for the sake of simplicity that the decision variables in $\mathscr{P}4.1, \widetilde{\mathscr{P}4.2}, \mathscr{P}4.5$ and $\mathscr{P}4.8$ are real-valued.

Hence, using these concepts, we now analyse the comutational complexity of $\mathscr{P}4.1, \widetilde{\mathscr{P}4.2}, \mathscr{P}4.5$ and $\mathscr{P}4.8$. First we consider SDP formulation of $\mathscr{P}4.1$, which has K LMI (trace) constraints of size 1, three J LMI (trace) constraints of size 1, K SOC constraints of size N and K LMI (trace) constraints of size N. Therefore,

the complexity of the SDP formulation of $\mathscr{P}4.1$ is on the order shown in the first row of Table I. Similarly, we can determine the complexity order of the formulations $\widetilde{\mathscr{P}4.2}$, $\mathscr{P}4.5$ and $\mathscr{P}4.8$ as shown in Table I, respectively. From Table I, we can show that the proposed MOOP formulation $\widetilde{\mathscr{P}4.2}$ has lower complexity than the SDP formulation of $\mathscr{P}4.1$ since it has lower order of variables to compute i.e lower cost of factorization (C_{fact}). Also, we can straightforwardly show that for the robust MOOP, the proposed formulation $\mathscr{P}4.8$ has a lower complexity than the conventional formulation $\mathscr{P}4.5$ since $\mathscr{P}4.5$ involves a more complicated set of constraints (5 LMI constraints and 1 SOC constraint). This is also consistent with our simulation results in the following Section.

At this point, we emphasize that as the MOOP formulations in $\mathscr{P}4.1$ and $\mathscr{P}4.5$ are data independent, they only need to be applied once during each channel coherence time. While as the proposed MOOP formulations in $\widetilde{\mathscr{P}4.2}$ and $\mathscr{P}4.8$ are data dependent, they need to be run on a symbol by symbol basis. In the following section we compare the resulting transmit complexity of conventional and proposed MOOP approaches for both slow and fast fading scenarios, and show that the average execution time per downlink frames is comparable for both techniques.

4.6.2 Receiver Complexity

At the receiver side, for the case of the conventional beamforming, the downlink users in our FD system scenario need to equalize the composite channel $\mathbf{h}_i^H \mathbf{w}_i^*$ to recover their data symbols, where $\{\mathbf{w}_i^*\}_{i=1}^K$ is the optimal solution of $\mathscr{P}4.1$. For the case of the proposed CI scheme, since the received symbols already lie in the constructive region of the constellation as shown in Fig. 4.2 and Fig. 4.3, equalization is not required by the downlink users. This automatically translates to reduced complexity at the receiver. Accordingly, this implies that CSI is not required for detection at the downlink users for the proposed CI scheme. Thus, depending on the signaling and pilots already involved for the SINR estimation, the proposed CI scheme may lead to further savings in training time and overhead. Most importantly, this makes the proposed scheme resistant to any quantization errors from the CSI acquisition at the receiver.

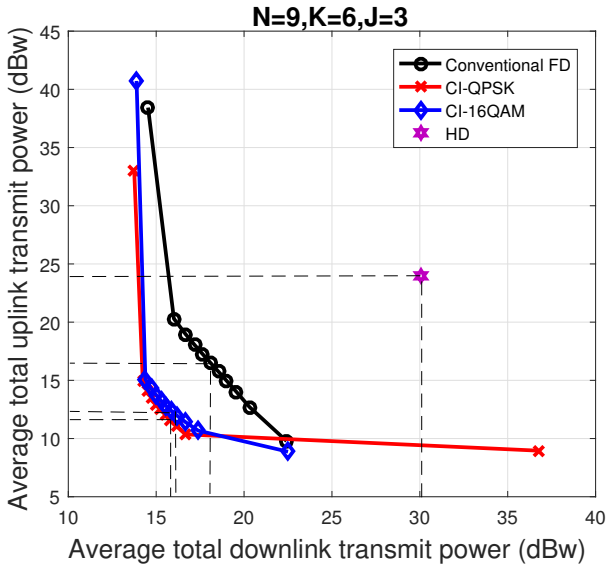

Figure 4.4: Weighted optimization plot for the proposed scheme versus the conventional scheme N = 9, K = 6, J = 3.

4.7 Simulation Results

In this section, we investigate the performance of our proposed system through simulations. We model all channels as independent and identically distributed Rayleigh fading for both the perfect and imperfect CSI cases. Systems with QPSK and 16QAM modulation are considered while it is clear that the benefit extends to any lower or higher order modulation. For comparison in every scenario, we compare the proposed technique, constructive interference (CI) with the conventional case i.e. when all interference is treated as harmful signal [115, 116]. We use $N \times K \times J$ to denote an FD radio BS with N antennas, K downlink users and J uplink users, respectively.

4.7.1 Uplink-Downlink Power Weighted Optimization

In Fig. 4.4, we investigate the weighted optimization between the downlink and uplink total transmit power for the case of $N = 9, K = 6, J = 3$ antennas. The plot is obtained by solving problem $\mathscr{P}4.1$, $\widetilde{\mathscr{P}4.2}$ and $\mathscr{P}4.3$ for the conventional and CI cases, respectively, for $0 \leq \lambda_a \leq 1, a \in (1,2)$ with a step size of 0.1. Note that λ_a determines the priority of the *a-th* objective. We assume the same required SINR for all downlink users to be $\Gamma_i^{DL} = 15dB$, $\Gamma_i^{UL} = 15dB$ for all uplink users, where $\varepsilon_G =$

0.1. It can be seen from the plot that there is a trade-off between the two objectives (uplink and downlink) by varying the priority weight λ_a. We note that, although, the downlink transmit power is not directly dependent on the uplink transmit power, this trade-off is as a result of the link between the downlink and uplink transmit power through the SI term. In addition, we would like to emphasize the usefulness of the uplink and downlink SINR constraints in the optimizations to ensure the required QoS is achieved even in critical scenarios such as when the uplink power is low or the SI is high. Thus, for comparison, making reference to the point when $\lambda_a = 0.5$ as indicated by the dotted lines, we can observe that the CI scheme has power savings of 4dB and 2.8dB for uplink and downlink users, respectively, for QPSK modulation. Accordingly, for 16QAM modulation, we can observe power savings of 3.5dB and 2.5dB for uplink and downlink users, respectively. Note that the proposed schemes are only outperformed by the conventional beamforming for the case $\lambda_1 = 0, \lambda_2 = 1$, where all priority is given to the uplink PM problem, where interference exploitation does not apply. The figure also depicts the performance of a HD system as a reference. Here the total uplink and downlink data rate of HD is set equal to the one for FD, which requires that the individual uplink and downlink data rate requirements are double the ones for the FD case, due to the slotted HD transmission. It can be seen that the HD operation results in increased uplink and downlink power to achieve the same total rate, which highlights the effectiveness of the FD approach.

In Fig. 4.5, we plot the case when we have $N = 8, K = 6, J = 3$. The same trend can be seen with Fig. 4.4, where we have when $\lambda_a = 0.5$, as indicated by the dotted lines, for QPSK modulation power savings of about 9dB and 2.1dB for the uplink and downlink users, respectively. For 16QAM modulation, we have power savings of about 7.5dB and 1.6dB for the uplink and downlink users, respectively. Again, it can be seen that the FD transmission outperforms the HD benchmark. Fig. 4.4 shows the scenario when the number of antennas at the FD BS is equal to the total number of uplink and downlink users, while Fig. 4.5 shows the scenario when there is one less antenna at the FD BS to serve the uplink and downlink users. This

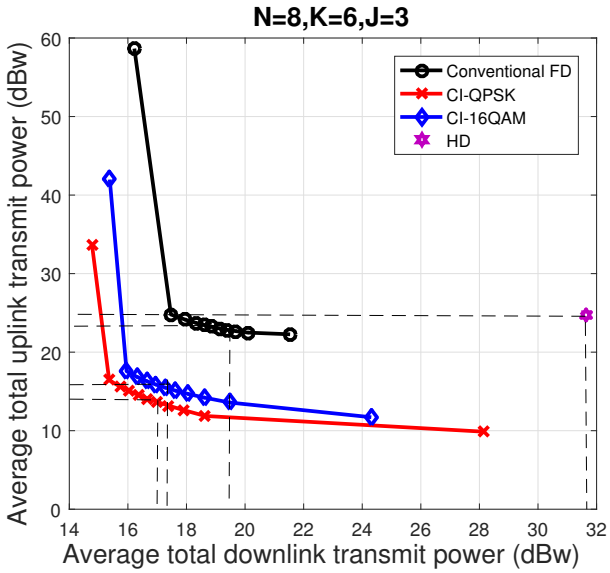

Figure 4.5: Weighted optimization plot for the proposed scheme versus the conventional scheme N = 8, K = 6, J = 3.

implies a lower degree of freedom compared to the scenario in Fig. 4.4, and is in fact a critical scenario where conventional approaches break down and lead to highly inefficient solutions. Thus, leading to increased uplink and dowlink power consumption compared to the CI scheme.

In Fig. 4.6, we show a scenario where we have equal number of antennas at the FD radio BS and at the users $N = K = J = 6$. With this setup, when $\lambda_a = 0.5$, we can see for QPSK modulation uplink and downlink user power savings of about 17dB and 2.4dB, respectively, and about 12.1dB and 0.8dB, respectively, for 16QAM modulation. The reason is because for $N = K = J = 6$ the problem is more restricted in the optimization variable dimensions and the conventional scheme in this scenario leads to greatly increased uplink and downlink powers while for the CI scheme this scenario can be accommodated and has higher feasibility so consumes lower power. Again, it can be observed that the FD transmission outperforms the HD benchmark. These results highlight a key advantage of the proposed scheme over the conventional approaches.

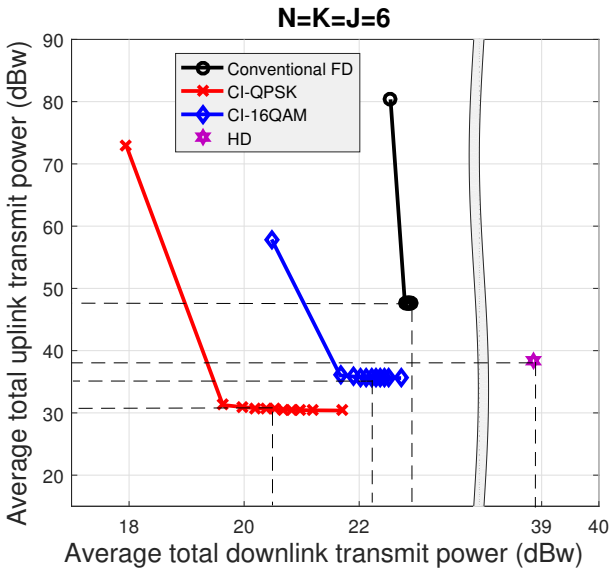

Figure 4.6: Weighted optimization plot for the proposed scheme versus the conventional scheme N = 6, K = 6, J = 6.

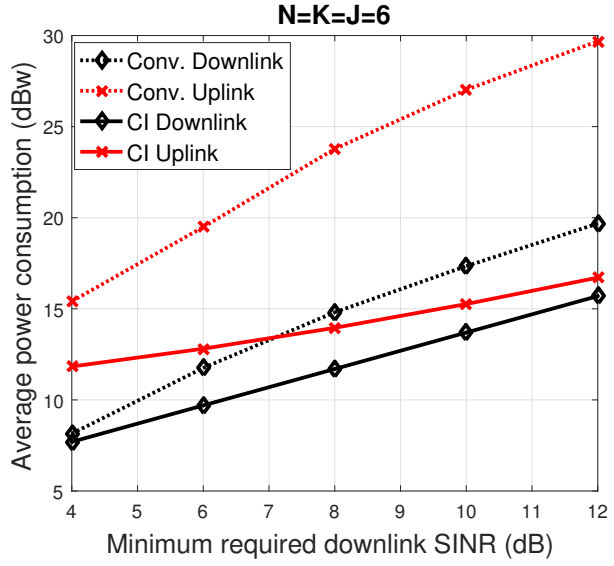

Figure 4.7: Average power consumption versus minimum required downlink SINR when $\lambda_1 = 0.9, \lambda_2 = 0.1, \varepsilon_G = 0.1$ and $\Gamma^{UL} = 0$dB for QPSK modulation

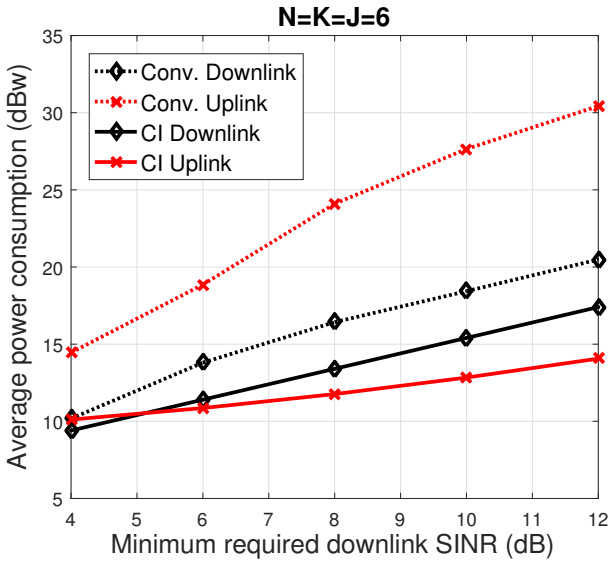

Figure 4.8: Average power consumption versus minimum required downlink SINR when $\lambda_1 = 0.1, \lambda_2 = 0.9, \varepsilon_G = 0.1$ and $\Gamma^{UL} = 0$dB for QPSK modulation

4.7.2 Average Transmit Power versus Minimum Required SINR

In Fig. 4.7 and Fig. 4.8, we investigate the power consumption of the downlink and uplink users for different minimum required downlink SINR (Γ_i^{DL}). For both plots we assume a minimum required uplink SINR $\Gamma_j^{UL} = 0dB$ for all uplink users. In Fig. 4.7, we select $\lambda_1 = 0.9$ and $\lambda_2 = 0.1$, which gives higher priority to the total downlink transmit power minimization problem. It can be observed that both the uplink and downlink power consumption increases with increase in Γ_i^{DL}. This is because an increase in the downlink SINR requirement translates to increase in downlink transmit power and hence increase in the SI power. Therefore, the uplink users have to transmit with a higher power to meet their QoS requirement (Γ_j^{UL}). However, we can still see power savings of up to 12dB and 4dB for the uplink and downlink users, respectively, for the CI scheme compared to the conventional scheme. Also, we note that while CI is applied to only the downlink users, more power is saved for the uplink users than the downlink users. This is because with CI the total downlink transmit power is reduced and this directly reduces the residual SI power at the FD BS. Accordingly, the constructive interference power has been traded off for both uplink and downlink power savings. The same trend can be seen in the Fig. 4.8, where $\lambda_1 = 0.1$ and $\lambda_2 = 0.9$. It can be observed that in this scenario

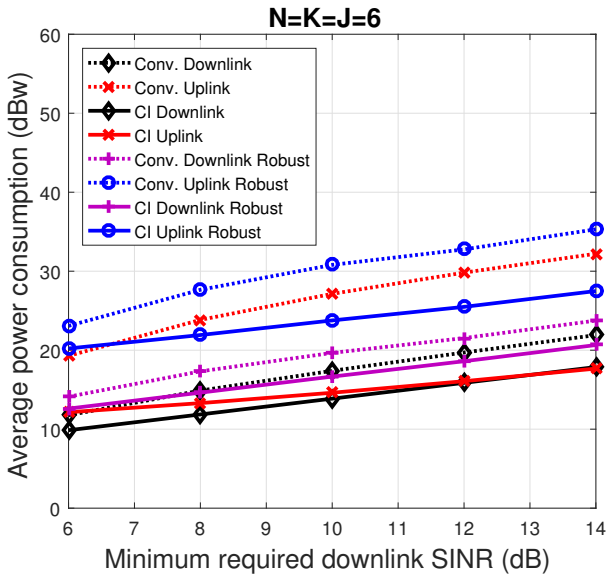

Figure 4.9: Average power consumption versus minimum required downlink SINR when $\lambda_1 = 0.9, \lambda_2 = 0.1, \Gamma^{UL} = 0$dB and $\varepsilon_h = \varepsilon_f = \varepsilon_G = 0.1$ for QPSK modulation

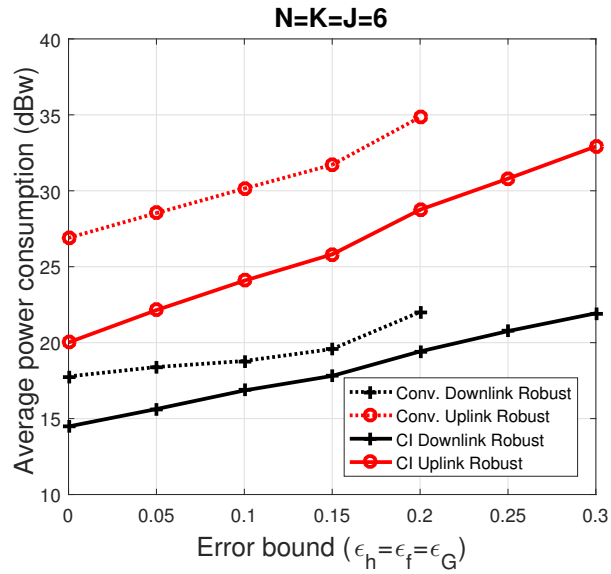

Figure 4.10: Average power consumption versus error bounds when $\lambda_1 = 0.9, \lambda_2 = 0.1, \Gamma^{UL} = 0dB$ and $\Gamma^{DL} = 10dB$ for QPSK modulation

since we give higher priority to the uplink power minimization problem, we have higher power savings for the uplink users and lower power savings for the downlink users compared to the Fig. 4.7.

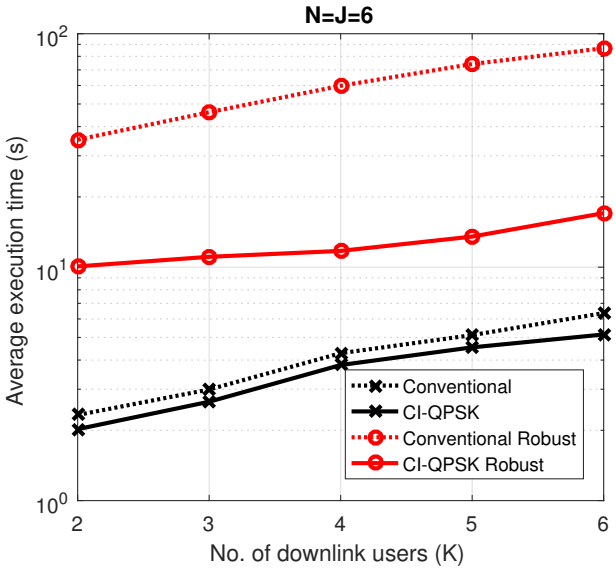

Figure 4.11: Average execution time per optimization versus number of downlink users with $N = J = 6$ when $\lambda_1 = 0.9, \lambda_2 = 0.1, \Gamma^{UL} = 0$dB, $\Gamma^{DL} = 5$dB and $\varepsilon_h = \varepsilon_f = \varepsilon_G = 0.01$

4.7.3 MOOP with Imperfect CSI

In Fig. 4.9 and 4.10, we investigate the performance of the proposed CSI-robust CI scheme for $N = K = J = 6$, we select $\lambda_1 = 0.9$ and $\lambda_2 = 0.1$. Fig. 4.9 shows the Average power consumption for the uplink and downlink users when the error bounds $\varepsilon_h = \varepsilon_f = \varepsilon_G = 0.1$. It can be seen that the CI scheme shows better performance than the conventional scheme with power savings of 8dB and 3dB for the uplink and downlink users, respectively. This is also shown in Fig. 4.10, which shows the average power consumption with increasing error bounds. It can be seen that feasible solutions can only be found for $\varepsilon_h = \varepsilon_f = \varepsilon_G \leq 0.2$. Besides, even if feasible results could be found, significant amount of power will be consumed as can be seen for error bound values between 0.15 and 0.2 for both uplink and downlink users.

4.7.4 Complexity

In Fig. 4.11, we compare the Average execution time per optimization of the conventional scheme and the proposed CI scheme for different number of downlink users (K) with $N = J = 6$. We fixed $\lambda_1 = 0.9, \lambda_2 = 0.1, \Gamma^{UL} = 0$dB, $\Gamma^{DL} = 5$dB and $\varepsilon_h = \varepsilon_f = \varepsilon_G = 0.01$. This plot shows the complexity comparison of the proposed

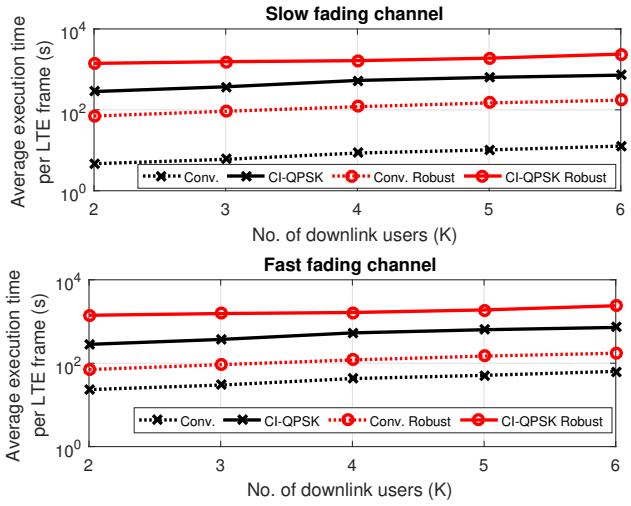

Figure 4.12: Average execution time versus number of downlink users for slow/fast fading channels with $N = J = 6$ when $\lambda_1 = 0.9, \lambda_2 = 0.1, \Gamma^{UL} = 0$dB, $\Gamma^{DL} = 5$dB and $\varepsilon_h = \varepsilon_f = \varepsilon_G = 0.01$.

and conventional schemes in terms of average execution time. This is computed by generating K random QPSK symbols for 100,000 channel realizations. Thus, taking into consideration 100,000 random symbol combinations over 100,000 iterations. We kindly want to emphasize that the execution time is not only dependent on the symbol combinations, but also on the channel realization and the problem formulation, i.e. the geometry and number of constraints, stemming from the number of users, antennas, e.t.c. It can be seen that for the perfect CSI case, the proposed CI scheme takes 83% of time taken by the conventional scheme. While for the imperfect CSI case, the proposed CI scheme takes about 28% of the time taken by the conventional scheme. This is because the conventional approach involves a more complicated set of constraints, hence, more computational cost as shown in Section 4.6.1 above. Besides, the proposed MOOP ($\mathscr{P}$4.8) formulation involves a multicast approach which reduces the number variables to compute.

As we have noted above however, the proposed data dependent optimization needs to be run on a symbol-by-symbol basis. To obtain a fairer comparison, we plot in Fig. 4.12 the average execution time per frame versus the number of downlink users for slow and fast fading channels. Here, we assume the LTE Type 2 TDD frame structure [137], where each frame is subdivided to 10 subframes each with

a duration $1ms$ and containing 14 symbol-time slots. Accordingly, we assume that for fast fading the channel is constant for the duration of a subframe with a number of symbols per coherence time $N_{coh} = 14$, while for slow fading we assume a coherence time equal to 5 subframes with $N_{coh} = 70$ [137]. The results for both slow and fast fading channels show the end complexity of the proposed CI approaches are comparable to those with the conventional approaches. Accordingly, and in conjunction with the performance improvements shown in the previous results, it can be seen that the proposed schemes provide a much more favorable performance complexity trade-off w.r.t. conventional interference mitigation.

4.8 Joint Iterative Optimization Schemes in FD Systems

In this Section, we design an iterative optimization algorithm to improve the proposed approach in Section 4.4. Sections 4.3 and 4.4 limit the MOOs to the downlink beamforming vectors and the uplink power allocation, employing a closed form ZF detector for the uplink. In this Section we aim to further increase the power savings in multiuser FD communication systems via an iterative algorithm that jointly optimizes the receive beamformer, transmit beamformer and the uplink power, respectively, which increases the degrees of freedom in the optimization, and allows a scalable performance-complexity trade-off. We provide simulation results and discussions to show the effectiveness of the proposed algorithm compared to the approach in Section 4.3 and 4.4.

4.8.1 Proposed Joint MOOP for Interference Cancellation

First, we study the conventional MOOP in Section 4.3 ($\mathscr{P}4.1$) where all interference are treated as harmful signals, by jointly optimizing all the transmit beamforming vectors $\mathbf{w}_i$, the receive beamfoming vectors $\mathbf{u}_j$ and the uplink transmit power P_j, respectively. Following the conventional MOOP formulation in $\mathscr{P}4.1$, the proposed

joint MOOP is written as

$$\begin{aligned} \mathscr{P}4.9: \quad & \min_{\mathbf{w}_i,P_j,\mathbf{u}_j} \quad \max_{a=1,2} \{\lambda_a (R_a^* - R_a)\} \\ \text{s.t.} \quad & \text{E1}: \frac{|\, \mathbf{h}_i^H \mathbf{w}_i \,|^2}{\sum_{k\neq i}^{K} |\, \mathbf{h}_i^H \mathbf{w}_k \,|^2 + \sigma_i^2} \geq \Gamma_i^{DL}, \forall i, \\ & \text{E2}: \min_{\Delta\mathbf{G}} \frac{P_j |\, \mathbf{f}_j^H \mathbf{u}_j \,|^2}{I_j + \sigma_N^2 \|\mathbf{u}_j\|^2} \geq \Gamma_j^{UL}, \forall j, \end{aligned} \tag{4.63}$$

where, $I_j = \sum_{n\neq j}^{J} P_n \mid \mathbf{f}_n^H \mathbf{u}_j \mid^2 + \sum_{k=1}^{K} \mid \mathbf{u}_j^H (\check{\mathbf{G}} + \Delta\mathbf{G}) \mathbf{w}_k \mid^2$. Problem $\mathscr{P}4.9$ is a non-convex problem due to the SINR constraints E1 and E2. To tackle the non-convexity, we transform $\mathscr{P}4.9$ as a semi-definite program (SDP) problem given by

$$\widetilde{\mathscr{P}4.9}: \min_{\mathbf{W}_i,P_j,\mathbf{U}_j} \max_{a=1,2} \{\lambda_a (R_a^* - R_a)\}$$

s.t.

$$\begin{aligned} & \widetilde{\text{E1}}: \frac{\text{Tr}\left\{\mathbf{H}_i^H \mathbf{W}_i\right\}}{\text{Tr}\left\{\mathbf{H}_i^H \mathbf{W}_k\right\} + \sigma_i^2} \geq \Gamma_i^{DL}, \forall i, \\ & \widetilde{\text{E2a}}: \frac{P_j \text{Tr}\left\{\mathbf{F}_j^H \mathbf{U}_j\right\}}{\sum_{n\neq j}^{J} P_n \text{Tr}\left\{\mathbf{F}_n^H \mathbf{U}_j\right\} + s_j^{SI} + \sigma_N^2 \text{Tr}\left\{\mathbf{U}_j\right\}} \geq \Gamma_j^{UL}, \forall j \\ & \widetilde{\text{E2b}}: \max_{\Delta\mathbf{G}} \text{Tr}\left\{ \left(\check{\mathbf{G}} + \Delta\mathbf{G}\right) \sum_{k=1}^{K} \mathbf{W}_k \left(\check{\mathbf{G}} + \Delta\mathbf{G}\right)^H \mathbf{U}_j \right\} - s_j^{SI} \leq 0, \forall j, \end{aligned} \tag{4.64}$$

where, $\mathbf{W}_k = \mathbf{w}_k \mathbf{w}_k^H, \mathbf{F}_j = \mathbf{f}_j \mathbf{f}_j^H$ and $\mathbf{U}_j = \mathbf{u}_j \mathbf{u}_j^H$. Here, we rewrite constraint E2 into two constraints by introducing slack variables $s_j^{SI} > 0, \forall j$, respectively. Following Lemma 1, the constraint $\widetilde{\text{E2b}}$ can be expanded, simplified and converted to LMI in

a similar fashion as in Section 4.5.1. Hence, the transformed $\mathscr{P}4.9$ is given as

$$
\begin{aligned}
\mathscr{P}4.10: \min_{\mathbf{W}_i, P_j, \mathbf{U}_j, t, \rho, s_j^{SI}} \quad & t \\
\text{s.t. } \widetilde{\text{A1}}: \; & \text{Tr}\left\{\mathbf{H}_i^H \mathbf{W}_i\right\} - \Gamma_i^{DL} \text{Tr}\left\{\mathbf{H}_i^H \mathbf{W}_k\right\} \geq \Gamma_i^{DL} \sigma_i^2, \forall i, \\
\widetilde{\text{A2a}}: \; & P_j \text{Tr}\left\{\mathbf{F}_j^H \mathbf{U}_j\right\} - \Gamma_j^{UL} \left(\sum_{n \neq j}^{J} P_n \text{Tr}\left\{\mathbf{F}_n^H \mathbf{U}_j\right\} + s_j^{SI} \right) \geq \Gamma_j^{UL} \sigma_N^2 \text{Tr}\left\{\mathbf{U}_j\right\}, \forall j, \\
\widetilde{\text{A2b}}: \; & \begin{bmatrix} \rho \mathbf{I} - \left(\mathbf{U}_j \otimes \sum_{k=1}^{K} \mathbf{W}_k\right) & -\left(\mathbf{U}_j \otimes \sum_{k=1}^{K} \mathbf{W}_k\right) \check{\mathbf{g}} \\ -\check{\mathbf{g}}^H \left(\mathbf{U}_j \otimes \sum_{k=1}^{K} \mathbf{W}_k\right) & s_j^{SI} - \check{\mathbf{g}}^H \left(\mathbf{U}_j \otimes \sum_{k=1}^{K} \mathbf{W}_k\right) \check{\mathbf{g}} - \rho \varepsilon_G^2 \end{bmatrix} \succeq 0, \forall j, \\
& \text{A3}: \lambda_a \left(R_a^* - R_a\right) \leq t, \forall a \in \{1,2\}, \\
& \text{A4}: \mathbf{W}_i \succeq 0, \forall i, \quad \text{A5}: \mathbf{U}_j \succeq 0, \forall j.
\end{aligned}
\tag{4.65}
$$

where, t is an auxiliary variable.

The problem $\mathscr{P}4.10$ is still non-convex due to the joint optimization of P_j and $\mathbf{U}_j$ in constraint $\widetilde{\text{E2a}}$. It is very difficult to obtain a closed-form solution that jointly optimizes $\mathbf{W}_i$, P_j and $\mathbf{U}_j, \forall i, j$, hence, to solve $\mathscr{P}4.10$, we propose a two-step iterative process. In the first step, we initialize a feasible $\mathbf{U}_j$ to solve problem $\mathscr{P}4.10$ obtaining the optimal values of $\mathbf{W}_i$ and P_j, using CVX [132]. In the second step, we solve problem $\mathscr{P}4.11$ below using the solution from the first step to obtain the optimal $\mathbf{U}_j^*$. We summarize the overall procedure in Algorithm 4.1.

Algorithm 4.1 Procedure for solving the problem $\mathscr{P}4.10$

1: **Input** : $\mathbf{h}_i, \mathbf{f}_j, \check{\mathbf{G}}, \Gamma_j^{DL}, \Gamma_j^{UL}, \sigma_i, \sigma_N$.
2: *Initialise:* $n = 0, \mathbf{U}_\mathbf{j}^{(\mathbf{0})} = \mathbf{u}_j \mathbf{u}_j^H$,
repeat,
3: $n = n + 1$,
4: solve the problem $\mathscr{P}4.10$ to obtain $\mathbf{W}_i$ and P_j,
5: use the solution from step 4 to solve the problem $\mathscr{P}4.11$ to obtain $\mathbf{U}_\mathbf{j}^{(\mathbf{n})}$,
6: until convergence.
7: **Output** : $\mathbf{W}_i^*$ and $P_j^*, \forall i, j$.

$$\begin{aligned}\mathscr{P}4.11: \min_{\mathbf{U}_j,\tau,\rho,s_j^{SI}} \ & \tau \\ \text{s.t.} \quad & \widetilde{\text{E2a}}, \quad \widetilde{\text{E2b}}, \\ & \mathbf{U}_j \succeq 0, \forall j, \\ & \lambda_a \left(R_a^* - R_a\right) \leq \tau, \forall a \in \{1,2\}.\end{aligned} \tag{4.66}$$

In problem $\mathscr{P}4.11$, we ignore constraint $\widetilde{\text{E1}}$ since it is independent of $\mathbf{U}_j$. Note that the problem $\mathscr{P}4.10$ and $\mathscr{P}4.11$ are relaxed form of $\mathscr{P}4.9$. While it is difficult to prove the rank-one solution, we have observed over multiple simulations, problem $\mathscr{P}4.10$ and $\mathscr{P}4.11$ always return rank-one solution $(\mathbf{W}_i, \forall i)$ and $(\mathbf{U}_j, \forall j)$. Nevertheless, in the unlikely case of a non rank-one solution the optimal solutions can always be obtained by randomization technique as in [134], such that $\mathbf{W}_i = \mathbf{w}_i \mathbf{w}_i^H, \forall i$ and $\mathbf{U}_j = \mathbf{u}_j \mathbf{u}_j^H, \forall j$, respectively.

4.8.2 Proposed Joint MOOP for Interference Exploitation

Here, we study the CI based MOOP in Section 4.4 where interference is exploited, by jointly optimizing all the transmit beamforming vectors $\mathbf{w}_i$, the receive beamfoming vectors $\mathbf{u}_j$ and the uplink transmit power P_j, respectively. Following the conventional MOOP formulation in $\mathscr{P}4.2$, the proposed joint MOOP is expressed as

$$\begin{aligned}&\mathscr{P}4.12: \min_{\mathbf{w}_i,P_j,\mathbf{u}_j,t} \ t \\ &\text{s.t. F1}: \left|\Im\left(\mathbf{h}_i^H \sum_{k=1}^{K} \mathbf{w}_k e^{j(\phi_k-\phi_i)}\right)\right| \leq \left(\Re\left(\mathbf{h}_i^H \sum_{k=1}^{K} \mathbf{w}_k e^{j(\phi_k-\phi_i)}\right) - \sqrt{\Gamma_i^{DL}\sigma_i^2}\right)\tan\theta, \forall i, \\ &\text{F2}: \min_{\Delta\mathbf{G}} \frac{P_j \left|\mathbf{f}_j^H \mathbf{u}_j\right|^2}{I_j^{PSK} + \sum_{k=1}^{K} \left|\mathbf{u}_j^H (\check{\mathbf{G}} + \Delta\mathbf{G}) \mathbf{w}_k e^{j(\phi_k-\phi_1)}\right|^2} \geq \Gamma_j^{UL}, \forall j, \\ &\text{F3}: \lambda_a \left(R_a^* - R_a(\mathbf{w}_i, P_j)\right) \leq t, \forall a \in \{1,2\},\end{aligned} \tag{4.67}$$

where t is an auxiliary variable, and $I_j^{PSK} = \sum_{n\neq j}^{J} P_n \left|\mathbf{f}_n^H \mathbf{u}_j\right|^2 + \sigma_N^2 \|\mathbf{u}_j\|^2$. Following similar procedure as in Section 4.4, the joint MOOP $\mathscr{P}4.12$ can be transformed to

$$
\begin{aligned}
&\mathscr{P}4.13: \min_{\mathbf{w}_i, P_j, \mathbf{u}_j, t, s_j^{SI}} \quad t \\
&\text{s.t.} \\
&\text{F1}: \left|\Im\left(\mathbf{h}_i^H \sum_{k=1}^{K} \mathbf{w}_k e^{j(\phi_k-\phi_i)}\right)\right| \leq \left(\Re\left(\mathbf{h}_i^H \sum_{k=1}^{K} \mathbf{w}_k e^{j(\phi_k-\phi_i)}\right) - \sqrt{\Gamma_i^{DL}\sigma_i^2}\right)\tan\theta, \forall i, \\
&\widetilde{\text{F2a}}: P_j \left|\mathbf{f}_j^H \mathbf{u}_j\right|^2 \geq \Gamma_j^{UL}\left(\sum_{n\neq j}^{J} P_n \left|\mathbf{f}_n^H \mathbf{u}_j\right|^2 + s_j^{SI} + \sigma_N^2\|\mathbf{u}_j\|^2\right), \forall j, \\
&\widetilde{\text{F2b}}: \sum_{k=1}^{K}\left(\left|\mathbf{u}_j^H \check{\mathbf{G}} \mathbf{w}_k e^{j(\phi_k-\phi_1)}\right| + \varepsilon_G \left|\mathbf{u}_j^H \mathbf{w}_k e^{j(\phi_k-\phi_1)}\right|\right)^2 \leq s_j^{SI}, \forall j, \\
&\text{F3}: \lambda_a\left(R_a^* - R_a\right) \leq t, \forall a \in \{1,2\}.
\end{aligned}
\tag{4.68}
$$

Problem $\mathscr{P}4.13$ is still non-convex due to the joint optimization of P_j and $\mathbf{u}_j$ in constraint $\widetilde{\text{F2a}}$. Hence, we propose a two-step iterative process to jointly optimize $\mathbf{w}_i$, P_j and $\mathbf{u}_j, \forall i, j$. In the first step, we initialize a feasible $\mathbf{u}_j, \forall j$ to solve $\mathscr{P}4.13$ to obtain the optimal values of $\mathbf{w}_i$ and P_j using CVX [132]. Then we use the values obtained from the first step to solve $\mathscr{P}4.14$ below to obtain the optimal values of the $\mathbf{U}_j{}^*, \forall j$. The iterative process is summarized in Algorithm 4.2.

$$
\begin{aligned}
&\mathscr{P}4.14: \min_{\mathbf{U}_j, \tau, \rho, s_j^{SI}} \quad \tau \\
\text{s.t.} \quad & P_j \text{Tr}\left\{\mathbf{F}_j^H \mathbf{U}_j\right\} - \Gamma_j^{UL}\left(\sum_{n\neq j}^{J} P_n \text{Tr}\left\{\mathbf{F}_n^H \mathbf{U}_j\right\} + s_j^{SI}\right) \geq \Gamma_j^{UL}\sigma_N^2 \text{Tr}\left\{\mathbf{U}_j\right\}, \forall j, \\
& \begin{bmatrix} \rho\mathbf{I} - \left(\mathbf{U}_j \otimes \sum_{k=1}^{K} \mathbf{W}_k\right) & -\left(\mathbf{U}_j \otimes \sum_{k=1}^{K} \mathbf{W}_k\right)\check{\mathbf{g}} \\ -\check{\mathbf{g}}^H\left(\mathbf{U}_j \otimes \sum_{k=1}^{K} \mathbf{W}_k\right) & s_j^{SI} - \check{\mathbf{g}}^H\left(\mathbf{U}_j \otimes \sum_{k=1}^{K} \mathbf{W}_k\right)\check{\mathbf{g}} - \rho\varepsilon_G^2 \end{bmatrix} \succeq 0, \forall j, \\
& \lambda_a\left(R_a^* - R_a\right) \leq \tau, \forall a \in \{1,2\}, \mathbf{U}_j \succeq 0, \forall j.
\end{aligned}
\tag{4.69}
$$

Note that the optimal $\mathbf{u}_j^*$ can be obtained by randomization as in [134].

Algorithm 4.2 Procedure for solving the problem $\mathscr{P}4.13$

1: **Input** : $\mathbf{h}_i, \mathbf{f}_j, \check{\mathbf{G}}, \Gamma_j^{DL}, \Gamma_j^{UL}, \sigma_i, \sigma_N$.
2: *Initialize:* $n = 0, \mathbf{u}_j$,
repeat,
3: $n = n + 1$,
4: solve the problem $\mathscr{P}4.13$ to obtain $\mathbf{w}_i$ and P_j,
5: use the solution from step 4 to solve the problem $\mathscr{P}4.14$ to obtain $\mathbf{U}_\mathbf{j}^{(\mathbf{n})}$,
6: until convergence.
7: **Output** : $\mathbf{w}_i^*$ and $P_j^*, \forall i, j$.

4.8.3 Numerical Results

In this subsection, we investigate the performance of our proposed iterative scheme through simulations. We model all channels as independent and identically distributed Rayleigh fading for systems with QPSK modulation are considered while it is clear that the benefit extends to any higher order modulation. For comparison in every scenario, we compare the iterative approach with the approach in Sections 4.3 and 4.4 (ZF) for both CI and conventional cases.

In Fig. 4.13a, we show the average power consumption versus the minimum required downlink SINR for QPSK modulated signals. This clearly shows power gains of up to 4dB and 2dB for conventional and CI schemes, respectively, of the proposed iterative approach for uplink users compared to the ZF approach in Sections 4.3 and 4.4. Similarly, less than 1dB power gains can be seen for the downlink users. In Fig. 4.13b, we compare the complexity of the two approaches, which shows that the iterative approach has a much high complexity in terms of running time until convergence. These two results clearly highlights the trade-off between the two proposed approaches in terms of performance and complexity, respectively.

4.9 Summary

In this chapter, we studied the application of the interference exploitation concept to a MU-MIMO system with a FD radio BS. The optimization problem was formulated as a MOOP via the weighted Tchebycheff method. The MOOP was formulated for both PSK and QAM modulated signals by adapting the decision thresholds in both cases to accommodate for constructive interference and by assuming zero-forcing

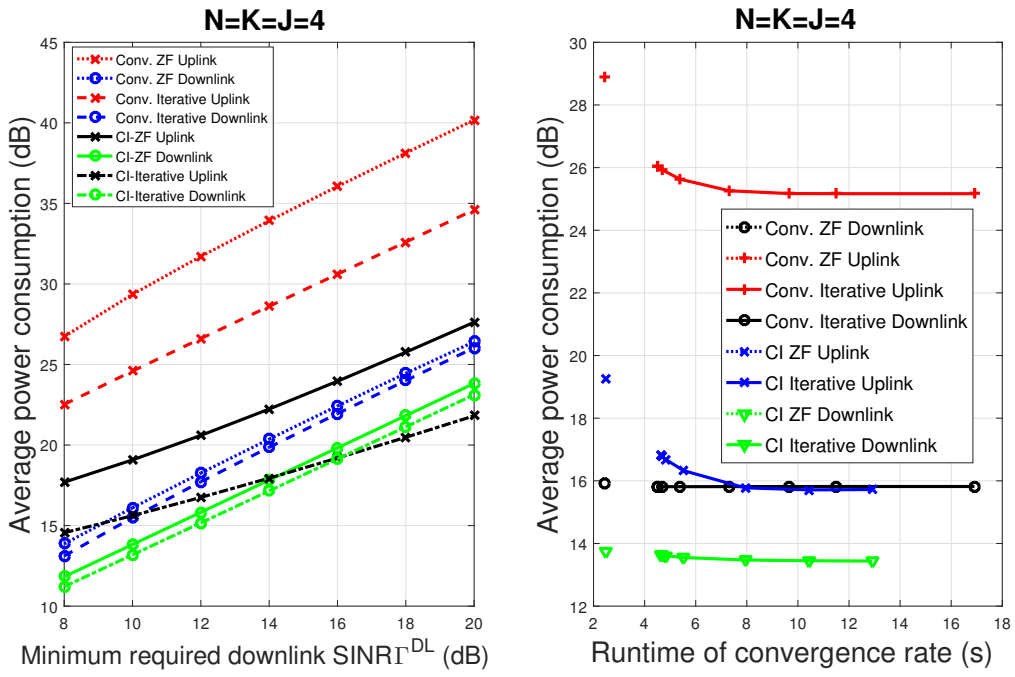

Figure 4.13: Average power consumption versus a) downlink SINR for $\Gamma^{UL} = 5$dB and b) runtime of convergence rate for $\Gamma^{UL} = 5$dB and $\Gamma^{DL} = 10$dB, respectively, for QPSK modulation.

for the receive beamformer. The CI scheme was also extended to robust designs for imperfect downlink, uplink and SI CSI with bounded CSI errors. Simulation results proved the significant power savings of the CI scheme over the conventional scheme in every scenario. More importantly, we have shown that through the FD MOOP formulation, constructive interference power can be traded off for both uplink and downlink power savings. To further improve the power savings, we proposed a two-step iterative algorithm. The algorithm jointly optimizes the transmit beamformer, receive beamformer and uplink transmit power, providing a step forward from employing ZF receive beamforming. Simulations results show improved power savings compared to the ZF approaches in both conventional and CI cases at the expense of a scalable complexity increase.

Chapter 5

Robust Energy Harvesting FD Transmission

This chapter is based on our publication in [J4].

5.1 Introduction

In this chapter, we investigate the resource allocation algorithm design for simultaneous wireless information and power transfer (SWIPT) systems by exploring robust designs to jointly minimize the total uplink and downlink transmit power, and maximize the total harvested energy in a full duplex system with imperfect channel state information.

As mention in Chapter 3, EH is one of the key technologies for the realization of the next generation 5G systems and beyond. Towards this direction research efforts have involved employing energy and information receivers (EIR) [32] as well as SWIPT relays [138]. The integration of FD with SWIPT is promising since the EIR can be simultaneously served thereby improving the spectrum and energy efficiency of the system [139]. In [140], a power splitting scheme was proposed to receive information and energy in order to maximize the energy harvested subject to SINR and maximum power constraints in a FD system. Likewise, [141] studied a joint transceiver design for FD cloud radio access networks with SWIPT. The authors proposed a system power minimization problem with uplink and downlink QoS constraints as well as EH constraints while optimizing the transceiver

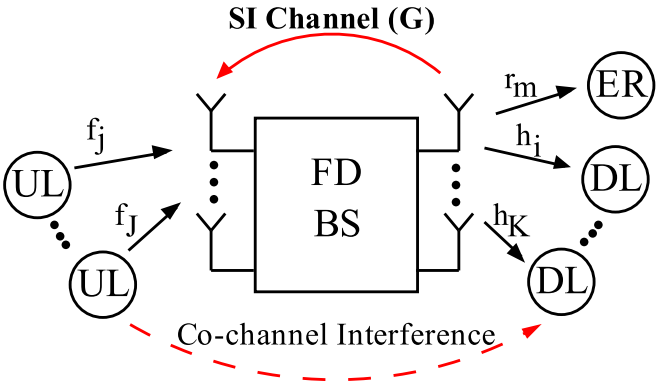

Figure 5.1: A multi-user FD SWIPT system

beamformers, the uplink transmit power, and the receive power splitting ratios, respectively. Most relevant to the focus of the work in this chapter, in [117], the authors proposed a multi-objective optimization problem (MOOP) via the weighted Tchebycheff method to investigate the resource allocation for FD-SWIPT systems with separated EIR. Their MOOP jointly minimizes the uplink and downlink transmit power and maximizes the total energy harvested. However, the authors assumed perfect CSI including the SI channel, this assumption deviates from practical scenarios for FD systems.

Accordingly, in this chapter, we aim to investigate precoding solutions for FD-SWIPT. Inspired by [117], here we first derive a channel state information (CSI)-robust MOOP based on suppressing interference. We then go one step further to reformulate the optimization such that the multi-user interference is exploited as a useful resource both for energy and information power. While the concept of interference exploitation has been studied thoroughly for half-duplex (HD) in [13, 102, 122], providing significant downlink power gains, the FD setup investigated here provides the opportunity to extend these gains to the uplink power budget.

5.2 System Model

We consider a multiuser communication system defined in [117] and shown in Fig. 5.1. A FD base station (BS) with N transmit and N receive antennas simultaneously serves K single-antenna downlink users, J uplink users and M energy receivers

(ERs). The transmitted signal by the FD BS is expressed as

$$\mathbf{t} = \sum_{i=1}^{K} \mathbf{w}_i d_i + \mathbf{q}, \tag{5.1}$$

where, $\mathbf{w}_i \in \mathbb{C}^{N\times 1}$ and d_i denote the beamforming vector and the unit data symbol for the *i-th* downlink user, respectively. The vector $\mathbf{q} \in \mathbb{C}^{N\times 1}$ is the energy signal sent by the FD BS to facilitate energy transfer [117]. Let $\mathbf{h}_i \in \mathbb{C}^{N\times 1}$, $\mathbf{f}_j \in \mathbb{C}^{N\times 1}$ and $\mathbf{r}_m \in \mathbb{C}^{N\times 1}$ be the channels between the FD BS and the *i-th* downlink user, the *j-th* uplink user, the *m-th* ER, respectively. Therefore, the received signals at the *i-th* downlink user, the FD BS and the *m-th* ER are respectively given by

$$y_i^{\mathrm{DL}} = \mathbf{h}_i^H \sum_{k=1}^{K} \mathbf{w}_k d_k + \mathbf{h}_i^H \mathbf{q} + \sum_{j=1}^{J} \sqrt{p_j}\ell_{j,i} x_j + n_i, \tag{5.2}$$

$$\mathbf{y}^{\mathrm{BS}} = \sum_{j=1}^{J} \sqrt{p_j}\mathbf{f}_j x_j + \mathbf{G}\mathbf{t} + \mathbf{n}_j, \tag{5.3}$$

$$y_m^{\mathrm{ER}1} = \mathbf{r}_m^H \mathbf{t} + n_m, \tag{5.4}$$

where, p_j and x_j denote the uplink transmit power and the data symbol from the *j-th* uplink user, respectively. $\ell_{j,i}$ is the channel between the *j-th* uplink user and the *i-th* downlink user. We denote $n_i \sim \mathscr{CN}\left(0, \sigma_i^2\right)$, $\mathbf{n}_j \sim \mathscr{CN}(0, \sigma_j^2)$ and $n_m \sim \mathscr{CN}(0, \sigma_m^2)$ as the additive white Gaussian noise at the *i-th* user, the FD BS and the *m-th* ER, respectively. The matrix $\mathbf{G} \in \mathbb{C}^{N\times N}$ denotes the SI channel at the FD BS. In order to isolate our proposed scheme from the specific implementation of any passive or active SI mitigation techniques, we consider the deterministic model to represent the residual-SI channel after cancellation, that is known imperfectly at the BS. Accordingly, the SI channel, which typically follows Rician distribution [117], is expressed as $\mathbf{G} = \check{\mathbf{G}} + \Delta\mathbf{G}$, where $\check{\mathbf{G}}$, denotes the SI channel estimate known to the FD BS which can be cancelled, and $\Delta\mathbf{G}$ represents the SI channel uncertainties, for which $\|\Delta\mathbf{G}\|_F^2 \leq \varepsilon_G^2$, for some $\varepsilon_G \geq 0$. We denote $\|\cdot\|_F$ as the Frobenius norm.

[1] In the adopted system model, the ERs only receive energy from the FD BS, while we ignore the potential energy received by the uplink users for simplicity.

We define the signal-to-interference plus noise ratio (SINR) at the *i-th* downlink user and at the FD radio BS respectively as

$$\Gamma_i^{\mathrm{DL}} = \frac{|\mathbf{h}_i^H \mathbf{w}_i|^2}{\sum_{k\neq i}^{K} |\mathbf{h}_i^H \mathbf{w}_k|^2 + |\mathbf{h}_i^H \mathbf{q}|^2 + \sum_{j=1}^{J} p_j |\ell_{j,i}|^2 + \sigma_i^2}, \tag{5.5}$$

$$\Gamma_j^{\mathrm{UL}} = \frac{p_j |\mathbf{f}_j^H \mathbf{u}_j|^2}{\sum_{n\neq j}^{J} p_n |\mathbf{f}_n^H \mathbf{u}_j|^2 + |\mathbf{u}_j \Delta \mathbf{G} \mathbf{t}|^2 + \sigma_j^2 \left\|\mathbf{u}_j\right\|^2}, \tag{5.6}$$

where, $\mathbf{u}_j \in^{N\times 1}$ is the receive beamforming vector for detecting the received symbol from the *j-th* uplink user. Following [117], we adopt zero-forcing (ZF) beamforming at the FD BS for the detection of uplink signals.

The total harvested energy at the *m-th* ER is modelled as [32] $E_m^{\mathrm{ER}} = \zeta_m \|\mathbf{r}_m^H \mathbf{t}\|^2$, where, $0 \leq \zeta_m \leq 1$ represents the energy conversion efficiency and we assume the noise power is negligibly small compared to the power of the received signal [117].

In contrast to [117], in this chapter, we focus on the case where imperfect CSI for the uplink, downlink, CCI and SI channels are available at the FD BS. We model these additive errors as norm-bounded, in the form $\mathbf{h}_i = \check{\mathbf{h}}_i + \mathbf{e}_{h,i}, \left\|\mathbf{e}_{h,i}\right\|^2 \leq \varepsilon_{h,i}^2, \forall i$, $\mathbf{f}_j = \check{\mathbf{f}}_j + \mathbf{e}_{f,j}, \left\|\mathbf{e}_{f,j}\right\|^2 \leq \varepsilon_{f,j}^2, \forall j$ and $\ell_{j,i} = \check{\ell}_{j,i} + e_{j,i}, |e_{j,i}|^2 \leq \varepsilon_{j,i}^2, \forall j,i$, where $\check{\mathbf{h}}_i, \check{\mathbf{f}}_j$ and $\check{\ell}_{j,i}$ denote the downlink, uplink and CCI CSI estimates known to the FD BS, respectively, and $\mathbf{e}_{h,i}, \mathbf{e}_{f,j}$ and $e_{j,i}$ represent the downlink, uplink and CCI CSI uncertainties, respectively. On the other hand, the FD BS need only to know the channel gain r_m of the ERs' channel to achieve a specified energy harvested target.

5.3 Robust Design with Interference Suppression

The system design objective is to jointly minimize the total downlink and uplink transmit power while maximizing the total harvested energy subject to QoS constraints (5.5) and (5.6), where multi-user interference is treated as harmful signal. Extending the non-robust design of [117], in this section, we jointly optimize the transmit beamformer ($\mathbf{w}_i$), the energy signal ($\mathbf{q}$) and uplink transmit power (p_j),

respectively. This can be mathematically formulated as

$$\begin{aligned}
\mathscr{P}5.1: \min_{\mathbf{w}_i,\mathbf{q},p_j} \quad & c_1 \cdot \left(\sum_{k=1}^{K} \|\mathbf{w}_k\|^2 + \|\mathbf{q}\|^2 \right) + c_2 \cdot \sum_{j=1}^{J} p_j - c_3 \cdot \sum_{m=1}^{M} E_m^{\mathrm{ER}} \\
\text{s.t.} \quad & \mathrm{A1}: \min_{\mathbf{e}_{h,i},e_{j,i}} \Gamma_i^{\mathrm{DL}} \geq \Gamma_i, \forall \left\|\mathbf{e}_{h,i}\right\|^2 \leq \varepsilon_{h,i}^2, \forall |e_{j,i}|^2 \leq \varepsilon_{j,i}^2, \forall i, \\
& \mathrm{A2}: \min_{\mathbf{e}_{f,j},\Delta\mathbf{G}} \Gamma_j^{\mathrm{UL}} \geq \Gamma_j, \forall \|\Delta\mathbf{G}\|_F^2 \leq \varepsilon_G^2, \forall \left\|\mathbf{e}_{f,j}\right\|^2 \leq \varepsilon_{f,j}^2, \forall j, \\
& \mathrm{A3}: \zeta_m r_m \left(\sum_{k=1}^{K} \|\mathbf{w}_k\|^2 + \|\mathbf{q}\|^2 \right) \geq P_m^{\min}, \forall m, \\
& \mathrm{A4}: \sum_{k=1}^{K} \|\mathbf{w}_k\|^2 + \|\mathbf{q}\|^2 \leq \mathrm{P}_{\max}^{\mathrm{DL}}, \\
& \mathrm{A5}: p_j \leq \mathrm{P}_{\max}^{\mathrm{UL}}, \forall j,
\end{aligned} \tag{5.7}$$

where $c_1 + c_2 + c_3 = 1$ are the weights given to each of the system's design objectives, respectively. Constraints A1 and A2 ensure that the minimum SINR, Γ_i and Γ_j, is achieved for the *i-th* downlink user and *j-th* uplink user, respectively. Constraint A3 ensures that the minimum harvested energy, P_m^{min}, for the *m-th* ER is achieved while A4 and A5 denote the maximum downlink and uplink transmit power constraints, respectively. The evidently non-convex problem (5.7) can be solved by formulating it as a semi-definite program (SDP) which can be transformed into linear matrix inequalities (LMI) by using the S-procedure. Accordingly, by defining $\mathbf{W}_i = \mathbf{w}_i\mathbf{w}_i^H, \mathbf{Q} = \mathbf{q}\mathbf{q}^H$ and $\mathbf{U}_j = \mathbf{u}_j\mathbf{u}_j^H$. Constraint A1 can be expressed as the following two constraints

$$\min_{\mathbf{e}_{h,i}} (\check{\mathbf{h}}_i + \mathbf{e}_{h,i})^H \mathbf{Y}_i (\check{\mathbf{h}}_i + \mathbf{e}_{h,i}) - \Gamma_i(\sigma_i^2 + L_i) \geq 0, \forall i, \tag{5.8}$$

$$\max_{e_{j,i}} \sum_{j=1}^{J} p_j (\check{\ell}_{j,i} + e_{j,i})^H (\check{\ell}_{j,i} + e_{j,i}) \leq L_i, \forall i, \tag{5.9}$$

where we introduce auxiliary variable $L_i \geq 0$ and

$$\mathbf{Y}_i \triangleq \mathbf{W}_i - \Gamma_i \left(\sum_{k \neq i}^{K} \mathbf{W}_k + \mathbf{Q} \right).$$

For constraint A2, we define two vectors $\widetilde{\mathbf{f}} = [\check{\mathbf{f}}_j^H, \ldots, \check{\mathbf{f}}_J^H]^H \in \mathbb{C}^{NJ\times 1}$ and $\widetilde{\mathbf{e}}_f = [\mathbf{e}_{f,j}^H, \ldots, \mathbf{e}_{f,J}^H]^H \in \mathbb{C}^{NJ\times 1}$. Hence, we can define any $\check{\mathbf{f}}_j = \mathbf{B}_j\widetilde{\mathbf{f}}$ and $\mathbf{e}_{f,j} = \mathbf{B}_j\widetilde{\mathbf{e}}_f$, for $j = 1,\ldots,J$, with $\mathbf{B}_j \in \mathbb{R}^{N\times NJ}$ defined as $\mathbf{B}_j = [\mathbf{B}_{j,1}, \ldots, \mathbf{B}_{j,J}]$, where $\mathbf{B}_{j,j} = \mathbf{I}_N$ and $\mathbf{B}_{j,n} = \mathbf{0}_N$, for $n = 1,\ldots,J, n \neq j$. We have $\mathbf{I}_N$ and $\mathbf{0}_N$ to be an $N \times N$ identity matrix and zero matrix, respectively. Hence, A2 can be rewritten as

$$\min_{\mathbf{e}_{f,j},\Delta\mathbf{G}} \frac{p_j\left((\mathbf{B}_j\widetilde{\mathbf{f}}+\mathbf{B}_j\widetilde{\mathbf{e}}_f)^H\mathbf{U}_j(\mathbf{B}_j\widetilde{\mathbf{f}}+\mathbf{B}_j\widetilde{\mathbf{e}}_f)\right)}{\sum_{n\neq j}^{J} p_n\left((\mathbf{B}_n\widetilde{\mathbf{f}}+\mathbf{B}_n\widetilde{\mathbf{e}}_f)^H\mathbf{U}_j(\mathbf{B}_n\widetilde{\mathbf{f}}+\mathbf{B}_n\widetilde{\mathbf{e}}_f)\right)+S_j} \geq \Gamma_j, \tag{5.10}$$

where

$$S_j = \mathrm{Tr}\left\{\mathbf{E}_G\left(\sum_{k=1}^{K}\mathbf{W}_k+\mathbf{Q}\right)\mathbf{E}_G^H\mathbf{U}_j\right\}+\sigma_N^2\mathrm{Tr}\left\{\mathbf{U}_j\right\}.$$

Furthermore, we introduce

$$\mathbf{Z}_j \triangleq P_j\mathbf{B}_j^T\mathbf{U}_j\mathbf{B}_j - \Gamma_j\sum_{n\neq j}^{J} P_n\mathbf{B}_n^T\mathbf{U}_j\mathbf{B}_n$$

and auxiliary variable S_j^{SI}, such that (5.10) can be written as the following two constraints

$$\min_{\mathbf{e}_{f,j}} \left(\widetilde{\mathbf{f}}+\widetilde{\mathbf{e}}_f\right)^H\mathbf{Z}_j\left(\widetilde{\mathbf{f}}+\widetilde{\mathbf{e}}_f\right) \geq S_j^{\mathrm{SI}}\Gamma_j, \forall j, \tag{5.11}$$

$$\max_{\Delta\mathbf{G}} \mathrm{Tr}\left\{\mathbf{E}_G\left(\sum_{k=1}^{K}\mathbf{W}_k+\mathbf{Q}\right)\mathbf{E}_G^H\mathbf{U}_j\right\}+\sigma_N^2\mathrm{Tr}\left\{\mathbf{U}_j\right\} \leq S_j^{\mathrm{SI}}, \forall j. \tag{5.12}$$

Thus, using $\mathrm{Tr}\{\mathbf{ABCD}\} = \mathrm{vec}\left(\mathbf{A}^H\right)^H\left(\mathbf{D}^T\otimes\mathbf{B}\right)\mathrm{vec}\left(\mathbf{C}\right)$, and defining $\mathbf{P} = \mathrm{diag}(p_1,\ldots,p_J), \check{\ell}_i = \left[\check{\ell}_{1,i},\ldots,\check{\ell}_{J,i}\right], \mathbf{e}_{\ell,i} = [e_{1,i},\ldots,e_{J,i}]$ and $\mathbf{e}_g = \mathrm{vec}(\Delta\mathbf{G}^H)$, where $\mathrm{vec}(\cdot)$ stacks the columns of a matrix into a vector and $\otimes$ stands for Kronecker product, constraints (5.8),(5.9), (5.11) and (5.12) can be expanded and transformed to LMIs using S-procedure as shown in the following, respectively.

$$\widetilde{\text{A1a}} \Rightarrow \begin{bmatrix} \delta_i\mathbf{I}+\mathbf{Y}_i & \mathbf{Y}_i\check{\mathbf{h}}_i \\ \check{\mathbf{h}}_i^H\mathbf{Y}_i & \check{\mathbf{h}}_i^H\mathbf{Y}_i\check{\mathbf{h}}_i - \Gamma_i\left(\sigma_i^2+L_i\right)-\delta_i\varepsilon_{h,i}^2 \end{bmatrix} \succeq 0, \tag{5.13}$$

$$\widetilde{\text{A1b}} \Rightarrow \begin{bmatrix} \lambda_i \mathbf{I} - \mathbf{P} & -\mathbf{P}\check{\ell}_i \\ -\check{\ell}_i^H \mathbf{P} & -\check{\ell}_i^H \mathbf{P}\check{\ell} - \lambda_i \varepsilon_{\ell,i}^2 - L_i \end{bmatrix} \succeq 0, \tag{5.14}$$

$$\widetilde{\text{A2a}} \Rightarrow \begin{bmatrix} \mu_j \mathbf{I} + \mathbf{Z}_j & \mathbf{Z}_j \widetilde{\mathbf{f}} \\ \widetilde{\mathbf{f}}^H \mathbf{Z}_j & \widetilde{\mathbf{f}}^H \mathbf{Z}_j \widetilde{\mathbf{f}} - S_j^{\text{SI}} \Gamma_j - \mu_j \varepsilon_f^2 \end{bmatrix} \succeq 0, \tag{5.15}$$

$$\widetilde{\text{A2b}} \Rightarrow \begin{bmatrix} \rho \mathbf{I} - \left(\mathbf{U}_j^T \otimes (\sum_{k=1}^K \mathbf{W}_k + \mathbf{Q}) \right) & 0 \\ 0 & S_j^{\text{SI}} - \sigma_N^2 \text{Tr}\left\{ \mathbf{U}_j \right\} - \rho \varepsilon_G^2 \end{bmatrix} \succeq 0. \tag{5.16}$$

Thus, (5.7) can be re-expressed as

$$\begin{aligned} \mathscr{P}5.2: \min_{\substack{\mathbf{W}_i, \mathbf{Q}, p_j, \\ \delta_i, \mu_j, \rho, S_j^{\text{SI}},}} \; & \text{Tr}\left\{ \sum_{k=1}^K \mathbf{W}_k + \mathbf{Q} \right\} \left(c_1 - c_3 \sum_{m=1}^M \zeta_m r_m \right) + c_2 \cdot \sum_{j=1}^J p_j \\ \text{s.t.} \quad & \widetilde{\text{A1a}}, \widetilde{\text{A1b}}, \widetilde{\text{A2a}}, \widetilde{\text{A2b}}, \text{A4}, \text{A5}, \\ & \widetilde{\text{A3}}: \zeta_m r_m \text{Tr}\left\{ \sum_{k=1}^K \mathbf{W}_k + \mathbf{Q} \right\} \geq P_m^{min}, \forall m, \\ & \mathbf{W}_i \succeq 0, \forall i, \mathbf{Q} \succeq 0, \delta_i \geq 0, \forall i, \mu_j \geq 0, \forall j, \rho \geq 0, \end{aligned} \tag{5.17}$$

where we have dropped the rank constraints on $\mathbf{W}_i, \forall i$. Note that the problem (5.17) is a relaxed form of (5.7). While it is difficult to prove analytically, our simulations have shown that problem (5.17) always returns rank-one solutions. Still, in the unlikely case of a non rank-one solution, valid solutions can always be obtained by randomization [134].

5.4 Robust Design with Interference Exploitation

In this section, we design our system to exploit interference rather than suppressing it as in Section 5.3. Constructive interference (CI) is the interference that pushes the received signal away from the detection thresholds [13]. The concept of CI has been thoroughly studied in the literature for both PSK and QAM modulation in [13] and references therein, where analytical criteria are also derived. For notational convenience, we focus on PSK here. To reformulate (5.7) for interference exploitation,

we first write the received signal at the *i-th* downlink user as

$$\widetilde{y}_i = \left(\check{\mathbf{h}}_i + \mathbf{e}_{h,i}\right)^H \left(\sum_{k=1}^{K} \mathbf{w}_k e^{j(\phi_k - \phi_i)} + \mathbf{q}e^{-j\phi_i}\right) = \left(\check{\mathbf{h}}_i + \mathbf{e}_{h,i}\right)^H \mathbf{a}, \tag{5.18}$$

where we have omitted the noise term, $\mathbf{a} = \sum_{k=1}^{K} \mathbf{w}_k e^{j(\phi_k - \phi_i)} + \mathbf{q}e^{-j\phi_i}$ and the unit-energy PSK symbol for the *i-th* downlink user is represented as $d_i = de^{\phi_i}$.

As detailed in [13], for any given PSK constellation point, to guarantee CI, $\widetilde{y}_i$ must fall within the CI region of the constellation. The size of the region is determined by $\theta = \pm\frac{\pi}{B}$, which is the maximum angle shift within the CI region for a modulation order B. Accordingly, the downlink SINR constraint that guarantees CI at the *i-th* downlink user [13] is

$$|\Im\left(\widetilde{y}_i\right)| \leq \left(\Re(\widetilde{y}_i) - \sqrt{\Gamma_i \sum_{j=1}^{J} p_j |\check{\ell}_{j,i} + e_{j,i}|^2 + \Gamma_i \sigma_i^2}\right) \tan\theta, \tag{5.19}$$

where $\Re$ and $\Im$ are the real and imaginary parts, respectively. In a similar fashion to Section 5.3, the robust system design for CI can be formulated as

$$\begin{aligned}
\mathscr{P}5.3: \min_{\mathbf{a},\{p_j\}} \quad & c_1 \cdot \|\mathbf{a}\|^2 + c_2 \cdot \sum_{j=1}^{J} p_j - c_3 \cdot \sum_{m=1}^{M} \zeta_m r_m \|\mathbf{a}\|^2 \\
\text{s.t.} \quad & \text{B1}: \max_{\mathbf{e}_{h,i}, e_{j,i}} (5.19), \forall \left\|\mathbf{e}_{h,i}\right\|^2 \leq \varepsilon_{h,i}^2, \forall |e_{j,i}|^2 \leq \varepsilon_{j,i}^2, \forall i, \\
& \text{B2}: \min_{\mathbf{e}_{f,j}, \Delta\mathbf{G}} \Gamma_j^{\text{UL}} \geq \Gamma_j, \forall \|\mathbf{E}_G\|_F^2 \leq \varepsilon_G^2, \forall \left\|\mathbf{e}_{f,j}\right\|^2 \leq \varepsilon_{f,j}^2, \forall j, \\
& \text{B3}: \zeta_m r_m \|\mathbf{a}\|^2 \geq P_m^{\min}, \forall m, \\
& \text{B4}: \|\mathbf{a}\|^2 \leq \text{P}_{\max}^{\text{DL}}, \\
& \text{B5}: p_j \leq \text{P}_{\max}^{\text{UL}}, \forall j.
\end{aligned} \tag{5.20}$$

Problem (5.20) is a non-convex problem. To solve (5.20), we transform each constraint to a convex form separately in the following. Let's consider the downlink SINR constraint B1, which for the worst-case scenario can be rewritten as the fol-

lowing two constraints

$$\max_{\mathbf{e}_{h,i}} \left|(\underline{\check{\mathbf{h}}}_i+\underline{\mathbf{e}}_{h,i})^H\underline{\mathbf{a}}\right| - ((\underline{\check{\mathbf{h}}}_i+\underline{\mathbf{e}}_{h,i})^H\Pi\underline{\mathbf{a}} - \sqrt{\Gamma_i}L_i^{\mathrm{CI}})\tan\theta \le 0, \forall i, \tag{5.21}$$

$$\max_{e_{j,i}} \sqrt{\sum_{j=1}^{J} p_j|\check{\ell}_{j,i}+e_{j,i}|^2+\sigma_i^2} \le L_i^{\mathrm{CI}}, \forall i. \tag{5.22}$$

Accordingly, (5.21) can be relaxed to the following two robust formulations

$$\underline{\check{\mathbf{h}}}_i^H(\underline{\mathbf{a}}-\Pi\underline{\mathbf{a}}\tan\theta)+\varepsilon_{h,i}\|\underline{\mathbf{a}}-\Pi\underline{\mathbf{a}}\tan\theta\|+\sqrt{\Gamma_i}L_i^{\mathrm{CI}}\tan\theta \le 0, \forall i, \tag{5.23}$$

$$\underline{\check{\mathbf{h}}}_i^H(-\underline{\mathbf{a}}-\Pi\underline{\mathbf{a}}\tan\theta)+\varepsilon_{h,i}\|-\underline{\mathbf{a}}-\Pi\underline{\mathbf{a}}\tan\theta\|+\sqrt{\Gamma_i}L_i^{\mathrm{CI}}\tan\theta \le 0, \forall i, \tag{5.24}$$

where $\underline{\mathbf{a}} = \begin{bmatrix}\Re(\mathbf{a})^H & \Im(\mathbf{a}^H)\end{bmatrix}^H$, $\Pi = \begin{bmatrix}\mathbf{0}_N & -\mathbf{I}_N \\ \mathbf{I}_N & \mathbf{0}_N\end{bmatrix}$, $\underline{\check{\mathbf{h}}}_i = \begin{bmatrix}\Im(\check{\mathbf{h}}_i)^H & \Re(\check{\mathbf{h}}_i)^H\end{bmatrix}^H$, $\underline{\mathbf{e}}_{h,i} = \begin{bmatrix}\Im(\mathbf{e}_{h,i})^H & \Re(\mathbf{e}_{h,i})^H\end{bmatrix}^H$. Furthermore, by using the inequality $\sqrt{x^2+y^2} \le |x|+|y|$, (5.22) can be relaxed to the following robust formulation

$$\left|\sum_{j=1}^{J}\sqrt{p_j}\left(|\check{\ell}_{j,i}|+\varepsilon_{j,i}\right)\right| + |\sigma_i| \le L_i^{\mathrm{CI}}, \forall i. \tag{5.25}$$

Next, we consider the uplink SINR constraint B2, which can be written as

$$p_j\left|\left(\check{\mathbf{f}}_j+\mathbf{e}_{f,j}\right)^H\mathbf{u}_j\right|^2 \ge \Gamma_j\left[\sum_{n\ne j}^{J} p_n\left|\left(\check{\mathbf{f}}_n+\mathbf{e}_{f,n}\right)^H\mathbf{u}_j\right|^2 + \left|\mathbf{u}_j\Delta\mathbf{G}\mathbf{a}\right|^2+\sigma_j^2\left\|\mathbf{u}_j\right\|^2\right], \tag{5.26}$$

which can be relaxed using the inequality $\|\mathbf{x}+\mathbf{y}\|^2 \le (\|\mathbf{x}\|+\|\mathbf{y}\|)^2$ to give the following robust formulation

$$p_j\left(|\check{\mathbf{f}}_j^H\mathbf{u}_j|+\varepsilon_{f,j}\|\mathbf{u}_j\|\right)^2 \ge \Gamma_j\left[\sum_{n\ne j}^{J} p_n\left(|\check{\mathbf{f}}_n^H\mathbf{u}_j|+\varepsilon_{f,n}\|\mathbf{u}_j\|\right)^2 + (\varepsilon_G\left\|\mathbf{u}_j\right\|\|\mathbf{a}\|)^2+\sigma_j^2\|\mathbf{u}_j\|^2\right] \tag{5.27}$$

Accordingly, from (5.23) we have

$$-\frac{\check{\underline{\mathbf{h}}}_i^H\left(\mathbf{I}-\Pi\tan\theta\right)\underline{\mathbf{a}}+\sqrt{\Gamma_i}L_i^{\mathrm{CI}}\tan\theta}{\varepsilon_{h,i}\left\|\mathbf{I}-\Pi\tan\theta\right\|}\leq\left\|\underline{\mathbf{a}}\right\|. \tag{5.28}$$

Hence, an upper bound for the ER constraint in (5.20) is

$$-\frac{\check{\underline{\mathbf{h}}}_i^H\left(\mathbf{I}-\Pi\tan\theta\right)\underline{\mathbf{a}}+\sqrt{\Gamma_i}L_i^{\mathrm{CI}}\tan\theta}{\varepsilon_{h,i}\left\|\mathbf{I}-\Pi\tan\theta\right\|}\geq\sqrt{\frac{P_m^{min}}{\zeta_m r_m}},\forall i,\forall m. \tag{5.29}$$

Finally, the transformed problem (5.20) can be expressed as

$$\begin{aligned}\mathscr{P}5.4:\min_{\substack{\mathbf{a},\underline{\mathbf{a}},p_j,\beta_m,\\ L_i^{\mathrm{CI}},S_j^{\text{SI-CI}}}}\quad & c_1\cdot\left\|\underline{\mathbf{a}}\right\|^2+c_2\cdot\sum_{j=1}^{J}p_j-c_3\cdot\sum_{m=1}^{M}\zeta_m\beta_m\\ \text{s.t.}\quad & (5.23),(5.24),(5.27),(5.29),\left\|\mathbf{a}\right\|^2\leq \mathrm{P}_{\max}^{\mathrm{DL}},\,p_j\leq \mathrm{P}_{\max}^{\mathrm{UL}},\forall j\\ & -\frac{\check{\underline{\mathbf{h}}}_i^H\left(\mathbf{I}-\Pi\tan\theta\right)\underline{\mathbf{a}}+\sqrt{\Gamma_i}L_i^{\mathrm{CI}}\tan\theta}{\varepsilon_{h,i}\left\|\mathbf{I}-\Pi\tan\theta\right\|}\geq\frac{\beta_m}{\sqrt{r_m}},\forall i,\forall m.\end{aligned} \tag{5.30}$$

$\mathscr{P}5.4$ is jointly convex with respect to the optimization variables, thus can be optimally solved using standard convex solvers.

At this point, we emphasize the flexibility provided by the MOOP $\mathscr{P}5.2$ and $\mathscr{P}5.4$ with respect to optimization variables. There is a strong interdependency between the optimization variables, in that, increasing the downlink transmit power to satisfy the SINR constraints increases the SI power, which hinders the reception of uplink signals. At the same time, if the uplink transmit power is increased in order to satisfy the SINR constraints, co-channel interference (CCI) is increased at the downlink users. Similarly, minimizing the downlink transmit power reduces the amount of energy transferred to ERs.

5.5 Simulation Results

We consider the system with the FD BS at the center of a cell with $N=6$. We assume $K=J=3$ downlink and uplink users, are randomly and uniformly distributed

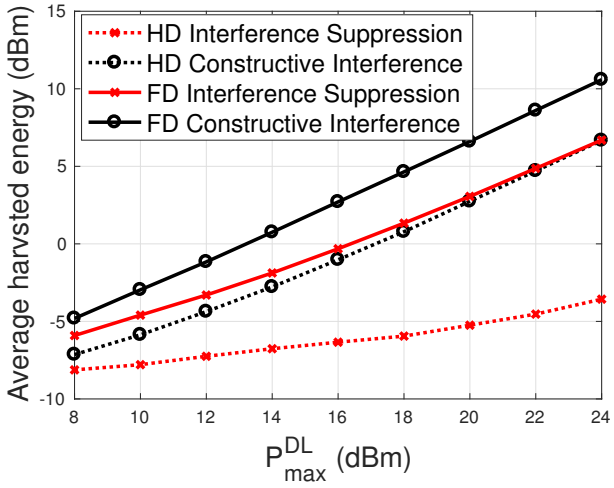

Figure 5.2: Average harvested energy vs P_{max}^{DL}

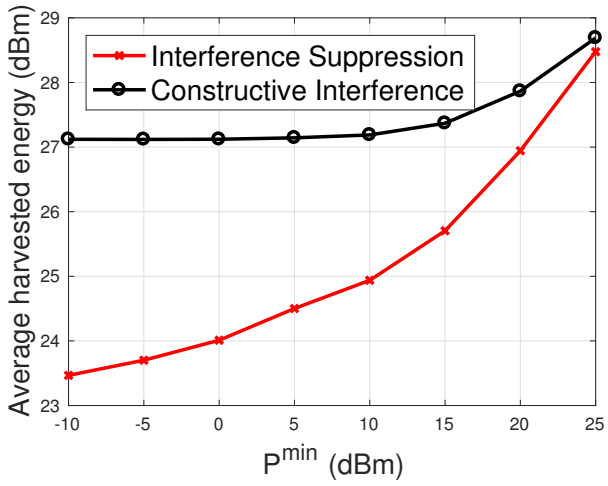

Figure 5.3: Average harvested energy vs P^{min}

between the distance of 10m and 50m and $M = 2$ ERs are randomly and uniformly distributed between the distance of 2m and 10m. We model the channels to the uplink and downlink users as Rayleigh fading. By assuming the same parameters as in [117], $G_t = 10\text{dBi}, G_r = 0\text{dBi}, freq = 915\text{MHz}, d = 5$, and using Friis equation we have an estimate channel gain $r_m = 0.00027$. Furthermore, we consider $\varepsilon_h = \varepsilon_f = \varepsilon_G = \varepsilon_\ell = 0.001, \Gamma^{\text{DL}} = 8\text{dB}, \Gamma^{\text{UL}} = 2\text{dB}, \zeta = 0.4, \sigma_i = -60\text{dBm}, \sigma_j = -70\text{dBm}$ and QPSK modulation in all cases.

First, we investigate the performance of our proposed schemes with $c_1 = 0.1, c_2 = 0.1$ and $c_3 = 0.8$. In Fig. 5.2, we show the average harvested energy

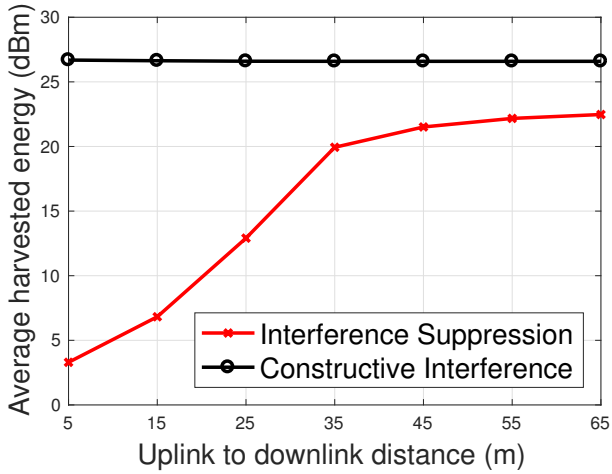

Figure 5.4: Average harvested energy vs uplink to downlink distance

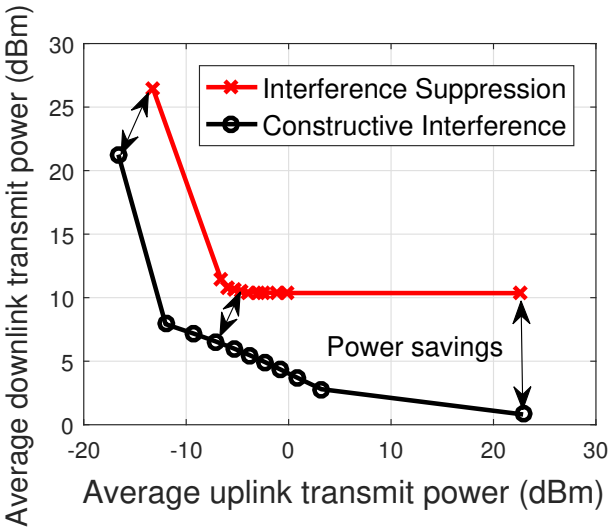

Figure 5.5: Uplink-downlink power trade-off

for varying P_{max}^{DL}. First, it can be seen that for the same overall data rate requirement the FD systems outperform the corresponding HD transmission. More importantly, it can be seen that with the proposed CI scheme more energy is harvested as P_{max}^{DL} increases. This occurs because less power is required to satisfy the downlink and uplink QoS constraints for the CI scheme compared to the interference suppression (IS) scheme, hence, more power is available to be harvested by the ERs. Furthermore, Fig. 5.3 shows the average harvested energy for different minimum harvested energy thresholds. Clearly, the CI scheme is less sensitive to the P^{min} threshold values since more transmit power is being saved from exploiting interference, while

for the IS scheme less energy can be harvested. In Fig. 5.4, we show the average harvested energy with respect to the distance between uplink and downlink users, that determines the CCI. The CI scheme is less sensitive to CCI compared to the IS schemes, which further highlights the effectiveness of the interference exploitation approach.

In Fig. 5.5, we show the uplink and downlink power trade-off by varying c_1 and c_2 between 0 and 1 with a step of 0.1 while $c_3 = 0$. Thus, it can be seen from Fig. 5.5 that a trade-off exist between the uplink and downlink transmit power for both CI and IS schemes. However, power savings can be seen for CI compared with the IS scheme, since interference is rather exploited as an additional source of useful power. In addition, we note that while CI is applied only to the downlink users, power savings can also be seen for the uplink since lower downlink transmit power translates to lower SI power and hence, lower uplink power consumption. This is unique for the FD scenario and has never been observed in the CI literature.

5.6 Summary

In this chapter, we studied the CSI-robust transmit power and harvested energy optimization problem in a multiuser FD SWIPT system. We first formulated an optimization where MUI is suppressed. Then, we formulated an optimization where MUI is rather exploited, both as useful energy and information power for guaranteeing QoS and energy harvesting constraints. By exploiting interference both as a source of energy and information power, the proposed CI scheme show a significant performance improvement over the conventional interference cancellation-based scheme.

Chapter 6

FD Mobile Edge Computing Systems

This chapter is based on our publications in [C1],[J2].

6.1 Introduction

Motivated by the ongoing research for the materialization of the 5G vision, in this chapter we investigate the offloading energy and latency trade-off in a multiuser FD MEC system.

The next generation 5G network aims at providing higher data rate and low latency communications. MEC has been identified as a promising solution to enable mobile devices (MD) offload their intensive and latency-critical computation tasks to the MEC servers for execution. In this way, the battery life at the MD can be enhanced while their data storage capabilities and computational resources can be relaxed [14]. In quest to reap the benefits of the MEC, several resource allocation designs have been proposed. [142] investigated resource allocation design for MEC systems based on time-division multiple access (TDMA) and orthogonal frequency division multiple access (OFDMA) offloading by considering the local computation capabilities of the users to minimize the mobile energy consumption. While in [143], an offline heuristic algorithm was designed to minimize the average completion time of multiple users for partitioning and scheduling the offloading of their computations. In [144], a wireless powered multiuser MEC system was proposed where the devices depend on their harvested energy to compute locally or offload tasks to the MEC server while the energy consumption of the MEC server is mini-

mized. [145] formulated an offloading problem to minimize the energy consumption by jointly optimizing the mobile precoding matrices and the computing frequency while meeting latency constraints. Similarly, [146] proposed a game theoretic approach for computation mobile offloading in a multi-user MEC system. However, in all the above works, the authors focused on half duplex transmission and on a single-objective i.e., either energy consumption or latency objectives. In [147], the authors studied the effects of using multiple access points (APs) with computation capabilities for offloading tasks in order to minimize the energy consumption and latency for fixed and elastic central processing unit (CPU) frequency. However, the authors assumed fixed transmitting and receiving power in their analysis, and in addition, the authors like the authors in [142–146], assumed that the APs have perfect channel state information (CSI). These assumptions may deviate from practical scenarios.

In the area of multi-user FD systems, only limited works have been done on mobile-edge computing (MEC). [148] studied energy harvesting with MEC, where a FD relay assists a mobile user to connect to an access point (AP) integrated with a MEC server. The user uploads part of its computation bits to the AP for execution and then, uses power splitting to download the results and harvest energy within a time frame. The paper minimizes the system energy consumption subject to latency and energy constraints by assuming perfect channel state information (CSI) with perfect self-interference (SI) cancellation at the FD relay. In [149], a similar system model is employed where users offload computation bits to a FD AP for execution and simultaneously the FD AP transmits energy to the users. The authors investigated the max-min energy efficiency problem to ensure fairness between users. Also, the authors [150, 151] investigated FD with MEC in wireless network virtualization. [150] studied the virtual resource allocation for heterogeneous services in FD-enabled small cell networks with MEC and caching while [151] proposed a MEC framework for a user virtualization scheme in the software-defined network virtualization cellular network.

Accordingly, in this chapter, we study a multiuser FD MEC-supported sys-

tem which comprises a FD BS equipped with a MEC server. The FD BS sends information signals in the downlink and receive intensive and latency-critical computation tasks to be executed by the MEC server through the uplink. Unlike existing works on MEC [142–147], we employ FD, which brings the need to optimize the variables for both uplink and downlink transmission i.e., the uplink transmit power and the downlink beamforming vectors, at the same time. However, when half duplex (HD) is employed as in [142–147], only the uplink or downlink variable is optimized. Also, FD introduces the self-interference (SI) signal, which is an additional term in the constraints that is non-trivial to handle as will be evident in later sections. In addition, we formulate an optimisation problem which involves minimising two desirable but conflicting system objectives, namely the total offloading energy and latency. Different to the existing works on FD [12, 116, 117, 152–156] and MEC [142–151], this calls for a weighted multi-objective formulation in order to study their trade-off which is highly dependent on the optimisation variables. Thus, existing methods in [142–151], can not be applied to solve the proposed optimization problems directly.

Furthermore, as will be shown later, the simulation results show the performance gains achieved by the FD proposed schemes compared to the existing HD schemes. We summarize our contributions below:

1. We first define the two system objectives namely, the total offloading energy and latency, then we formulate two weighted multi-objective optimization problems (MOOPs) subject to offloading latency constraints and downlink QoS constraints. One, based on interference suppression (IS) and the other, based on constructive interference (CI).

2. To solve the non-convex problems, we employ the Lagrangian method in order to design a tractable iterative algorithm for both the IS scheme and IE scheme.

3. We further extend our designs to robust formulations of the optimization problems for both IS and CI schemes by considering the worst-case perfor-

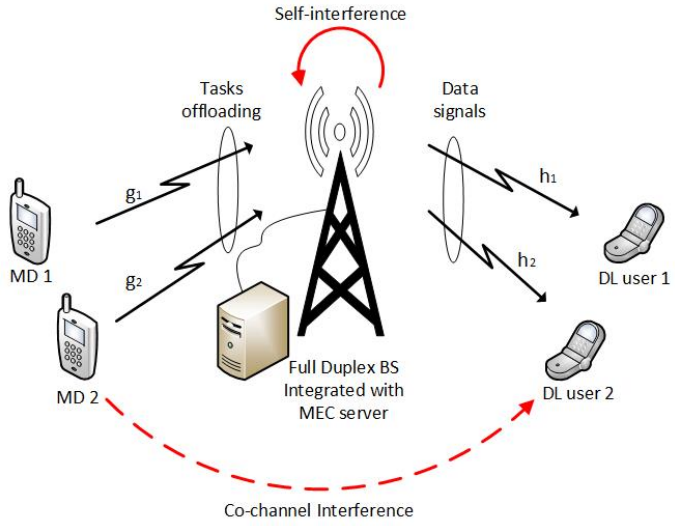

Figure 6.1: A multiuser FD MEC system

mance model. To tackle the non-convexity of the formulations, we simplify and relax the constraints using auxiliary variables and then we use the S-procedure to transmform the constraints into linear matrix inequalities.

6.2 System Model

We consider a multiuser wireless communication system as shown in Fig. 6.1. The system consists of a FD BS, integrated with a MEC server, with N transmit and N receive antennas simultaneously serving K single-antenna downlink users and J single-antenna mobile devices. In this system, the downlink users receive information signals from the FD BS, while, the mobile devices leverage the MEC server at the FD BS to offload its latency-sensitive computation tasks, which can not be locally executed, to be executed by the MEC server. Please note that for user scheduling in the resource block, we assume that this can be dealt with by existing protocols like the time-division multiple access or the orthogonal frequency-division multiple access as in [142, 144].

6.2.1 Downlink Transmission

For the transmission of information signal from the FD BS to the *i-th* downlink user, let $d_i, \mathbf{h}_i \in \mathbb{C}^{N\times 1}$ and $\mathbf{w}_i \in \mathbb{C}^{N\times 1}$ be the unit data symbol, the channel vector and the beamforming vector between the FD BS and the *i-th* downlink user, respectively.

Hence, the received signals at the *i-th* downlink user is given by

$$y_i = \mathbf{h}_i^H \sum_{k=1}^{K} \mathbf{w}_k d_k + \sum_{j=1}^{J} \sqrt{p_j}\ell_{j,i} + n_i, \tag{6.1}$$

where, p_j and $n_i \sim \mathscr{CN}\left(0, \sigma_i^2\right)$ denote the transmit power for the *j-th* mobile device and the additive white Gaussian noise at the *i-th* user, respectively. $\ell_{j,i}$ is the channel between the *j-th* mobile device and the *i-th* downlink user.

6.2.2 Computation Offloading

We denote the computation task to be offloaded to the MEC server for execution in bits at the *j-th* mobile device as q_j, which are classified as either energy consuming or time consuming tasks for the battery-constrained and time-constrained mobile device [14]. Computation offloading to the MEC server involves the transmission of the computation tasks to the FD BS by each mobile device and downloading[1] of the results by each user. Hence, we define the transmission rate of the *j-th* mobile device with bandwidth B as

$$r_j = B\log_2\left(1+\gamma_j\right), \tag{6.2}$$

where

$$\gamma_j = \frac{p_j \left|\mathbf{g}_j^H \mathbf{u}_j\right|^2}{\sum_{n\neq j}^{J} p_n \left|\mathbf{g}_n^H \mathbf{u}_j\right|^2 + s_j + \sigma_j^2 \left\|\mathbf{u}_j\right\|^2}. \tag{6.3}$$

In addition, $\mathbf{g}_j \in \mathbb{C}^{N\times 1}$ denotes the channel between the FD BS and the *j-th* mobile device and σ_j^2 is the noise power at the FD BS. We denote $\mathbf{u}_j \in^{N\times 1}$ as the receive beamforming vector for the *j-th* mobile device. In this chapter, to reduce complexity, we adopt ZF beamforming at the FD BS for the detection of the offloaded tasks. ZF is adopted since it provides a good trade-off between complexity and performance [131]. Hence, the receive beamforming vector for the *j-th* mobile device is

[1] As the computational results are usually small, in our analysis we ignore the downloading time and the power consumed during transmitting and receiving the results [14,144]. Thus, in this chapter, our focus is particularly on the offloading of the tasks. We set aside the consideration of the results downloading from the FD BS to the mobile devices for our future work.

given as

$$\mathbf{u}_j = (\mathbf{c}_j \mathbf{G}^{\dagger})^H, \tag{6.4}$$

where $\mathbf{c}_j = [\underbrace{0,\ldots,0}_{j-1},1,\underbrace{0,\ldots,0}_{J-j}]$, $\mathbf{G}^{\dagger} = (\mathbf{G}^H\mathbf{G})^{-1}\mathbf{G}^H$,† denotes the pseudo-inverse operation and $\mathbf{G} = [\mathbf{g}_1,\ldots,\mathbf{g}_J]$. Furthermore, due to the simultaneous transmission and reception at the FD BS, there is a strong SI that degrades the reception of the offloaded computation tasks at the FD BS. In the literature, there are different SI mitigation techniques which could be employed to reduce the effects of SI. In order to isolate our proposed scheme from the specific implementation of any passive or active SI mitigation techniques, we model the SI after cancellation as $s_j = \sum_{i=1}^{K} \mathrm{Tr}\left\{\mathbf{w}_i\mathbf{w}_i^H\mathbf{H}_{\mathrm{SI}}^H\mathbf{u}_j\mathbf{u}_j^H\mathbf{H}_{\mathrm{SI}}\right\}$ [6, 117], where the matrix $\mathbf{H}_{\mathrm{SI}} \in \mathbb{C}^{N\times N}$ denotes the SI channel at the FD BS. Accordingly, given the computation task q_j to be offloaded by the *j-th* mobile device, the total offloading latency is defined as the time taken to offload the task q_j to the FD BS plus the time taken for the FD BS to compute the corresponding result. This can be expressed as [147]

$$T_j^{\mathrm{total}} = \underbrace{\frac{q_j}{r_j}}_{t_{off,j}} + \underbrace{\frac{q_j L_{\mathrm{BS},j}}{f_{\mathrm{BS}}}}_{t_{\mathrm{BS},j}}. \tag{6.5}$$

We denote $t_{off,j}$ as the time it takes to offload task q_j to the FD BS and $t_{\mathrm{BS},j}$ as the computation time at the FD BS for task q_j, where $L_{\mathrm{BS},j}$ (cycles/bit) is the number of CPU cycles required to compute 1 input bit of q_j at the FD BS and f_{BS} (cycles/s) is the CPU frequency of the FD BS. Thus, the corresponding total computation energy consumed in the offloading process by all the mobile devices is [37]

$$E_{off} = \sum_{j=1}^{J} p_j t_{off,j}. \tag{6.6}$$

We note here the dependency of the transmit power of the mobile devices and the downlink beamforming vectors, in that, p_j through the SI term (s_j) is a function of $\mathbf{w}_i$, which in turn is a function of p_j through (6.1).

6.3 Problem Formulation

Our main objective in this chapter is to study the trade-off between two important and desirable system objectives, namely, the total offloading energy and the total offloading latency. In practice, there always exist a trade-off between these two objectives, in that, on one hand, an increase in the offloading energy implies increase in transmit power of the mobile devices and in essence, leads to a decrease in the offloading latency and vice versa. In the literature, multi-objective optimization (MOO) is often employed to study the trade-off between conflicting objectives via the concept of Pareto optimality. A point is said to be Pareto optimal if there is no other point that improves any of the objectives without decreasing the others [118]. It has been shown in [118] that, one way to capture the complete Pareto optimal set of the MOOP is through the weighted-sum formulation, which can achieve the complete Pareto optimal set with low computational complexity. Thus, in order to efficiently analyse and address this trade-off between these objectives, we adopt the sum- weighted MOO that aims at minimizing the two objectives by jointly optimizing the downlink beamforming vectors and the transmit power for each mobile device, while satisfying the total offloading latency requirement constraint and downlink users QoS constraints as well as the power constraints. In the following subsections, we present two strategies for the trade-off design, one based on classical interference suppression and one based on interference exploitation.

We note that in this section, we assume that the FD BS knows all the channel state information (CSI) from and to all the users in the system. We focus on slow fading channel scenario, where the channels change at the beginning of each frame. Thus, to facilitate the channel realization in practice, handshaking is performed between the FD BS and all users. As the channel changes slowly, pilot signals are usually embedded in the data packets, which allows the FD BS to constantly update the CSI estimation of the transmission links of the users and devices. However, we explicitly treat the case of imperfect CSI in Section 6.4.

6.3.1 Trade-off Optimization based on Interference Suppression

First, in this section, we define the signal-to-interference plus noise ratio (SINR) at the *i-th* downlink user that promotes interference suppression (IS) transmission based on (6.1) as

$$\Gamma_i^{\mathrm{DL}} = \frac{|\mathbf{h}_i^H \mathbf{w}_i|^2}{\sum_{k\neq i}^{K} |\mathbf{h}_i^H \mathbf{w}_k|^2 + \sum_{j=1}^{J} p_j |\ell_{j,i}|^2 + \sigma_i^2}. \tag{6.7}$$

Thus, based on the DL SINR expression in (6.7) the MOOP based on IS can be mathematically formulated as

$$\begin{aligned} \mathscr{P}6.1: \min_{\{\mathbf{w}_i\},\{p_j\}} \; & c_1 \cdot E_{off} + c_2 \cdot \sum_{j=1}^{J} T_j^{\mathrm{total}} \\ \text{s.t.} \quad & \mathrm{A1}: \frac{q_j}{r_j} + \frac{q_j L_{\mathrm{BS},j}}{f_{\mathrm{BS}}} \leq T_j, \forall j, \\ & \mathrm{A2}: \Gamma_i^{\mathrm{DL}} \geq \Gamma_i, \forall i, \\ & \mathrm{A3}: 0 \leq p_j \leq P_{\max}^{\mathrm{MD}}, \forall j, \\ & \mathrm{A4}: \sum_{i=1}^{K} \|\mathbf{w}_i\|^2 \leq P_{\max}^{\mathrm{DL}}, \end{aligned} \tag{6.8}$$

where c_1 and c_2 are the weights given to the two objectives, respectively, with $c_1 + c_2 = 1$. Constraints A1 ensures the total offloading latency of each mobile device does not exceed the required threshold T_j. Constraint A2 ensures a certain QoS for the downlink user and constraints A3 and A4 are the maximum power constraints for each mobile device and for downlink transmission, respectively.

At this point, we emphasize the flexibility provided by the MOOP (6.8) with respect to optimization variables. There is a strong interdependency between the optimization variables, in that, increasing the transmit power of the mobile devices in order to satisfy the latency constraints increases the co-channel interference (CCI) to the downlink users. At the same time, increasing the downlink transmit power to satisfy the downlink SINR constraints due to the increase in CCI, increases the SI power, which hinders the reception of the offloaded computation tasks.

The optimization problem (6.8) is non-convex and in general difficult to solve

partly due to the fractional objective functions. In order to solve (6.8), in the following we develop a tractable approach to obtain the optimal resource allocation in an iterative manner.

First, given a fixed power p_j for each mobile device, the problem reduces to obtaining the beamforming vectors for the downlink users. Thus, it can be seen that obtaining the beamforming vectors $\mathbf{w}_i$, for $i = 1,\ldots,K$ in (6.8) aims at minimizing the downlink transmit power in order minimize the SI power to satisfy the constraints. Thus, this can be obtained by solving the following subproblem

$$\begin{aligned} \mathscr{P}6.1\text{a}: \min_{\{\mathbf{w}_i\}} \quad & \sum_{i=1}^{K} \|\mathbf{w}_i\|^2 \\ \text{s.t.} \quad & \text{A1, A2, A4.} \end{aligned} \tag{6.9}$$

The optimization problem (6.9) is non-convex but can be easily solved through semidefinite relaxation (SDR). The SDR formulation of (6.9) is given by

$$\begin{aligned} \widetilde{\mathscr{P}6.1\text{a}}: \min_{\{\mathbf{W}_i \succeq 0\}} & \sum_{i=1}^{K} \mathrm{Tr}\{\mathbf{W}_i\} \\ \text{s.t.} \quad & \widetilde{\text{A1}}: \tau_j - \gamma_j \leq 0, \forall j, \\ & \widetilde{\text{A2}}: \frac{\mathrm{Tr}(\mathbf{H}_i\mathbf{W}_i)}{\Gamma_i} \geq \sum_{k\neq i}^{K} \mathrm{Tr}(\mathbf{H}_i\mathbf{W}_k) + \sum_{j=1}^{J} p_j|\ell_{j,i}|^2 + \sigma_i^2, \forall i, \\ & \widetilde{\text{A4}}: \sum_{i=1}^{K} \mathrm{Tr}(\mathbf{W}_i) \leq P_{\max}^{\mathrm{DL}}, \end{aligned} \tag{6.10}$$

where $\tau_j = 2^{\frac{q_j}{B\left(T_j - \frac{q_j L_{\mathrm{BS},j}}{f_{\mathrm{BS}}}\right)}} - 1$.

The SDR formulation (6.10) is convex and can be solved by standard convex solvers. Please note that, the formulation in (6.10) is a relaxed form of (6.9) where the rank one constraint on $\mathbf{W}_i$ has been dropped. If the resulting solution $\mathbf{W}_i$ after solving (6.10) is rank one, the optimal $\mathbf{w}_i$ can be obtained by applying eigenvalue-decomposition (EVD), otherwise, ramdomization technique [134] can be used to retrieve $\mathbf{w}_i$.

Accordingly, for fixed downlink beamforming vectors $\mathbf{w}_i$, for $i = 1,\ldots,K$, the

transmit power for the mobile devices can be obtained by solving the following subproblem

$$\begin{aligned}\mathscr{P}6.1\text{b}: \min_{\substack{\{p_j\},\{a_j\},\\ \{b_j\}}} \; & c_1 \cdot \left(\sum_{j=1}^{J} q_j a_j\right) + c_2 \cdot \left(\sum_{j=1}^{J} q_j b_j\right) \\ \text{s.t.} \quad & \text{A5}: \frac{p_j}{r_j} \le a_j, \quad \text{A6}: \frac{1}{r_j} \le b_j, \\ & \widetilde{\text{A1}}: \tau_j - \gamma_j \le 0, \forall j, \\ & \text{A3}: 0 \le p_j \le P_{\max}^{\text{MD}}, \forall j.\end{aligned} \tag{6.11}$$

Here, we introduce auxiliary variables a_j and b_j for $j = 1,\ldots,J$. In order to solve (6.11) we analyse the problem using Lagrangian method. Thus, the Lagrange function of problem (6.11) is

$$\begin{aligned}\mathscr{L}\left(p_j,a_j,b_j,\lambda_j,\mu_j,\beta_j,\nu_j\right) = c_1 \sum_{j=1}^{J} q_j a_j + c_2 \sum_{j=1}^{J} q_j b_j + \sum_{j=1}^{J} \lambda_j \left(p_j - a_j r_j\left(\mathbf{w}_i, p_j\right)\right) \\ + \sum_{j=1}^{J} \mu_j \left(1 - b_j r_j\left(\mathbf{w}_i, p_j\right)\right) + \sum_{j=1}^{J} \beta_j \left(\tau_j - \gamma_j\left(\mathbf{w}_i, p_j\right)\right) + \sum_{j=1}^{J} \nu_j \left(p_j - P_{\max}^{\text{MD}}\right),\end{aligned} \tag{6.12}$$

where $\lambda_j, \mu_j, \beta_j, \nu_j$ are the Lagrange multipliers for constraints A5, A6, $\widetilde{\text{A1}}$ and A3, respectively. Based on the definition of Karush-Kuhn-Tucker (KKT) conditions, we have

$$\frac{\partial \mathscr{L}}{\partial p_j} = \lambda_j - \lambda_j a_j \frac{\partial r_j}{\partial p_j} - \mu_j b_j \frac{\partial r_j}{\partial p_j} - \beta_j \frac{\partial \gamma_j}{\partial p_j} + \nu_j = 0, \tag{6.13}$$

$$\frac{\partial \mathscr{L}}{\partial a_j} = c_1 q_j - \lambda_j r_j = 0, \quad \frac{\partial \mathscr{L}}{\partial b_j} = c_2 q_j - \mu_j r_j = 0, \tag{6.14}$$

$$\lambda_j \left(p_j - a_j r_j\right) = 0, \quad \mu_j \left(1 - b_j r_j\right) = 0, \tag{6.15}$$

$$\beta_j \left(\tau_j - \gamma_j\right) = 0, \quad \nu_j \left(p_j - P_{\max}^{\text{MD}}\right) = 0. \tag{6.16}$$

From (6.14) and (6.15) we have $\lambda_j = \frac{c_1 q_j}{r_j}$, $\mu_j = \frac{c_2 q_j}{r_j}$, $a_j = \frac{p_j}{r_j}$ and $b_j = \frac{1}{r_j}$, respectively. Furthermore, notice that the optimal solution (p_j^*, a_j^*, b_j^*) of problem (6.11)

satisfies the KKT conditions of the following J subproblems

$$\begin{aligned} \min_{p_j} \quad & \lambda_j p_j - \lambda_j a_j r_j\left(\mathbf{w}_i, p_j\right) - \mu_j b_j r_j\left(\mathbf{w}_i, p_j\right) \\ \text{s.t.} \quad & \widetilde{\text{A1}} : \tau_j - \gamma_j \leq 0, \\ & \text{A3} : 0 \leq p_j \leq P_{\max}^{\text{MD}}. \end{aligned} \tag{6.17}$$

It is easy to see that the KKT conditions for the subproblem (6.17) are the same as that of problem (6.11) and are given by

$$\lambda_j - \lambda_j a_j \frac{B}{\ln 2}\frac{\Xi_j}{(1+\gamma_j)} - \mu_j b_j \frac{B}{\ln 2}\frac{\Xi_j}{(1+\gamma_j)} - \beta_j \Xi_j + \nu_j = 0, \tag{6.18}$$

$$\beta_j\left(\tau_j - \gamma_j\right) = 0, \tag{6.19}$$

$$\nu_j\left(p_j - P_{\max}^{\text{MD}}\right) = 0. \tag{6.20}$$

where $\Xi_j = \frac{\left|\mathbf{g}_j^H \mathbf{u}_j\right|^2}{s_j + \sigma_j^2 \left\|\mathbf{u}_j\right\|^2}$. From (6.18), we see that the optimal p_j^* is

$$p_j^* = \frac{B}{\ln 2}\frac{\lambda_j a_j + \mu_j b_j}{\lambda_j - \beta_j^* \Xi_j + \nu_j^*} - \frac{1}{\Xi_j}, \tag{6.21}$$

where β_j^* and ν_j^* satisfy the KKT conditions (6.19) and (6.20), respectively. In the following, we examine 3 cases in order to obtain $\{p_j^*, \beta_j^*, \nu_j^*\}$:

1. From (6.19) and (6.20) we have $p_j^* \in \left(\frac{\tau_j}{\Xi_j}, P_{\max}^{\text{MD}}\right)$ for $\beta_j^* = \nu_j^* = 0$. In this case, $p_j^* = M_j$ where $M_j = \frac{B}{\ln 2}\frac{\lambda_j a_j + \mu_j b_j}{\lambda_j} - \frac{1}{\Xi_j}$ according to (6.21). Thus, we have $p_j^* = M_j$ and $\beta_j^* = \nu_j^* = 0$ if $M_j \in \left[\frac{\tau_j}{\Xi_j}, P_{\max}^{\text{MD}}\right]$.

2. If $M_j < \frac{\tau_j}{\Xi_j}$ implies that $\beta_j^* > 0$ from the constraints (6.21). Therefore, $p_j^* = \frac{\tau_j}{\Xi_j}$ and $\nu_j^* = 0$ according to (6.19) and (6.20). By substituting these in (6.21) gives $\beta_j^* = \frac{\lambda_j}{\Xi_j} - \frac{B}{\ln 2}\frac{\lambda_j a_j + \mu_j b_j}{\tau_j + 1}$.

3. Similarly, if $M_j > P_{\max}^{\text{MD}}$ implies that $\nu_j^* > 0$. In this case, $p_j^* = P_{\max}^{\text{MD}}$ and $\beta_j^* = 0$ according to (6.20) and (6.19) and putting these into (6.21) gives $\nu_j^* = \frac{B}{\ln 2}\frac{\Xi_j(\lambda_j a_j + \mu_j b_j)}{P_{\max}^{\text{MD}}\Xi_j + 1} - \lambda_j$.

Accordingly, from these cases the solution to the subproblem shown in (6.11) is

Algorithm 6.3 Iterative algorithm for solving problem (6.8)

1: **Initialization:**
Set $p_j = P_{\max}^{\mathrm{MD}}$, for $j = 1, \ldots, J$,
Obtain $\mathbf{w}_i$, for $i = 1, \ldots, K$, by solving subproblem (6.10)
Repeat
Loop
2: Compute λ_j, μ_j, a_j and b_j, for $j = 1, \ldots, J$,
3: Update p_j, β_j and ν_j, for $j = 1, \ldots, J$,
until convergence. End Loop
4: Update $\mathbf{w}_i$, for $i = 1, \ldots, K$ through solving (6.10)
Until stopping criterion is satisfied.
5: **Output**: $\{\mathbf{w}_i^*\}$ and $\{p_j^*\}$.

given by

$$p_j^* = \begin{cases} \frac{\tau_j}{\Xi_j}, & \text{for } M_j < \frac{\tau_j}{\Xi_j}, \\ M_j, & \text{for } \frac{\tau_j}{\Xi_j} \leq M_j \leq P_{\max}^{\mathrm{MD}}, \\ P_{\max}^{\mathrm{MD}}, & \text{for } M_j > P_{\max}^{\mathrm{MD}}, \end{cases} \tag{6.22}$$

$$\beta_j^* = \begin{cases} \frac{\lambda_j}{\Xi_j} - \frac{B}{\ln 2} \frac{\lambda_j a_j + \mu_j b_j}{\tau_j + 1}, & \text{for } M_j < \frac{\tau_j}{\Xi_j}, \\ 0, & \text{elsewhere}, \end{cases} \tag{6.23}$$

$$\nu_j^* = \begin{cases} 0, & \text{for } M_j \leq P_{\max}^{\mathrm{MD}}, \\ \frac{B}{\ln 2} \frac{\Xi_j (\lambda_j a_j + \mu_j b_j)}{P_{\max}^{\mathrm{MD}} \Xi_j + 1} - \lambda_j, & \text{elsewhere}. \end{cases} \tag{6.24}$$

Algorithm 6.3 summarizes the step by step procedure for solving the optimization (6.8) based on IS.

6.3.2 Trade-off Optimization based on Constructive Interference

In this section, we formulate the MOOP based on constructive interference (CI). The basic idea of CI is that, the knowledge of the downlink data signals at the

FD BS can be used to exploit the multiuser interference rather than suppress it as in the conventional case. The concept of CI has been thoroughly studied in the literature for both PSK and QAM modulation in [13, 105, 106, 121, 122, 157–161] and references therein, where analytical criteria are also derived. For notational convenience, we focus on PSK here. To formulate the MOOP based on CI, we first write the received symbol at the *i-th* downlink user as

$$\widetilde{y}_i = \mathbf{h}_i^H \left(\sum_{k=1}^{K} \mathbf{w}_k e^{j(\phi_k - \phi_i)} \right) = \mathbf{h}_i^H \mathbf{x}, \tag{6.25}$$

where we have omitted the noise term, $\mathbf{x} = \sum_{k=1}^{K} \mathbf{w}_k e^{j(\phi_k - \phi_i)}$ and the unit-energy PSK symbol for the *i-th* downlink user is represented as $d_i = de^{\phi_i}$.

As detailed in [13], for any given PSK constellation point, to guarantee CI, $\widetilde{y}_i$ must fall within the CI region of the constellation. The size of the region is determined by $\theta = \pm\frac{\pi}{Y}$, which is the maximum angle shift within the CI region for a modulation order Y. Accordingly, the downlink SINR constraint that guarantees CI at the *i-th* downlink user [13] is

$$|\Im(\widetilde{y}_i)| \leq \left(\Re(\widetilde{y}_i) - \sqrt{\Gamma_i \sum_{j=1}^{J} p_j^{\text{CI}} |\ell_{j,i}|^2 + \Gamma_i \sigma_i^2} \right) \tan\theta, \tag{6.26}$$

where $\Re$ and $\Im$ are the real and imaginary parts, respectively. Therefore, the MOOP based on CI can be mathematically formulated as

$$\begin{aligned} \mathscr{P}6.2: \min_{\mathbf{x}, \{p_j^{\text{CI}}\}} \quad & c_1 \cdot E_{off}^{\text{CI}} + c_2 \cdot \sum_{j=1}^{J} T_j^{\text{total-CI}} \\ \text{s.t.} \quad & \text{B1}: \frac{q_j}{r_j^{\text{CI}}} + \frac{q_j L_{\text{BS},j}}{f_{\text{BS}}} \leq T_j, \forall j, \\ & \text{B2}: (6.26), \forall i, \\ & \text{B3}: p_j^{\text{CI}} \leq P_{\max}^{\text{MD}}, \forall j, \quad \text{B4}: \|\mathbf{x}\|^2 \leq P_{\max}^{\text{DL}}. \end{aligned} \tag{6.27}$$

Here, $T_j^{\text{total-CI}} = \frac{q_j}{r_j^{\text{CI}}} + \frac{q_j L_{\text{BS},j}}{f_{\text{BS}}}$ and $E_{off}^{\text{CI}} = \sum_{j=1}^{J} p_j^{\text{CI}} t_{off,j}^{\text{CI}}$, where $r_j^{\text{CI}} = B\log_2\left(1+\gamma_j^{\text{CI}}\right)$, $\gamma_j^{\text{CI}} =$

$\frac{p_j\left|\mathbf{g}_j^H\mathbf{u}_j\right|^2}{s_j^{\mathrm{CI}}+\sigma_j^2\left\|\mathbf{u}_j\right\|^2}$ and $s_j^{\mathrm{CI}}=\left|\mathbf{u}_j^H\mathbf{H}_{\mathbf{SI}}\mathbf{x}\right|^2$. The MOOP (6.27) is non-convex. We solve (6.27) in a similar fashion to Section 6.3.1.

For fixed power p_j^{CI}, the variable $\{\mathbf{x}\}$ can be obtained by solving the following subproblem

$$\begin{aligned}\mathscr{P}6.2\mathrm{a}: \min_{\mathbf{x}} \quad & \|\mathbf{x}\|^2 \\ \text{s.t.} \quad & \mathrm{B1}, \mathrm{B2}, \mathrm{B4}.\end{aligned} \tag{6.28}$$

Unlike the conventional scheme, the subproblem (6.28) is convex and can be solved using standard convex solvers. Accordingly, given the variable $\{\mathbf{x}\}$, the transmit power for the mobile devices can be obtained by solving the following subproblem

$$\begin{aligned}\mathscr{P}6.2\mathrm{b}: \min_{\substack{\{p_j^{\mathrm{CI}}\},\{a_j^{\mathrm{CI}}\},\\ \{b_j^{\mathrm{CI}}\}}} \; & c_1\cdot\left(\sum_{j=1}^{J} q_j a_j^{\mathrm{CI}}\right)+c_2\cdot\left(\sum_{j=1}^{J} q_j b_j^{\mathrm{CI}}\right) \\ \text{s.t.} \quad & \mathrm{B5}: \frac{p_j^{\mathrm{CI}}}{r_j^{\mathrm{CI}}}\le a_j^{\mathrm{CI}}, \quad \mathrm{B6}: \frac{1}{r_j^{\mathrm{CI}}}\le b_j^{\mathrm{CI}}, \\ & \widetilde{\mathrm{B1}}: \tau_j-\gamma_j^{\mathrm{CI}}\le 0, \forall j, \\ & \mathrm{B3}: p_j^{\mathrm{CI}}\le P_{\max}^{\mathrm{MD}}, \forall j,\end{aligned} \tag{6.29}$$

To solve (6.29), we analyse the problem using Lagrangian method in a similar fashion to Section 6.3.1. Accordingly, we obtain the following as the corresponding solutions to the problem (6.29)

$$\lambda_j^{\mathrm{CI}}=\frac{c_1 q_j}{r_j^{\mathrm{CI}}}, \mu_j^{\mathrm{CI}}=\frac{c_2 q_j}{r_j^{\mathrm{CI}}}, a_j^{\mathrm{CI}}=\frac{p_j^{\mathrm{CI}}}{r_j^{\mathrm{CI}}}, b_j^{\mathrm{CI}}=\frac{1}{r_j^{\mathrm{CI}}},$$

$$p_j^{\mathrm{CI}^*}=\begin{cases}\frac{\tau_j}{\Xi_j^{\mathrm{CI}}}, & \text{for } M_j^{\mathrm{CI}}<\frac{\tau_j}{\Xi_j^{\mathrm{CI}}}, \\ M_j^{\mathrm{CI}}, & \text{for } \frac{\tau_j}{\Xi_j^{\mathrm{CI}}}\le M_j^{\mathrm{CI}}\le P_{\max}^{\mathrm{MD}}, \\ P_{\max}^{\mathrm{MD}}, & \text{for } M_j^{\mathrm{CI}}>P_{\max}^{\mathrm{MD}},\end{cases}$$

$$\beta_j^{\mathrm{CI}^*} = \begin{cases} \frac{\lambda_j^{\mathrm{CI}}}{\Xi_j^{\mathrm{CI}}} - \frac{B}{\ln 2}\frac{\lambda_j^{\mathrm{CI}} a_j^{\mathrm{CI}} + \mu_j^{\mathrm{CI}} b_j^{\mathrm{CI}}}{\tau_j + 1}, & \text{for } M_j^{\mathrm{CI}} < \frac{\tau_j}{\Xi_j^{\mathrm{CI}}}, \\ 0, & \text{elsewhere,} \end{cases}$$

$$\nu_j^{\mathrm{CI}^*} = \begin{cases} 0, & \text{for } M_j^{\mathrm{CI}} \leq P_{\max}^{\mathrm{MD}}, \\ \frac{B}{\ln 2}\frac{\Xi_j^{\mathrm{CI}}(\lambda_j^{\mathrm{CI}} a_j^{\mathrm{CI}} + \mu_j^{\mathrm{CI}} b_j^{\mathrm{CI}})}{P_{\max}^{\mathrm{MD}} \Xi_j^{\mathrm{CI}} + 1} - \lambda_j^{\mathrm{CI}}, & \text{elsewhere,} \end{cases}$$

where $\Xi_j^{\mathrm{CI}} = \frac{\left|\mathbf{g}_j^H \mathbf{u}_j\right|^2}{s_j^{\mathrm{CI}} + \sigma_j^2 \left\|\mathbf{u}_j\right\|^2}$ and $M_j^{\mathrm{CI}} = \frac{B}{\ln 2}\frac{\lambda_j^{\mathrm{CI}} a_j^{\mathrm{CI}} + \mu_j^{\mathrm{CI}} b_j^{\mathrm{CI}}}{\lambda_j^{\mathrm{CI}}} - \frac{1}{\Xi_j^{\mathrm{CI}}}$. Please note that, a summary of the Algorithm to solve (6.27) based on CI is omitted, however, (6.27) can be solved by following the same steps as shown in Algorithm 6.3 with the corresponding CI based solutions shown in Section 6.3.2.

6.4 MOOP Designs based on Imperfect CSI

In the previous section, it is assumed that the FD BS has perfect knowledge of the CSI for all the channel links. However, in practice this is not always the case. Thus, in this section in order to investigate the robustness of the considered system, we extend the MOOP algorithm designs in the previous section to accommodate for the case where the FD BS does not have perfect CSI knowledge of the channel links.

In the literature, robust designs can generally be categorized into two main designs: the probabilistic and the deterministic based designs. In probabilistic based designs, the error in the CSI knowledge is assumed to have a certain statistical characteristic like the mean or covariance of the channel. In deterministic based designs, which is adopted in this Section, the error in the CSI is assumed to belong to a given uncertainty set. The size of the set determines the amount of uncertainty on the channel and the system optimizes the worst-case performance which achieves a guaranteed performance level for any channel realization in the set. Therefore, for convenience and to avoid any statistical assumptions on the channel, we adopt the worst-case approach which corresponds well to quantization errors and is also suitable for handling slow-fading channels [89].

Accordingly, to model the imperfect CSI, we assume that the actual chan-

nels $\mathbf{h}_i, \ell_{j,i}, \mathbf{H}_{\mathrm{SI}}$ and $\mathbf{g}_j$, for $i = 1,\ldots,K$ and $j = 1,\ldots,J$, respectively, lie in the neighbourhood of the estimated channels $\hat{\mathbf{h}}_i, \hat{\ell}_{j,i}, \hat{\mathbf{H}}_{\mathrm{SI}}$ and $\hat{\mathbf{g}}_j$, for $i = 1,\ldots,K$ and $j = 1,\ldots,J$, respectively. Hence, the actual channels are modelled as

$$\begin{aligned}
&\mathbf{h}_i = \hat{\mathbf{h}}_i + \mathbf{e}_{h,i}, \text{ such that } \left\|\mathbf{e}_{h,i}\right\| \leq \varepsilon_{h,i}, \forall i,\\
&\ell_{j,i} = \hat{\ell}_{j,i} + e_{j,i}, \text{ such that } \left|e_{j,i}\right| \leq \varepsilon_{j,i}, \forall j,i,\\
&\mathbf{g}_j = \hat{\mathbf{g}}_j + \mathbf{e}_{g,j}, \text{ such that } \left\|\mathbf{e}_{g,j}\right\| \leq \varepsilon_{g,j}, \forall j,\\
&\mathbf{H}_{\mathrm{SI}} = \hat{\mathbf{H}}_{\mathrm{SI}} + \mathbf{E}_{\mathrm{SI}} \text{ such that } \left\|\mathbf{E}_{\mathrm{SI}}\right\|_F \leq \varepsilon_{\mathrm{SI}},
\end{aligned}$$

where $\mathbf{e}_{h,i}, e_{j,i}, \mathbf{e}_{g,j}$ and $\mathbf{E}_{\mathrm{SI}}$ represent the channel uncertainties that are assumed to be bounded. We assume the FD BS has no knowledge of the channel uncertainties except their bounds, hence, we take the worst case approach for our algorithm designs. In the following subsections, we present the robust solutions for the proposed interference suppression and interference exploitation designs presented in Section 6.3.

6.4.1 Robust Trade-off Design based on IS

The robust formulation of the MOOP based on IS in (6.8) can be expressed as

$$\begin{aligned}
\mathscr{P}6.3: \min_{\{\mathbf{w}_i\},\{p_j\}} \; & c_1 \cdot \hat{E}_{off} + c_2 \cdot \sum_{j=1}^{J} \hat{T}_j^{\mathrm{total}} \\
\text{s.t.} \quad & \mathrm{C1}: \max_{\mathbf{e}_{g,j},\mathbf{E}_{\mathrm{SI}}} \frac{q_j}{\hat{r}_j} + \frac{q_j L_{\mathrm{BS},j}}{f_{\mathrm{BS}}} \leq T_j, \forall \left\|\mathbf{e}_{g,j}\right\| \leq \varepsilon_{g,j}, \left\|\mathbf{E}_{\mathrm{SI}}\right\|_F \leq \varepsilon_{\mathrm{SI}}, \forall j, \\
& \mathrm{C2}: \min_{\mathbf{e}_{h,i},e_{j,i}} \hat{\Gamma}_i^{\mathrm{DL}} \geq \Gamma_i, \forall \left\|\mathbf{e}_{h,i}\right\| \leq \varepsilon_{h,i}, \left\|e_{j,i}\right\| \leq \varepsilon_{j,i}, \forall i, \\
& \mathrm{C3}: 0 \leq p_j \leq P_{\max}^{\mathrm{MD}}, \forall j, \\
& \mathrm{C4}: \sum_{i=1}^{K} \left\|\mathbf{w}_i\right\|^2 \leq P_{\max}^{\mathrm{DL}},
\end{aligned} \tag{6.30}$$

where we have

$$\hat{\Gamma}_i^{\mathrm{DL}} = \frac{\left|\left(\hat{\mathbf{h}}_i + \mathbf{e}_{h,i}\right)^H \mathbf{w}_i\right|^2}{\sum_{k\neq i}^{K} \left|\left(\hat{\mathbf{h}}_i + \mathbf{e}_{h,i}\right)^H \mathbf{w}_k\right|^2 + \sum_{j=1}^{J} p_j \left|\hat{\ell}_{j,i} + e_{j,i}\right|^2 + \sigma_i^2},$$

$$\hat{\gamma}_j = \frac{p_j \left| \left(\hat{\mathbf{g}}_j + \mathbf{e}_{g,j}\right)^H \mathbf{u}_j \right|^2}{\sum_{n\neq j}^{J} p_n \left| \left(\hat{\mathbf{g}}_n + \mathbf{e}_{g,n}\right)^H \mathbf{u}_j \right|^2 + \hat{s}_j + \sigma_j^2 \left\| \mathbf{u}_j \right\|^2},$$

$$\hat{s}_j = \sum_{i=1}^{K} \left| \mathbf{u}_j^H \left(\hat{\mathbf{H}}_{\mathrm{SI}} + \mathbf{E}_{\mathrm{SI}}\right) \mathbf{w}_i \right|^2,$$

$$\hat{r}_j = B \log_2 \left(1 + \hat{\gamma}_j\right),$$

$$\hat{E}_{off} = \sum_{j=1}^{J} p_j \hat{t}_{off,j},$$

$$\sum_{j=1}^{J} \hat{T}_j^{\mathrm{total}} = \frac{q_j}{\hat{r}_j} + \frac{q_j L_{\mathrm{BS},j}}{f_{\mathrm{BS}}}.$$

The formulation in (6.30) is evidently a non-convex problem, in addition, it contains many inequalities that makes the worst-case design particularly challenging to solve. To solve (6.30), we simply follow the algorithm design in Section 6.3.1. Hence, the SDR formulations of constraint C1 and C2 can be written respectively as

$$\frac{p_j \left| \left(\hat{\mathbf{g}}_j + \mathbf{e}_{g,j}\right)^H \mathbf{u}_j \right|^2}{\sum_{n\neq j}^{J} p_n \left| \left(\hat{\mathbf{g}}_n + \mathbf{e}_{g,n}\right)^H \mathbf{u}_j \right|^2 + \hat{s}_j^{\mathrm{SI}} + \sigma_j^2 \left\| \mathbf{u}_j \right\|^2} \geq \tau_j, \tag{6.31}$$

where $\hat{s}_j^{\mathrm{SI}} = \mathrm{Tr}\left\{ \left(\hat{\mathbf{H}}_{\mathrm{SI}} + \mathbf{E}_{\mathrm{SI}}\right) \sum_{i=1}^{K} \mathbf{W}_i \left(\hat{\mathbf{H}}_{\mathrm{SI}} + \mathbf{E}_{\mathrm{SI}}\right)^H \mathbf{U}_j \right\}$, and

$$\frac{\left(\hat{\mathbf{h}}_i + \mathbf{e}_{h,i}\right)^H \mathbf{W}_i \left(\hat{\mathbf{h}}_i + \mathbf{e}_{h,i}\right)}{\sum_{k\neq i}^{K} \left(\hat{\mathbf{h}}_i + \mathbf{e}_{h,i}\right)^H \mathbf{W}_k \left(\hat{\mathbf{h}}_i + \mathbf{e}_{h,i}\right) + \sum_{j=1}^{J} p_j \left| \hat{\ell}_{j,i} + e_{j,i} \right|^2 + \sigma_i^2} \geq \Gamma_i. \tag{6.32}$$

Therefore, the robust formulation of (6.10) becomes

$$\begin{aligned}
\mathscr{P}6.3\mathrm{a}: \min_{\{\mathbf{W}_i \succeq 0\}} \quad & \sum_{i=1}^{K} \mathrm{Tr}\{\mathbf{W}_i\} \\
\text{s.t.} \quad & \overline{\mathrm{C1}}: \min_{\mathbf{e}_{g,j}, \mathbf{E}_{\mathrm{SI}}} (6.31), \forall \left\|\mathbf{e}_{g,j}\right\| \leq \varepsilon_{g,j}, \left\|\mathbf{E}_{\mathrm{SI}}\right\|_F \leq \varepsilon_{\mathrm{SI}}, \forall j, \\
& \overline{\mathrm{C2}}: \min_{\mathbf{e}_{h,i}, e_{j,i}} (6.32), \forall \left\|\mathbf{e}_{h,i}\right\| \leq \varepsilon_{h,i}, \left\|e_{j,i}\right\| \leq \varepsilon_{j,i}, \forall i, \\
& \overline{\mathrm{C4}}: \sum_{i=1}^{K} \mathrm{Tr}\left(\mathbf{W}_i\right) \leq P_{\max}^{\mathrm{DL}}.
\end{aligned} \tag{6.33}$$

To make (6.33) more tractable to analyze and solve, we first simplify and relax part of constraints $\overline{\text{C1}}$ and $\overline{\text{C2}}$, and then transform them into linear matrix inequalities (LMIs) using the so-called S-procedure [84]. First, notice that $\overline{\text{C1}}$ can be simplified by introducing auxiliary variables such that $\overline{\text{C1}}$ can be written as the following two constraints

$$\min_{\mathbf{e}_{g,j}} p_j \left| \left(\hat{\mathbf{g}}_j + \mathbf{e}_{g,j}\right)^H \mathbf{u}_j \right|^2 \geq \tau_j \left(\sum_{n \neq j}^{J} p_n \left| \left(\hat{\mathbf{g}}_n + \mathbf{e}_{g,n}\right)^H \mathbf{u}_j \right|^2 + \hat{S}_j^{\text{SI}} \right), \tag{6.34}$$

$$\max_{\mathbf{E}_{\text{SI}}} \text{Tr} \left\{ \left(\hat{\mathbf{H}}_{\text{SI}} + \mathbf{E}_{\text{SI}}\right) \sum_{i=1}^{K} \mathbf{W}_i \left(\hat{\mathbf{H}}_{\text{SI}} + \mathbf{E}_{\text{SI}}\right)^H \mathbf{U}_j \right\} + \sigma_j^2 \left\|\mathbf{u}_j\right\|^2 \leq \hat{S}_j^{\text{SI}}. \tag{6.35}$$

By using the inequalities $\left|\mathbf{x}^H \mathbf{y}\right| \leq \|\mathbf{x}\| \|\mathbf{y}\|$ and $\|\mathbf{x}+\mathbf{y}\|^2 \leq (\|\mathbf{x}\| + \|\mathbf{y}\|)^2$, (6.34) can be relaxed to the following robust formulation

$$p_j \left(|\hat{\mathbf{g}}_j^H \mathbf{u}_j| + \varepsilon_{g,j} \|\mathbf{u}_j\|\right)^2 \geq \tau_j \left(\sum_{n \neq j}^{J} p_n \left(|\hat{\mathbf{g}}_n^H \mathbf{u}_j| + \varepsilon_{g,n} \|\mathbf{u}_j\|\right)^2 + \hat{S}_j^{\text{SI}} \right), \forall j. \tag{6.36}$$

Also, notice that $\overline{\text{C2}}$ can be simplified to the following two constraints,

$$\min_{\mathbf{e}_{h,i}} \left(\hat{\mathbf{h}}_i + \mathbf{e}_{h,i}\right)^H \mathbf{Q}_i \left(\hat{\mathbf{h}}_i + \mathbf{e}_{h,i}\right) - \Gamma_i \left(L_i + \sigma_i^2\right) \geq 0, \forall i, \tag{6.37}$$

$$\max_{e_{j,i}} \sum_{j=1}^{J} p_j \left|\hat{\ell}_{j,i} + e_{j,i}\right|^2 - L_i \leq 0, \forall i, \tag{6.38}$$

where $\mathbf{Q}_i = \mathbf{W}_i - \Gamma_i \sum_{k \neq i}^{K} \mathbf{W}_k$. (6.38) can be relaxed to give the following robust formultion

$$\sum_{j=1}^{J} p_j \left(\left|\hat{\ell}_{j,i}\right| + \varepsilon_{j,i}\right)^2 \leq L_i, \forall i. \tag{6.39}$$

Next, we transform the constraints (6.35) and (6.37) to LMIs using the S-procedure [84]. First, we expand constraints (6.35) and (6.37) by using the fact

that $\mathrm{Tr}\{\mathbf{ABCD}\} = \mathrm{vec}\left(\mathbf{A}^H\right)^H \left(\mathbf{D}^H \otimes \mathbf{B}\right) \mathrm{vec}\left(\mathbf{C}\right)$ as follows

$$\mathbf{e}_{\mathrm{SI}}^H \left(\mathbf{U}_j \otimes \sum_{k=1}^{K} \mathbf{W}_k \right) \mathbf{e}_{\mathrm{SI}} + 2Re\left\{ \hat{\mathbf{h}}_{\mathrm{SI}}^H \left(\mathbf{U}_j \otimes \sum_{k=1}^{K} \mathbf{W}_k \right) \mathbf{e}_{\mathrm{SI}} \right\} + \hat{\mathbf{h}}_{\mathrm{SI}}^H \left(\mathbf{U}_j \otimes \sum_{k=1}^{K} \mathbf{W}_k \right) \hat{\mathbf{h}}_{\mathrm{SI}}^H + \sigma_j^2 \mathrm{Tr}\left\{\mathbf{U}_j\right\} - \hat{S}_j^{\mathrm{SI}} \leq 0 \quad (6.40)$$

$$\mathbf{e}_{h,i}^H \mathbf{Q}_i \mathbf{e}_{h,i} + 2Re\left\{\hat{\mathbf{h}}_i^H \mathbf{Q}_i \mathbf{e}_{h,i}\right\} + \hat{\mathbf{h}}_i^H \mathbf{Q}_i \hat{\mathbf{h}}_i - \Gamma_i \left(L_i + \sigma_i^2\right) \geq 0, \quad (6.41)$$

We denote $\hat{\mathbf{h}}_{\mathrm{SI}} = \mathrm{vec}\left(\hat{\mathbf{H}}_{\mathrm{SI}}^H\right)$ and $\mathbf{e}_{\mathrm{SI}} = \mathrm{vec}\left(\mathbf{E}_{\mathrm{SI}}^H\right)$ where, $\mathrm{vec}\left(\cdot\right)$ stacks the columns of a matrix into a vector and $\otimes$ stands for Kronecker product. Thus, following Lemma 1, (6.40) and (6.41) can be transform into the following LMIs, respectively

$$\begin{bmatrix} \rho\mathbf{I} - Z_j & -Z_j\hat{\mathbf{h}}_{\mathrm{SI}} \\ -\hat{\mathbf{h}}_{\mathrm{SI}}^H Z_j & \hat{S}_j^{\mathrm{SI}} - \hat{\mathbf{h}}_{\mathrm{SI}}^H Z_j \hat{\mathbf{h}}_{\mathrm{SI}} - \sigma_N^2 \mathrm{Tr}\left\{\mathbf{U}_j\right\} - \rho\varepsilon_{\mathrm{SI}}^2 \end{bmatrix} \succeq 0, \forall j, \quad (6.42)$$

where $Z_j = \left(\mathbf{U}_j \otimes \sum_{i=1}^{K} \mathbf{W}_i\right)$, and

$$\begin{bmatrix} \delta_i\mathbf{I} + \mathbf{Q}_i & \mathbf{Q}_i\hat{\mathbf{h}}_i \\ \hat{\mathbf{h}}_i^H\mathbf{Q}_i & \hat{\mathbf{h}}_i^H\mathbf{Q}_i\hat{\mathbf{h}}_i - \Gamma_i\left(L_i + \sigma_i^2\right) - \delta_i\varepsilon_{h,i}^2 \end{bmatrix} \succeq 0, \forall i. \quad (6.43)$$

Therefore, (6.33) can be re-expressed as

$$\begin{aligned} \widetilde{\mathscr{P}6.3\mathrm{a}}: \min_{\{\mathbf{W}_i \succeq 0\}} \quad & \sum_{i=1}^{K} \mathrm{Tr}\{\mathbf{W}_i\} \\ \text{s.t.} \quad & (6.36), \quad (6.39), \quad (6.42), \quad (6.43), \quad \overline{\mathrm{C4}}. \end{aligned} \quad (6.44)$$

The problem (6.44) is convex and can be solved by standard convex solvers. We note that the formulation in (6.44) is a relaxed form of (6.30). If the resulting solution $\mathbf{W}_i$ after solving (6.44) is rank one, the optimal $\mathbf{w}_i$ can be obtained by applying eigenvalue-decomposition (EVD), otherwise, ramdomization technique [134] can be used to retrieve $\mathbf{w}_i$.

Next, for fixed beamforming vectors the transmit power for the mobile devices

can be obtained by solving the following robust subproblem

$$\begin{aligned}\mathscr{P}6.3\text{b}: \min_{\substack{\{p_j\},\{\hat{a}_j\},\\ \{\hat{b}_j\}}} \; & c_1 \cdot \left(\sum_{j=1}^{J} q_j \hat{a}_j\right) + c_2 \cdot \left(\sum_{j=1}^{J} q_j \hat{b}_j\right) \\ \text{s.t.} \quad & \text{C5}: \frac{p_j}{\hat{r}_j} \le \hat{a}_j, \quad \text{C6}: \frac{1}{\hat{r}_j} \le \hat{b}_j, \\ & \widetilde{\text{C1}}: \tau_j - \hat{\gamma}_j \le 0, \forall j, \\ & \text{C3}: 0 \le p_j \le P_{\max}^{\text{MD}}, \forall j.\end{aligned} \tag{6.45}$$

The Lagrange function of problem (6.45) is

$$\begin{aligned}\mathscr{L}\left(p_j, \hat{a}_j, \hat{b}_j, \hat{\lambda}_j, \hat{\mu}_j, \hat{\beta}_j, \hat{\nu}_j\right) = & c_1 \sum_{j=1}^{J} q_j \hat{a}_j + c_2 \sum_{j=1}^{J} q_j \hat{b}_j + \sum_{j=1}^{J} \hat{\lambda}_j \left(p_j - \hat{a}_j \hat{r}_j\right) \\ & + \sum_{j=1}^{J} \hat{\mu}_j \left(1 - \hat{b}_j \hat{r}_j\right) + \sum_{j=1}^{J} \hat{\beta}_j \left(\tau_j - \hat{\gamma}_j\right) + \sum_{j=1}^{J} \hat{\nu}_j \left(p_j - P_{\max}^{\text{MD}}\right),\end{aligned} \tag{6.46}$$

where $\hat{\lambda}_j, \hat{\mu}_j, \hat{\beta}_j, \hat{\nu}_j$ are Lagrange multipliers. The KKT conditions are given by

$$\begin{aligned}\frac{\partial \mathscr{L}}{\partial p_j} = & \hat{\lambda}_j - \hat{\lambda}_j \hat{a}_j \frac{\partial \hat{r}_j}{\partial p_j} - \hat{\mu}_j \hat{b}_j \frac{\partial \hat{r}_j}{\partial p_j} - \hat{\beta}_j \frac{\partial \hat{\gamma}_j}{\partial p_j} - \sum_{n \ne j}^{J} \hat{\lambda}_n \hat{a}_n \frac{\partial \hat{r}_n}{\partial p_j} - \sum_{n \ne j}^{J} \hat{\mu}_n \hat{b}_n \frac{\partial \hat{r}_n}{\partial p_j} \\ & - \sum_{n \ne j}^{J} \hat{\beta}_n \frac{\partial \hat{\gamma}_n}{\partial p_j} + \hat{\nu}_j = 0,\end{aligned} \tag{6.47}$$

$$\frac{\partial \mathscr{L}}{\partial \hat{a}_j} = c_1 q_j - \hat{\lambda}_j \hat{r}_j = 0, \; \frac{\partial \mathscr{L}}{\partial \hat{b}_j} = c_2 q_j - \hat{\mu}_j \hat{r}_j = 0, \tag{6.48}$$

$$\hat{\lambda}_j \left(p_j - \hat{a}_j \hat{r}_j\right) = 0, \; \hat{\mu}_j \left(1 - \hat{b}_j \hat{r}_j\right) = 0, \tag{6.49}$$

$$\hat{\beta}_j \left(\tau_j - \hat{\gamma}_j\right) = 0, \; \hat{\nu}_j \left(p_j - P_{\max}^{\text{MD}}\right) = 0. \tag{6.50}$$

From (6.48) and (6.49) we have $\hat{\lambda}_j = \frac{c_1 q_j}{\hat{r}_j}$, $\hat{\mu}_j = \frac{c_2 q_j}{\hat{r}_j}$, $\hat{a}_j = \frac{p_j}{\hat{r}_j}$ and $\hat{b}_j = \frac{1}{\hat{r}_j}$, respec-

tively. Also, we have

$$\frac{\partial \hat{\gamma}_j}{\partial p_j} = \frac{\left|\left(\hat{\mathbf{g}}_j + \mathbf{e}_{g,j}\right)^H \mathbf{u}_j\right|^2}{\sum_{n\neq j}^{J} p_n \left|\left(\hat{\mathbf{g}}_n + \mathbf{e}_{g,n}\right)^H \mathbf{u}_j\right|^2 + \hat{s}_j + \sigma_j^2 \left\|\mathbf{u}_j\right\|^2},$$

$$\frac{\partial \hat{r}_j}{\partial p_j} = \frac{B}{\ln 2\left(1+\hat{\gamma}_j\right)} \cdot \frac{\partial \hat{\gamma}_j}{\partial p_j},$$

$$\frac{\partial \hat{\gamma}_n}{\partial p_j} = -\frac{\hat{\gamma}_n^2 \left|\left(\hat{\mathbf{g}}_j + \mathbf{e}_{g,j}\right)^H \mathbf{u}_n\right|^2}{p_n \left|\left(\hat{\mathbf{g}}_n + \mathbf{e}_{g,n}\right)^H \mathbf{u}_n\right|^2},$$

$$\frac{\partial \hat{r}_n}{\partial p_j} = -\frac{B}{\ln 2\left(1+\hat{\gamma}_n\right)} \cdot \frac{\partial \hat{\gamma}_n}{\partial p_j},$$

which can be relaxed to give the following robust formulations, respectively,

$$\begin{aligned}
&\frac{\partial \overline{\gamma}_j}{\partial p_j} = \hat{\Xi}_j, \quad \frac{\partial \overline{r}_j}{\partial p_j} = \frac{B}{\ln 2\left(1+p_j\hat{\Xi}_j\right)} \cdot \hat{\Xi}_j, \\
&\frac{\partial \overline{\gamma}_n}{\partial p_j} = -\frac{\left(p_n\hat{\Xi}_n\right)^2 \left(\left|\hat{\mathbf{g}}_j^H \mathbf{u}_n\right| + \varepsilon_{g,j}\|\mathbf{u}_n\|\right)^2}{p_n\left(\left|\hat{\mathbf{g}}_n^H \mathbf{u}_n\right| + \varepsilon_{g,n}\|\mathbf{u}_n\|\right)^2}, \\
&\frac{\partial \overline{r}_n}{\partial p_j} = -\frac{B}{\ln 2\left(1+p_n\hat{\Xi}_n\right)} \cdot \frac{-\partial \overline{\gamma}_n}{\partial p_j},
\end{aligned}$$

where $\hat{\Xi}_j = \frac{\left(\left|\hat{\mathbf{g}}_j^H \mathbf{u}_j\right| + \varepsilon_{g,j}\|\mathbf{u}_j\|\right)^2}{\sum_{n\neq j}^{J} p_n\left(\left|\hat{\mathbf{g}}_n^H \mathbf{u}_j\right| + \varepsilon_{g,n}\|\mathbf{u}_j\|\right)^2 + \overline{s}_j + \sigma_j^2\left\|\mathbf{u}_j\right\|^2}$ and $\overline{s}_j = \sum_{i=1}^{K}\left(\left|\mathbf{u}_j^H \hat{\mathbf{H}}_{\mathrm{SI}} \mathbf{w}_i\right| + \varepsilon_{\mathrm{SI}}\|\mathbf{u}_j\|\|\mathbf{w}_i\|\right)^2$. Here, we used the inequalities $\left|\mathbf{x}^H\mathbf{y}\right| \leq \|\mathbf{x}\|\,\|\mathbf{y}\|$ and $\|\mathbf{x}+\mathbf{y}\|^2 \leq \left(\|\mathbf{x}\| + \|\mathbf{y}\|\right)^2$. Further notice that, the optimal solutions of (6.45) can be obtained by solving the following J subproblems since they have the same KKT conditions

$$\begin{aligned}
\min_{p_j} \quad & \hat{\lambda}_j p_j + D_j p_j - \hat{\lambda}_j \hat{a}_j \hat{r}_j - \hat{\mu}_j \hat{b}_j \hat{r}_j \\
\text{s.t.} \quad & \widetilde{\mathrm{C1}} : \tau_j - \hat{\gamma}_j \leq 0, \\
& \mathrm{C3} : 0 \leq p_j \leq P_{\max}^{\mathrm{MD}},
\end{aligned} \tag{6.51}$$

where

$$D_j = -\sum_{n\neq j}^{J} \hat{\beta}_n \frac{\partial \overline{\gamma}_n}{\partial p_j} - \sum_{n\neq j}^{J} \hat{\lambda}_n \hat{a}_n \frac{\partial \overline{r}_n}{\partial p_j} - \sum_{n\neq j}^{J} \hat{\mu}_n \hat{b}_n \frac{\partial \overline{r}_n}{\partial p_j}.$$

The KKT conditions are given by

$$\hat{\lambda}_j + D_j - \hat{\lambda}_j \hat{a}_j \frac{\partial \overline{r}_j}{\partial p_j} - \hat{\mu}_j \hat{b}_j \frac{\partial \overline{r}_j}{\partial p_j} - \hat{\beta}_j \frac{\partial \overline{\gamma}_j}{\partial p_j} + \hat{v}_j = 0, \tag{6.52}$$

$$\hat{\beta}_j \left(\tau_j - \hat{\gamma}_j\right) = 0, \tag{6.53}$$

$$\hat{v}_j \left(p_j - P_{\max}^{\mathrm{MD}}\right) = 0. \tag{6.54}$$

From (6.52), we have

$$p_j^* = \frac{B}{\ln 2} \frac{\hat{\lambda}_j \hat{a}_j + \hat{\mu}_j \hat{b}_j}{\hat{\lambda}_j + D_j - \hat{\beta}_j^* \hat{\Xi}_j + \hat{v}_j^*} - \frac{1}{\hat{\Xi}_j}, \tag{6.55}$$

where $\hat{\beta}_j^*$ and $\hat{v}_j^*$ satisfy the KKT conditions (6.53) and (6.54), respectively. After examining the KKT conditions in similar fashion as in Section 6.3.1, we obtain the following optimal solutions

$$p_j^* = \begin{cases} \frac{\tau_j}{\hat{\Xi}_j}, & \text{for } \hat{M}_j < \frac{\tau_j}{\hat{\Xi}_j}, \\ \hat{M}_j, & \text{for } \frac{\tau_j}{\hat{\Xi}_j} \leq \hat{M}_j \leq P_{\max}^{\mathrm{MD}}, \\ P_{\max}^{\mathrm{MD}}, & \text{for } \hat{M}_j > P_{\max}^{\mathrm{MD}}, \end{cases} \tag{6.56}$$

$$\hat{\beta}_j^* = \begin{cases} \frac{\hat{\lambda}_j + D_j}{\hat{\Xi}_j} - \frac{B}{\ln 2} \frac{\hat{\lambda}_j \hat{a}_j + \hat{\mu}_j \hat{b}_j}{\tau_j + 1}, & \text{for } \hat{M}_j < \frac{\tau_j}{\hat{\Xi}_j}, \\ 0, & \text{elsewhere}, \end{cases} \tag{6.57}$$

$$\hat{v}_j^* = \begin{cases} 0, & \text{for } \hat{M}_j \leq P_{\max}^{\mathrm{MD}}, \\ \frac{B}{\ln 2} \frac{\hat{\Xi}_j (\hat{\lambda}_j \hat{a}_j + \hat{\mu}_j \hat{b}_j)}{P_{\max}^{\mathrm{MD}} \hat{\Xi}_j + 1} - \hat{\lambda}_j - D_j, & \text{elsewhere}, \end{cases} \tag{6.58}$$

where $\hat{M}_j = \frac{B}{\ln 2} \frac{\hat{\lambda}_j \hat{a}_j + \hat{\mu}_j \hat{b}_j}{\hat{\lambda}_j + D_j} - \frac{1}{\hat{\Xi}_j}$. We note that, the same procedure as shown in Algorithm 6.3 can be used to solve the robust optimization problem (6.30) based on IS with the corresponding solutions shown in Section 6.4.1.

6.4.2 Robust Trade-off Design based on CI

For the robust design based on CI, we start by writing the robust formulation of (6.26) as

$$|\Im(\hat{y}_i)| \leq \left(\Re(\hat{y}_i) - \sqrt{\Gamma_i \sum_{j=1}^{J} p_j^{\text{CI}} \left| \hat{\ell}_{j,i} + e_{j,i} \right|^2 + \Gamma_i \sigma_i^2} \right) \tan\theta, \tag{6.59}$$

where $\hat{y}_i = \left(\hat{\mathbf{h}}_i + \mathbf{e}_{h,i}\right)^H \mathbf{x}$. Thus, the robust formulation of (6.27) becomes

$$\begin{aligned} \mathscr{P}6.4: \min_{\mathbf{x},\{p_j^{\text{CI}}\}} \quad & c_1 \cdot \hat{E}_{off}^{\text{CI}} + c_2 \cdot \sum_{j=1}^{J} \hat{T}_j^{\text{total-CI}} \\ \text{s.t.} \quad & \text{D1}: \max_{\mathbf{e}_{g,j},\mathbf{E}_{\text{SI}}} \frac{q_j}{\hat{r}_j^{\text{CI}}} + \frac{q_j L_{\text{BS},j}}{f_{\text{BS}}} \leq T_j, \forall \left\|\mathbf{e}_{g,j}\right\| \leq \varepsilon_{g,j}, \|\mathbf{E}_{\text{SI}}\|_F \leq \varepsilon_{\text{SI}}, \forall j, \\ & \text{D2}: \max_{\mathbf{e}_{h,i},e_{j,i}} (6.59), \forall \left\|\mathbf{e}_{h,i}\right\| \leq \varepsilon_{h,i}, \left\|e_{j,i}\right\| \leq \varepsilon_{j,i}, \forall i, \\ & \text{D3}: p_j^{\text{CI}} \leq P_{\max}^{\text{MD}}, \forall j, \\ & \text{D4}: \|\mathbf{x}\|^2 \leq P_{\max}^{\text{DL}}. \end{aligned} \tag{6.60}$$

Here, $\hat{T}_j^{\text{total-CI}} = \frac{q_j}{\hat{r}_j^{\text{CI}}} + \frac{q_j L_{\text{BS},j}}{f_{\text{BS}}}$ and $\hat{E}_{off}^{\text{CI}} = \sum_{j=1}^{J} p_j^{\text{CI}} \hat{t}_{off,j}^{\text{CI}}$, where $\hat{r}_j^{\text{CI}} = B\log_2\left(1+\hat{\gamma}_j^{\text{CI}}\right)$, $\hat{\gamma}_j^{\text{CI}} = \frac{p_j^{\text{CI}} \left| \left(\hat{\mathbf{g}}_j + \mathbf{e}_{g,j}\right)^H \mathbf{u}_j \right|^2}{\sum_{n\neq j}^{J} p_n^{\text{CI}} \left| \left(\hat{\mathbf{g}}_n + \mathbf{e}_{g,n}\right)^H \mathbf{u}_j \right|^2 + \hat{s}_j^{\text{CI}} + \sigma_j^2 \|\mathbf{u}_j\|^2}$ and $\hat{s}_j^{\text{CI}} = \left| \mathbf{u}_j^H \left(\hat{\mathbf{H}}_{\text{SI}} + \mathbf{E}_{\text{SI}}\right) \mathbf{x} \right|^2$. Following the algorithm design in Section 6.3.2, for fixed $\{p_j^{\text{CI}}\}$ we obtain $\mathbf{x}$ by solving

$$\begin{aligned} \mathscr{P}6.4\text{a}: \min_{\mathbf{x}} \quad & \|\mathbf{x}\|^2 \\ \text{s.t.} \quad & \text{D1, D2, D4.} \end{aligned} \tag{6.61}$$

Problem (6.61) is non-convex. We solve (6.61) as follows. First, consider constraint D1 which can be written as

$$p_j^{\text{CI}} \left| \left(\hat{\mathbf{g}}_j + \mathbf{e}_{g,j}\right)^H \mathbf{u}_j \right|^2 \geq \tau_j \left[\sum_{n\neq j}^{J} p_n^{\text{CI}} \left| \left(\hat{\mathbf{g}}_n + \mathbf{e}_{g,n}\right)^H \mathbf{u}_j \right|^2 + \hat{s}_j^{\text{CI}} + \sigma_j^2 \left\|\mathbf{u}_j\right\|^2 \right], \tag{6.62}$$

which can be relaxed to give the following robust formulation

$$p_j\left(|\hat{\mathbf{g}}_j^H\mathbf{u}_j|+\varepsilon_{g,j}\|\mathbf{u}_j\|\right)^2 \geq \tau_j\left[\sum_{n\neq j}^{J} p_n\left(|\hat{\mathbf{g}}_n^H\mathbf{u}_j|+\varepsilon_{g,n}\|\mathbf{u}_j\|\right)^2 + \left(|\mathbf{u}_j^H\hat{\mathbf{H}}_{\mathrm{SI}}\mathbf{x}|^2+\varepsilon_{\mathrm{SI}}\|\mathbf{u}_j\|\|\mathbf{x}\|\right)^2+\sigma_j^2\left\|\mathbf{u}_j\right\|^2\right], \forall j. \quad (6.63)$$

Constraint D2 can be written as

$$\left|(\underline{\hat{\mathbf{h}}}_i+\underline{\mathbf{e}}_{h,i})^H\underline{\mathbf{x}}\right| - \left[(\underline{\hat{\mathbf{h}}}_i+\underline{\mathbf{e}}_{h,i})^H\Pi\underline{\mathbf{x}} - \sqrt{\Gamma_i\left(\sum_{j=1}^{J} p_j\left|\hat{\ell}_{j,i}+e_{j,i}\right|^2+\sigma_i^2\right)}\right]\tan\theta \leq 0, \forall i, \quad (6.64)$$

which can be relaxed to the following two robust formulations

$$\underline{\hat{\mathbf{h}}}_i^H(\underline{\mathbf{x}}-\Pi\underline{\mathbf{x}}\tan\theta)+\varepsilon_{h,i}\|\underline{\mathbf{x}}-\Pi\underline{\mathbf{x}}\tan\theta\|+\sqrt{\Gamma_i\left(\sum_{j=1}^{J} p_j\left(\left|\hat{\ell}_{j,i}\right|+\varepsilon_{j,i}\right)^2\right)}\tan\theta\leq 0, \forall i, \quad (6.65)$$

$$\underline{\hat{\mathbf{h}}}_i^H(-\underline{\mathbf{x}}-\Pi\underline{\mathbf{x}}\tan\theta)+\varepsilon_{h,i}\|-\underline{\mathbf{x}}-\Pi\underline{\mathbf{x}}\tan\theta\|+\sqrt{\Gamma_i\left(\sum_{j=1}^{J} p_j\left(\left|\hat{\ell}_{j,i}\right|+\varepsilon_{j,i}\right)^2\right)}\tan\theta\leq 0, \forall i, \quad (6.66)$$

where $\underline{\mathbf{x}}=\begin{bmatrix}\Re(\mathbf{x})^H & \Im(\mathbf{x}^H)\end{bmatrix}^H$, $\Pi=\begin{bmatrix}\mathbf{0}_N & -\mathbf{I}_N\\ \mathbf{I}_N & \mathbf{0}_N\end{bmatrix}$, $\underline{\hat{\mathbf{h}}}_i=\begin{bmatrix}\Im(\hat{\mathbf{h}}_i)^H & \Re(\hat{\mathbf{h}}_i)^H\end{bmatrix}^H$, $\underline{\mathbf{e}}_{h,i}=\begin{bmatrix}\Im(\mathbf{e}_{h,i})^H & \Re(\mathbf{e}_{h,i})^H\end{bmatrix}^H$. Therefore, problem the transformed problem (6.61) can be expressed as

$$\begin{aligned}\widetilde{\mathscr{P}6.4\mathrm{a}}: \min_{\mathbf{x}} \quad & \|\mathbf{x}\|^2\\ \text{s.t.} \quad & (6.63), (6.65), (6.66), \mathrm{D4}.\end{aligned} \quad (6.67)$$

(6.67) is convex and can be solved using standard convex solvers.

Accordingly, given the variable $\{\mathbf{x}\}$, the transmit power for the mobile devices

can be obtained by solving the following subproblem

$$\begin{aligned}\mathscr{P}6.4\text{b}: \min_{\substack{\{p_j^{\mathrm{CI}}\},\{\hat{a}_j^{\mathrm{CI}}\},\\ \{\hat{b}_j^{\mathrm{CI}}\}}} & c_1\cdot\left(\sum_{j=1}^{J} q_j\hat{a}_j^{\mathrm{CI}}\right)+c_2\cdot\left(\sum_{j=1}^{J} q_j\hat{b}_j^{\mathrm{CI}}\right)\\ \text{s.t.}\quad & \mathrm{D5}: \frac{p_j^{\mathrm{CI}}}{\hat{r}_j^{\mathrm{CI}}}\le \hat{a}_j^{\mathrm{CI}},\quad \mathrm{D6}: \frac{1}{\hat{r}_j^{\mathrm{CI}}}\le \hat{b}_j^{\mathrm{CI}},\\ & \widetilde{\mathrm{D1}}: \tau_j-\hat{\gamma}_j^{\mathrm{CI}}\le 0,\forall j,\\ & \mathrm{D3}: p_j^{\mathrm{CI}}\le P_{\max}^{\mathrm{MD}},\forall j,\end{aligned} \tag{6.68}$$

To solve (6.68), we analyse the problem using Lagrangian method in a similar fashion to Section 6.4.1. Accordingly, we obtain the following as the corresponding solutions to the problem (6.68)

$$\hat{\lambda}_j^{\mathrm{CI}}=\frac{c_1q_j}{\hat{r}_j^{\mathrm{CI}}},\hat{\mu}_j^{\mathrm{CI}}=\frac{c_2q_j}{\hat{r}_j^{\mathrm{CI}}},\hat{a}_j^{\mathrm{CI}}=\frac{p_j^{\mathrm{CI}}}{\hat{r}_j^{\mathrm{CI}}},\hat{b}_j^{\mathrm{CI}}=\frac{1}{\hat{r}_j^{\mathrm{CI}}},$$

$$p_j^{\mathrm{CI}^*}=\begin{cases}\frac{\tau_j}{\hat{\Xi}_j^{\mathrm{CI}}}, & \text{for } \hat{M}_j^{\mathrm{CI}}<\frac{\tau_j}{\hat{\Xi}_j^{\mathrm{CI}}},\\ \hat{M}_j^{\mathrm{CI}}, & \text{for } \frac{\tau_j}{\hat{\Xi}_j^{\mathrm{CI}}}\le\hat{M}_j^{\mathrm{CI}}\le P_{\max}^{\mathrm{MD}},\\ P_{\max}^{\mathrm{MD}}, & \text{for } \hat{M}_j^{\mathrm{CI}}>P_{\max}^{\mathrm{MD}},\end{cases}$$

$$\hat{\beta}_j^{\mathrm{CI}^*}=\begin{cases}\frac{\hat{\lambda}_j^{\mathrm{CI}}+D_j^{\mathrm{CI}}}{\hat{\Xi}_j^{\mathrm{CI}}}-\frac{B}{\ln 2}\frac{\hat{\lambda}_j^{\mathrm{CI}}\hat{a}_j^{\mathrm{CI}}+\hat{\mu}_j^{\mathrm{CI}}\hat{b}_j^{\mathrm{CI}}}{\tau_j+1}, & \text{for } \hat{M}_j^{\mathrm{CI}}<\frac{\tau_j}{\hat{\Xi}_j^{\mathrm{CI}}},\\ 0, & \text{elsewhere},\end{cases}$$

$$\hat{\nu}_j^{\mathrm{CI}^*}=\begin{cases}0, & \text{for } \hat{M}_j^{\mathrm{CI}}\le P_{\max}^{\mathrm{MD}},\\ \frac{B}{\ln 2}\frac{\hat{\Xi}_j^{\mathrm{CI}}(\hat{\lambda}_j^{\mathrm{CI}}\hat{a}_j^{\mathrm{CI}}+\hat{\mu}_j^{\mathrm{CI}}\hat{b}_j^{\mathrm{CI}})}{P_{\max}^{\mathrm{MD}}\hat{\Xi}_j^{\mathrm{CI}}+1}-\hat{\lambda}_j^{\mathrm{CI}}-D_j^{\mathrm{CI}}, & \text{elsewhere},\end{cases}$$

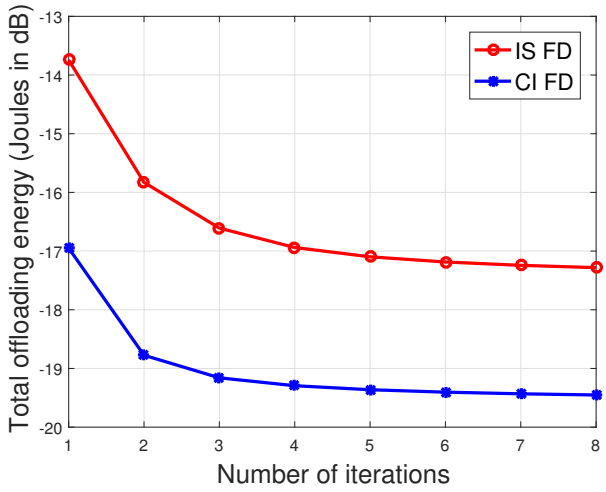

Figure 6.2: Total offloading energy vers[width=8cm]us number of iterations.

where

$$\hat{\Xi}_j^{\mathrm{CI}} = \frac{\left(|\hat{\mathbf{g}}_j^H \mathbf{u}_j| + \varepsilon_{g,j}\|\mathbf{u}_j\|\right)^2}{\sum_{n\neq j}^{J} p_n \left(|\hat{\mathbf{g}}_n^H \mathbf{u}_j| + \varepsilon_{g,n}\|\mathbf{u}_j\|\right)^2 + \bar{s}_j^{\mathrm{CI}} + \sigma_j^2 \left\|\mathbf{u}_j\right\|^2},$$

$$\bar{s}_j^{\mathrm{CI}} = \left(|\mathbf{u}_j^H \hat{\mathbf{H}}_{\mathrm{SI}} \mathbf{x}|^2 + \varepsilon_{\mathrm{SI}}\|\mathbf{u}_j\|\|\mathbf{x}\|\right)^2,$$

$$\hat{M}_j^{\mathrm{CI}} = \frac{B}{\ln 2} \frac{\hat{\lambda}_j \hat{a}_j^{\mathrm{CI}} + \hat{\mu}_j^{\mathrm{CI}} \hat{b}_j^{\mathrm{CI}}}{\hat{\lambda}_j^{\mathrm{CI}} + D_j^{\mathrm{CI}}} - \frac{1}{\hat{\Xi}_j^{\mathrm{CI}}}.$$

To solve the robust design problem in (6.60), similar steps as in Algorithm 6.3 are followed by adopting the corresponding CI based solutions as detailed in Section 6.4.2, respectively.

6.5 Simulation Results

In this section, we investigate the performance of our proposed schemes through Monte Carlo simulations. We consider the system with the FD BS at the centre of a cell with $N = 6$. We assume $K = 4$ DL users and $J = 2$ MDs, are randomly and uniformly distributed between the distance of 2m and 20m. We model the channels to the MDs and DL users as Rayleigh fading. The SI channel is modelled as Rician fading channel with Rician factor 6dB [117]. Furthermore, we consider a similar system set-up as in [116] with $\sigma_i = \sigma_j = -90\text{dB}, P_{\max}^{\mathrm{MD}} = 32\text{dBm}$ and $P_{\max}^{\mathrm{DL}} = 40\text{dBm}$.

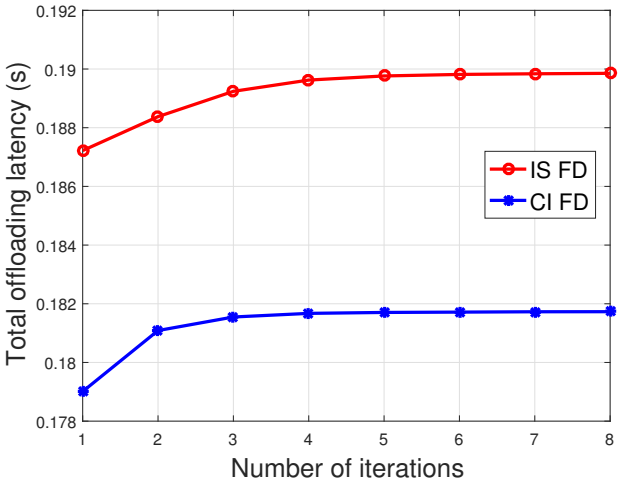

Figure 6.3: Total offloading latency versus number of iterations.

Moreover, we assume $T = 100\text{ms}, \Gamma_i = 4\text{dB}, B = 1\text{MHz}, q_j = 10^5, L_{\text{BS},j} = 10^3$ and $f_{\text{BS}} = 10^{10}$ as in [14, 144], and QPSK modulation is considered for the CI scheme.

Our baseline is the HD scheme as in [147]. In order to make the comparison fair, we consider that the HD BS is equipped with N number of transmit and N number of receive antennas which are utilized for transmitting or receiving in non-overlapping equal-length time intervals. This implies that both SI and CCI are avoided. In addition, we set the data rate of HD equal to the one for FD, which requires that the individual mobile devices' and downlink users' data rates are double the ones for the FD case, due to the slotted HD transmission. Furthermore, the power consumption for the uplink and downlink transmission is divided by two since only uplink or downlink transmission is performed at a given time.

6.5.1 Convergence and Complexity of Algorithms

In this subsection, we show the convergence and complexity to the solutions for the proposed MOOPs in (6.8) and (6.27), respectively. Since the objective functions in (6.8) and (6.27) decrease in every iteration the convergence of Algorithm 6.3 is guaranteed, which can realized from optimizing all $\mathbf{w}_k$ and p_j in each iteration as shown in Algorithm 6.3. In Figs. 6.2 and 6.3, we show the convergence rate of the proposed solutions with respect to number of iterations. Each point in the curves is obtained by solving the MOOPs in (6.8) and (6.27) for the correspond-

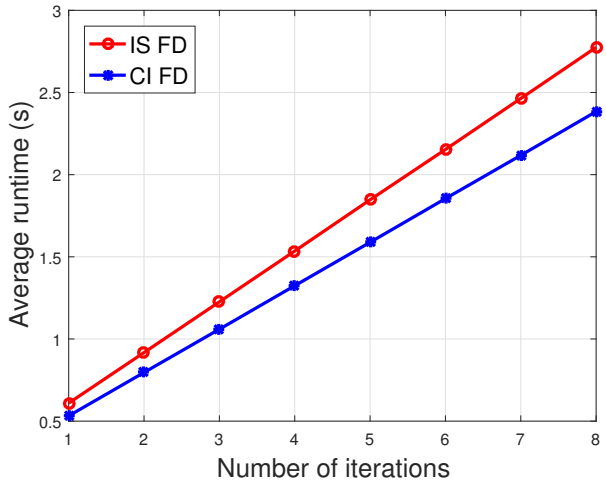

Figure 6.4: Average Run time versus number of iterations.

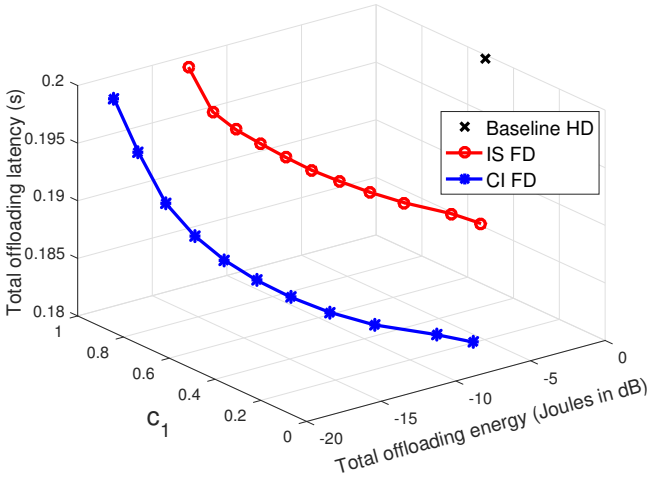

Figure 6.5: Trade-off plot total offloading energy versus latency with $N = 6, K = 4, J = 2, T = 100\text{ms}, \Gamma_i = 4\text{dB}, B = 1\text{MHz}, q_j = 10^5, L_{\text{BS},j} = 10^3$ and $f_{\text{BS}} = 10^{10}$.

ing number of iteration(s). Generally, we have observed that both the proposed IS and CI schemes converge with the same number of iterations in terms of both the offloading energy and latency respectively, although, it takes fewer iterations for the case of the offloading latency. This is attributed to the strictness of the offloading latency threshold imposed for each mobile device. In addition, even with the same convergence rate, the CI scheme shows improved performance in both plots compared to the IS scheme since multi-user inference in exploited rather than suppressed. Furthermore, in Fig. 6.4, we show the corresponding complexity of the

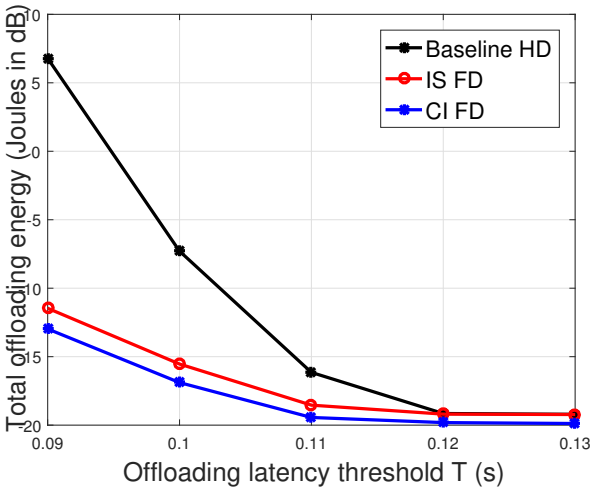

Figure 6.6: Total offloading energy versus latency threshold T, with $N = 6, K = 4, J = 2, c_1 = c_2 = 0.5, \Gamma_i = 4\text{dB}, B = 1\text{MHz}, q_j = 10^5, L_{\text{BS},j} = 10^3$ and $f_{\text{BS}} = 10^{10}$.

proposed solutions in terms of the average run time in seconds per iteration. We can observe that, although the solutions to proposed schemes have the same convergence rate, the average run time in seconds per iteration of the CI scheme is faster than the IS scheme. This difference in complexity mainly comes from optimizing the beamforming vectors $\mathbf{w}_k$ through solving subproblems (6.10) and (6.28) for the IS scheme and CI scheme, respectively. The formulation in (6.10) is a standard SDP problem which basically finds the optimal covariance matrix $\mathbf{W}_k$ before retrieving the beamforming vector $\mathbf{w}_k$, while (6.28) is a second-order cone program (SOCP) that finds the optimal beamforming vectors directly. In general, the solutions to the proposed MOOPs show an acceptable complexity as shown in Fig. 6.4.

6.5.2 Numerical Results

Fig. 6.5 shows the trade-off between the total offloading energy and latency. The trade-off region is obtained by varying the weights c_1 and c_2 between 0 to 1, respectively, with a step size of 0.1. First, it can be seen that, where before one could only optimize either the offloading energy with a fixed latency constraint, or the latency with a fixed energy constraint, our proposed MOOP allows for a scalable tradeoff between the two objectives. It is evident that an increase in the offloading energy leads to the decrease in the offloading latency and vice versa. This is as a

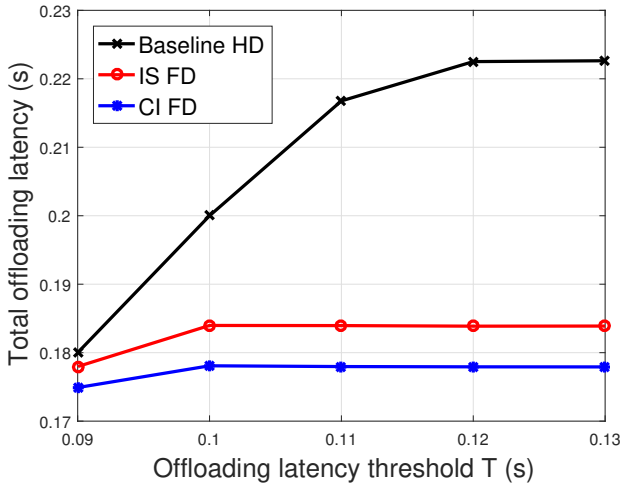

Figure 6.7: Total offloading latency versus latency threshold T with $N = 6, K = 4, J = 2, c_1 = c_2 = 0.5, \Gamma_i = 4\text{dB}, B = 1\text{MHz}, q_j = 10^5, L_{\text{BS},j} = 10^3$ and $f_{\text{BS}} = 10^{10}$.

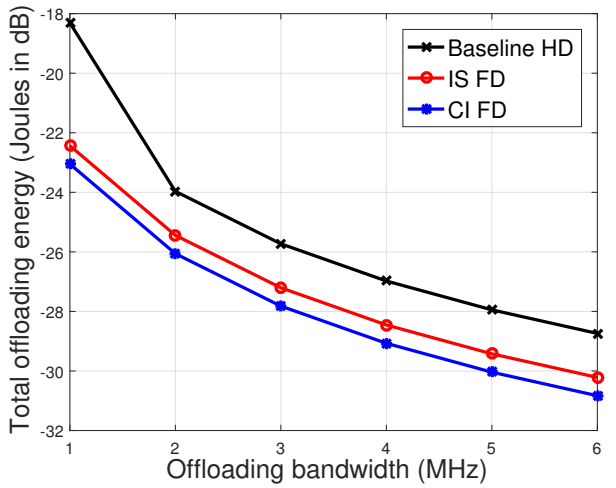

Figure 6.8: Total offloading energy versus offloading bandwidth B, with $N = 6, K = 4, J = 2, c_1 = c_2 = 0.5, \Gamma_i = 4\text{dB}, T = 100\text{ms}, q_j = 10^5, L_{\text{BS},j} = 10^3$ and $f_{\text{BS}} = 10^{10}$.

result of the dependency of the optimization variables. On one hand, increasing the transmit power of the mobile devices in order to satisfy the latency constraints and minimize the offloading latency, increases the CCI to the downlink users. Hence, the downlink transmit power is increased to accommodate for the increase in CCI, which in turn increases the SI. In essence, this leads a continuous increase in the uplink and downlink transmit power, thus, the offloading energy increases. On the contrary, reducing the transmit powers in order to reduce the CCI and SI, and minimize the offloading energy, gives rise to an increase in the offloading latency. In

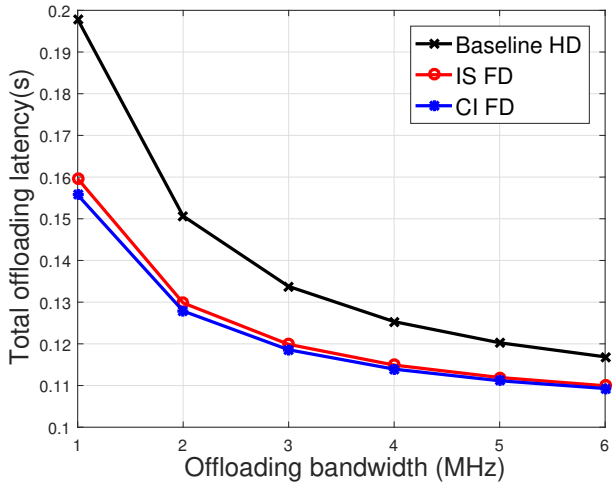

Figure 6.9: Total offloading latency versus offloading bandwidth B, with $N = 6, K = 4, J = 2, c_1 = c_2 = 0.5, \Gamma_i = 4\text{dB}, T = 100\text{ms}, q_j = 10^5, L_{\text{BS},j} = 10^3$ and $f_{\text{BS}} = 10^{10}$.

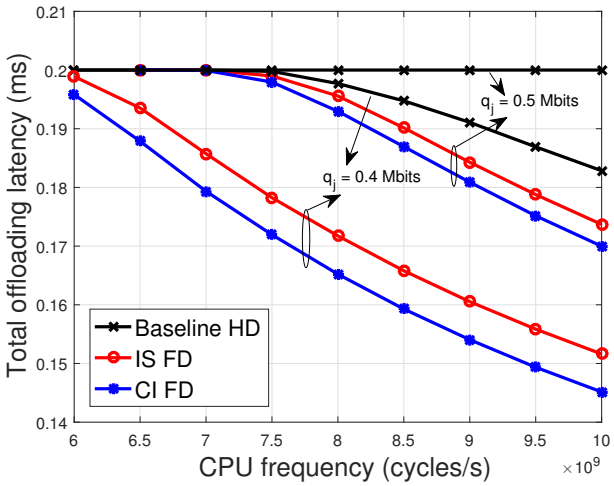

Figure 6.10: Total offloading latency versus CPU frequency f_{BS}, with $N = 6, K = 4, J = 2, c_1 = c_2 = 0.5, \Gamma_i = 4\text{dB}, T = 100\text{ms}, B = 1\text{MHz}$ and $L_{\text{BS},j} = 10^3$.

addition, this results show the proposed CI scheme consumes less energy and time as compared to the conventional FD scheme. This is because less downlink transmit power is required to satisfy the downlink SINR constraints, hence, reduced SI, as compared to the conventional case where interference is rather suppressed. Furthermore, the points $c_1 = 0$ and $c_1 = 1$ is equivalent to the having only the offloading energy minimization problem [142, 144–146] and the offloading latency minimization problem [143], respectively. Again, this shows the flexibility provided by the proposed MOOP by varying the weights. More importantly, it can be seen that the

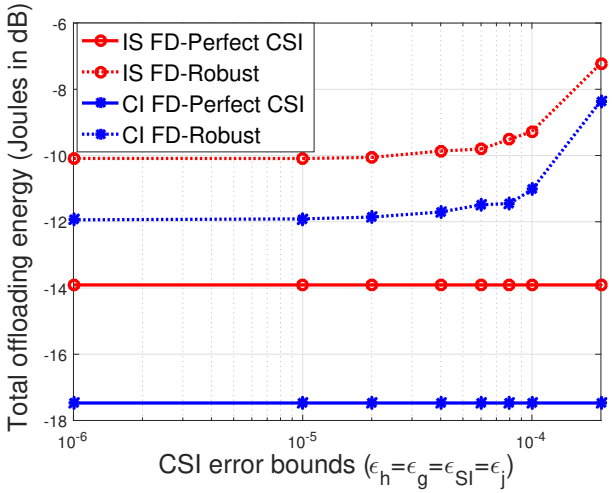

Figure 6.11: Total offloading energy versus Error bounds ($\varepsilon_h = \varepsilon_g = \varepsilon_{SI} = \varepsilon_j$), with $N = 6, K = 4, J = 2, c_1 = c_2 = 0.5, \Gamma_i = 4\text{dB}, B = 1\text{MHz}, T = 100\text{ms}, q_j = 10^5, L_{\text{BS},j} = 10^3$ and $f_{\text{BS}} = 10^{10}$.

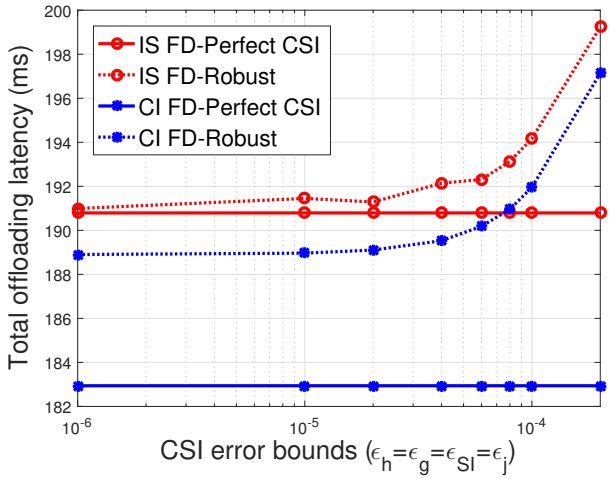

Figure 6.12: Total offloading latency versus Error bounds ($\varepsilon_h = \varepsilon_g = \varepsilon_{SI} = \varepsilon_j$), with $N = 6, K = 4, J = 2, c_1 = c_2 = 0.5, \Gamma_i = 4\text{dB}, B = 1\text{MHz}, T = 100\text{ms}, q_j = 10^5, L_{\text{BS},j} = 10^3$ and $f_{\text{BS}} = 10^{10}$.

proposed FD schemes out perform their baseline HD [147] counterpart in terms of energy consumption and latency reduction.

In Figs. 6.6 and 6.7, we study the effect of different offloading latency thresholds T on the considered system. Here, for the purpose of analyses we set $c_1 = c_2 = 0.5$. Fig. 6.6 shows the total offloading energy for the different latency thresholds. As expected for all the schemes, since increasing the latency thresh-

old requires less transmit powers, thus, the total offloading energy consumption reduces, respectively. However, in terms of offloading latency in Fig. 6.7, all schemes are proportional to increase in latency requirement. Besides, in both plots the FD schemes outperforms the HD scheme. This further highlights the effectiveness of the proposed FD schemes.

Next, we show the effect of the offloading bandwidth (B) in the considered FD system. Fig. 6.8 shows that the total offloading energy consumption decreases as B increases. This indicates that as B increase the offloading rate increases and also energy consumption is saved by all schemes. However, still the proposed FD schemes outperforms the HD counterpart even at large bandwidth. Similar trend can be seen in Fig. 6.9, which shows that increasing B results in latency reduction. This is as a result of the increase in offloading rate which translates directly to reduction in latency. These plots highlight the importance of the offloading bandwidth in the considered FD system.

In addition, Fig. 6.10 shows the total offloading latency versus the CPU frequency of the FD BS. As the CPU frequency increases, less time is required by the FD BS to complete the computation of the offloaded tasks. This is reported in Fig. 6.10 for all schemes. The figure also shows the effect of the computation task size with regards to the CPU frequency. It can be seen that an increase in the computation task size increases the overall offloading latency. This is obviously due the fact that increasing the task size implies more cycles/s is required to complete the task, hence, an increase in the overall latency. Besides, our proposed FD schemes outperform the HD scheme in all cases.

Furthermore, in Figs. 6.11 and 6.12 we investigate the performance of the proposed robust FD schemes. Fig. 6.11 shows the obtained total energy consumption with increasing CSI error bounds where it can be seen that increasing error bound increases the energy consumption. The reason is that increasing the error bounds implies reduced CSI knowledge at the FD BS. Similarly, in Fig. 6.12, the total latency increases with increase in the CSI error bounds.

6.6 Summary

In this chapter, we studied the offloading energy and latency trade-off in a multiuser FD system that performs both data transmission and MEC. We proposed one FD scheme based on the traditional downlink MUI interference suppression and the other based on downlink MUI exploitation. We further extended the two proposed schemes to consider practical scenarios with imperfect CSI knowledge. The proposed FD schemes show a promising performance improvement over the baseline HD schemes.

Chapter 7

Delay-Constrained BF and Resource Allocation in FD Systems

This chapter is based on our publication in [J1].

7.1 Introduction

The strict requirements on latency and reliability for the next generation 5G communication system has set new priorities for researchers and has led to the development of various techniques and algorithms in order to match these requirements. Motivated by this and the fact that the rapid growth of high data rate services leads to the increase in the power consumption in communication networks, it has become important to design power efficient communication systems in order to reduce the amount of greenhouse gases emission and operational expenses of communication systems. In this chapter, we study a delay-constrained beamforming (BF) and resource allocation problem in a multiuser FD system.

In traditional system design, the main goal is to minimize the system power consumption while satisfying some QoS constraints [79]. For example, [12] studied the resource allocation for distributed antenna systems with a FD base station (BS) that simultaneously serves uplink and downlink users where the network power consumption is minimized by jointly optimizing the downlink beamformer and uplink transmit power. Similarly, in [116], the authors investigated a power efficient resource allocation design for secure communications in a similar FD system setup.

Also, the trade-off between the uplink and downlink power consumption was investigated in [116, 154]. In [154], the authors used the knowledge of the downlink signals at the FD BS to exploit multi-user interference (MUI) instead of treating the MUI as unwanted as in traditional interference suppression techniques.

Delay is a critical performance metric that determines the reliability of a wireless system and it is directly related to the system queue length [162]. [163] studied the trade-off between energy efficiency (EE) and delay in time-varying wireless systems by maximizes the system EE subject to network stability constraints. Similarly, in [164] the authors studied EE maximization in a bufffer-aided relay system while maintaining queue stability. In [165], the authors studied resource allocation in LTE-A system by maximizing a utility function of the transmission rate with queue stability constraints. The authors in [166] proposed a QoS-aware resource allocation for vehicle-to-vehicle (V2V) communications by minimizing the transmission power subject to queueing latency constraints.

In contrast to the above mentioned works, which study either resource allocation in FD system without stability constraints or half-duplex (HD) resource allocation with stability constraints, we design a power-efficient resource allocation algorithm in multi-user FD system. Unlike existing FD works in [12, 116, 154], we aim at minimizing the long-term average system transmit power while ensuring system queue stability. Likewise, the existing HD methods in [163–166] can not be applied to our considered problem due to the introduction of SI and CCI in our FD study. This requires the joint optimization of the downlink beamforming vectors and uplink transmit power, which is not trivial to handle given the nature of the problem. Thus, in this chapter we aim at addressing these gaps by means of weighted and delay constrained optimization.

7.2 System Model

We consider a multiuser communication system where a FD BS with N transmit and N receive antennas simultaneously serves K single-antenna downlink users and J uplink users [12, 116, 154]. In the considered system, we assume communication

is time slotted and slot t refers to the interval $[t, t+1)$, where $t \in \{0,1,2,\ldots\}$. We assume that the duration of one time slot is enough to transmit 1 bit of data. Accordingly, by letting $\mathbf{h}_k \in \mathbb{C}^{N\times 1}$ and $\mathbf{g}_j \in \mathbb{C}^{N\times 1}$ be the channels between the FD BS and the *k-th* downlink user, the *j-th* uplink user, respectively, the downlink and uplink transmission rates at slot t in unit of bits/slot/Hz are defined respectively by

$$R_{\mathrm{DL},k}(t) = \log_2\left(1+\gamma_{\mathrm{DL},k}\right), \tag{7.1}$$

$$R_{\mathrm{UL},j}(t) = \log_2\left(1+\gamma_{\mathrm{UL},j}\right), \tag{7.2}$$

where

$$\begin{aligned}\gamma_{\mathrm{DL},k}(t) &= \frac{\left|\mathbf{h}_k^H \mathbf{w}_k\right|^2}{\sum_{i\neq k}^{K}\left|\mathbf{h}_k^H \mathbf{w}_i\right|^2 + \sum_{j=1}^{J} P_{\mathrm{UL},j}\left|\ell_{j,k}\right|^2 + \sigma_k^2}, \\ &= \frac{\mathbf{h}_k^H \mathbf{W}_k \mathbf{h}_k}{\sum_{i\neq k}^{K}\mathbf{h}_k^H \mathbf{W}_i \mathbf{h}_k + \sum_{j=1}^{J} P_{\mathrm{UL},j}\left|\ell_{j,k}\right|^2 + \sigma_k^2},\end{aligned} \tag{7.3}$$

$$\gamma_{\mathrm{UL},j}(t) = \frac{P_{\mathrm{UL},j}\left|\mathbf{g}_j^H \mathbf{u}_j\right|^2}{\sum_{n\neq j}^{J} p_n\left|\mathbf{g}_n^H \mathbf{u}_j\right|^2 + s_j + \sigma_j^2\left\|\mathbf{u}_j\right\|^2}, \tag{7.4}$$

are the signal-to-interference plus noise ratio (SINR) at the *k-th* downlink user and at the FD BS, respectively. In (7.3) and (7.4), $\mathbf{w}_k \in \mathbb{C}^{N\times 1}$, $P_{\mathrm{UL},j}$ and $\ell_{j,k}$ denote the beamforming vector for the *k-th* downlink user with $\mathbf{W}_k = \mathbf{w}_k \mathbf{w}_k^H$, the *j-th* uplink transmit power and the channel between the *j-th* uplink user and the *k-th* downlink user, respectively. In addition, $n_k \sim \mathscr{CN}(0,\sigma_k^2)$ and $\mathbf{n}_j \sim \mathscr{CN}(0,\sigma_j^2)$ are the additive white Gaussian noise at the *k-th* downlink user and the FD BS, respectively, and $\mathbf{u}_j \in^{N\times 1}$ is the receive beamforming vector for the *j-th* uplink user. In this chapter, to reduce complexity, we adopt ZF receive beamforming at the FD BS for the detection of the uplink signals.

Furthermore, due to the simultaneous transmission and reception at the FD BS, there is a strong SI that degrades the reception of the uplink signals at the FD BS. In the literature, there are several SI mitigation techniques which could be employed to reduce the effects of SI. In order to isolate our proposed scheme from

the specific implementation of any passive or active SI mitigation techniques, we model the SI after cancellation as $s_j = \rho \left\{ \mathbf{u}_j^H \mathbf{H_{SI}} \left(\sum_{k=1}^{K} \mathbf{W}_k \right) \mathbf{H_{SI}}^H \mathbf{u}_j \right\}$ [116], where the matrix $\mathbf{H_{SI}} \in \mathbb{C}^{N \times N}$ denotes the SI channel at the FD BS and $0 \leq \rho \ll 1$ is the SI cancellation constant.

The FD BS has separate queue buffers to store data for each downlink user. Similarly, at each uplink user a queue buffer is used to store the data to be transmitted to the FD BS. Data arrive through a random process every slot at the FD BS and the uplink users. At slot t, the queue length for the *k-th* downlink user and the *j-th* uplink user are denoted by $Q_{\mathrm{DL},k}(t)$ and $Q_{\mathrm{UL},j}(t)$, respectively, and these queues evolve as follows:

$$Q_{\mathrm{DL},k}(t+1) = \max\left\{ Q_{\mathrm{DL},k}(t) - R_{\mathrm{DL},k}(t), 0 \right\} + A_{\mathrm{DL},k}(t), \tag{7.5}$$

$$Q_{\mathrm{UL},j}(t+1) = \max\left\{ Q_{\mathrm{UL},j}(t) - R_{\mathrm{UL},j}(t), 0 \right\} + A_{\mathrm{UL},j}(t), \tag{7.6}$$

where $A_{\mathrm{DL},k}(t)$ and $A_{\mathrm{UL},j}(t)$ are the data arrival rate for the *k-th* downlink user and the *j-th* uplink user, which follow Poisson distributions, with mean arrival rates of $\overline{A}_{\mathrm{DL},k}$ and $\overline{A}_{\mathrm{UL},j}$, respectively. Accordingly, as data keeps arriving in every slot t, the queue buffers become overloaded which may result to packet drop. In essence, the queue buffers become unstable and communication becomes unreliable in the system.

As such, a discrete time queue process $Q(t)$ is mean-stable if $\lim_{t\to\infty} \frac{\mathbb{E}[|Q(t)|]}{t} = 0$ [167], and a system of queues is said to be stable if all individual queues are stable. This implies that to stabilize the system, it is required to control the size of the queues. In addition, according to Little's law [162], for a given arrival rate the average queue length is proportional to the average delay. Thus, the system delay is dependent on the queue length and stability. As a result, we can address the transmission delay by the queue length and stability. To this end, in our problem formulation we impose a queue stability constraint to ensure that the data in the buffers are not trapped and are delivered with a finite delay. This is equivalent to ensuring that the long-term average transmission rates are greater or equal to the average arrival rates.

7.3 Delay-constrained Power Minimization and Algorithm Design

Due to the stochastic nature of the channel conditions and data arrivals in the considered system and following [163–165], we consider the long-term average system performance metrics in our design. Thus, our main objective is to design an optimal resource allocation optimization problem that minimizes the the time-averaged total system transmit power while satisfying queue stability constraints, quality of service (QoS) constraints as well as maximum power constraints. This can be mathematically formulated as

$$
\begin{aligned}
\mathscr{P}7.1: \quad \min_{\substack{\{\mathbf{W}_k \succeq 0\} \\ \{P_{\mathrm{UL},j}\}}} \quad & c_1 \cdot \sum_{k=1}^{K} \overline{P}_{\mathrm{DL},k} + c_2 \cdot \sum_{j=1}^{J} \overline{P}_{\mathrm{UL},j} \\
\text{s.t.} \quad & \mathrm{A1}: \overline{R}_{\mathrm{DL},k} \geq \overline{A}_{\mathrm{DL},k}, \forall k, \\
& \mathrm{A2}: \overline{R}_{\mathrm{UL},j} \geq \overline{A}_{\mathrm{UL},j}, \forall j, \\
& \mathrm{A3}: \gamma_{\mathrm{DL},k}(t) \geq \Gamma_{\mathrm{DL}}, \forall k, \forall t, \\
& \mathrm{A4}: \gamma_{\mathrm{UL},j}(t) \geq \Gamma_{\mathrm{UL}}, \forall j, \forall t, \\
& \mathrm{A5}: \sum_{k=1}^{K} P_{\mathrm{DL},k}(t) \leq P_{\max}^{\mathrm{DL}}, \forall t, \\
& \mathrm{A6}: 0 \leq P_{\mathrm{UL},j}(t) \leq P_{\max}^{\mathrm{UL}}, \forall j, \forall t,
\end{aligned}
\tag{7.7}
$$

where $P_{\mathrm{DL},k}(t) = \mathrm{Tr}\{\mathbf{W}_k\}$, and c_1 and c_2 are weights attached to the total downlink and uplink transmit powers, respectively. Here, we define $\overline{x} = \lim_{T\to\infty} \frac{1}{T} \sum_{t=1}^{T} \mathbb{E}[x(t)]$ as the time average expectation of the variable $x(t)$. Accordingly, constraints A1 and A2 ensure that the time-averaged transmission rate is greater or equal to the average arrival rate, which guarantee queue stability for the uplink and downlink queues. Constraints A3 and A4 ensure a minimum QoS for all users and constraint A5 and A6 impose the maximum power on the the FD BS and uplink users, respectively. The problem (7.7) is a non-convex problem due the time-averaged objective and constraints, thus, classified as a stochastic problem [167]. In order to solve (7.7) we resort to the classical drift-plus-penalty approach based

on Lyapunov framework [167].

To tackle (7.7), let $\Theta(t) = \left\{Q_{\mathrm{DL},k}(t), Q_{\mathrm{UL},j}(t)\right\}$ represent the queuing states of all queues. Then, the Lyapunov function is defined as

$$L(\Theta(t)) = \mathbb{E}\left[\frac{1}{2}\sum_{k=1}^{K} Q_{\mathrm{DL},k}(t)^2 + \frac{1}{2}\sum_{j=1}^{J} Q_{\mathrm{UL},j}(t)^2\right], \tag{7.8}$$

and the conditional drift-plus-penalty is defined as

$$D(\Theta(t)) \hat{=} \mathbb{E}\left[L(\Theta(t+1)) - L(\Theta(t)) + V \cdot \left(c_1 \sum_{k=1}^{K} P_{\mathrm{DL},k}(t) + c_2 \sum_{j=1}^{J} P_{\mathrm{UL},j}(t)\right) \Big| \Theta(t)\right]. \tag{7.9}$$

The non-negative parameter V is the control parameter that is chosen as desired, which captures the trade-off between the queue length and the total system transmit power [167]. Accordingly, following straightforward calculations and using $(\max\{x,0\})^2 \leq x^2$, we obtain the following upper bound for (7.9)

$$\begin{aligned} D(\Theta(t)) \leq \mathbb{E}\Bigg[M + V \cdot \Bigg(c_1 \sum_{k=1}^{K} P_{\mathrm{DL},k}(t) + c_2 \sum_{j=1}^{J} P_{\mathrm{UL},j}(t)\Bigg) \\ - \sum_{k=1}^{K} Q_{\mathrm{DL},k}(t) R_{\mathrm{DL},k}(t) - \sum_{j=1}^{J} Q_{\mathrm{UL},j}(t) R_{\mathrm{UL},j}(t) \Big| \Theta(t)\Bigg], \end{aligned} \tag{7.10}$$

where M is a constant which does not influence the system performance [167]. According to [167], the solution to (7.7) can be acquired by minimizing the righthand side of (7.10) in each slot t. Specifically, the optimisation problem is given by

$$\begin{aligned} \mathscr{P}7.2: \quad \max_{\substack{\{\mathbf{W}_k \succeq 0\} \\ \{P_{\mathrm{UL},j}\}}} \quad & \sum_{k=1}^{K} Q_{\mathrm{DL},k}(t) R_{\mathrm{DL},k}(t) + \sum_{j=1}^{J} Q_{\mathrm{UL},j}(t) R_{\mathrm{UL},j}(t) \\ & - V \cdot \left(c_1 \sum_{k=1}^{K} P_{\mathrm{DL},k}(t) + c_2 \sum_{j=1}^{J} P_{\mathrm{UL},j}(t)\right) \\ \text{s.t.} \quad & \text{A3, A4, A5, A6.} \end{aligned} \tag{7.11}$$

The minimization problem (7.11) is not trivial to handle due to the rate expressions in the objective term. Thus, we simplify the objective as shown in (7.12) by

expanding the non-linear log terms into linear log terms.

$$\sum_{k=1}^{K} Q_{\mathrm{DL},k}(t)\left[\log_2\left(\sum_{i=1}^{K}\mathbf{h}_k^H\mathbf{W}_i\mathbf{h}_k+\sum_{j=1}^{J}P_{\mathrm{UL},j}\left|\ell_{j,k}\right|^2+\sigma_k^2\right)\right.$$
$$\left.-\log_2\left(\sum_{i\neq k}^{K}\mathbf{h}_k^H\mathbf{W}_i\mathbf{h}_k+\sum_{j=1}^{J}P_{\mathrm{UL},j}\left|\ell_{j,k}\right|^2+\sigma_k^2\right)\right]-V\cdot\left(c_1\sum_{k=1}^{K}P_{\mathrm{DL},k}(t)+c_2\sum_{j=1}^{J}P_{\mathrm{UL},j}(t)\right)$$
$$+\sum_{j=1}^{J}Q_{\mathrm{UL},j}(t)\left[\log_2\left(s_j+\sigma_j^2\left\|\mathbf{u}_j\right\|^2+P_{\mathrm{UL},j}\left|\mathbf{g}_j^H\mathbf{u}_j\right|^2\right)-\log_2\left(s_j+\sigma_j^2\left\|\mathbf{u}_j\right\|^2\right)\right]. \tag{7.12}$$

The objective function in (7.12) is still non-convex, however, by close observation (7.12) can be written as a difference of two concave functions. Thus, in order to solve (7.11), we employ the convex-concave procedure (CCP) [168] to convexify the objective function. The basic idea of the CCP is to convexify the DC problem by replacing the convex part of the function by their first order Taylor series expansions. This then makes the convex part affine functions. Hence, the CCP solves a series of concave problems successively and iteratively by initiating the procedure with a feasible point. In addition, the CCP has been proven to converge to the local optima of DC programming, we refer the reader to [168] for a formal proof.

Accordingly, the objective function in (7.12) can be written as a difference of two concave functions, i.e., $f_{\mathrm{DL},k}(t)-r_{\mathrm{DL},k}(t)$ and $f_{\mathrm{UL},j}(t)-r_{\mathrm{UL},j}(t)$, where,

$$f_{\mathrm{DL},k}(t)=\log_2\left(\sum_{i=1}^{K}\mathbf{h}_k^H\mathbf{W}_i\mathbf{h}_k+\sum_{j=1}^{J}P_{\mathrm{UL},j}\left|\ell_{j,k}\right|^2+\sigma_k^2\right),$$
$$r_{\mathrm{DL},k}(t)=\log_2\left(\sum_{i\neq k}^{K}\mathbf{h}_k^H\mathbf{W}_i\mathbf{h}_k+\sum_{j=1}^{J}P_{\mathrm{UL},j}\left|\ell_{j,k}\right|^2+\sigma_k^2\right),$$
$$f_{\mathrm{UL},j}(t)=\log_2\left(s_j+\sigma_j^2\left\|\mathbf{u}_j\right\|^2+P_{\mathrm{UL},j}\left|\mathbf{g}_j^H\mathbf{u}_j\right|^2\right),$$
$$r_{\mathrm{UL},j}(t)=\log_2\left(s_j+\sigma_j^2\left\|\mathbf{u}_j\right\|^2\right).$$

Based on the above analysis, the optimization problem (7.11) can be reformulated

as a standard DC problem as shown below

$$\widetilde{\mathscr{P}7.2}: \max_{\substack{\{\mathbf{W}_k \succeq 0\} \\ \{P_{\mathrm{UL},j}\}}} \sum_{k=1}^{K} Q_{\mathrm{DL},k}(t)\left(f_{\mathrm{DL},k}(t) - r_{\mathrm{DL},k}(t)\right) + \sum_{j=1}^{J} Q_{\mathrm{UL},j}(t)\left(f_{\mathrm{UL},j}(t) - r_{\mathrm{UL},j}(t)\right) - V \cdot \left(c_1 \sum_{k=1}^{K} P_{\mathrm{DL},k}(t) + c_2 \sum_{j=1}^{J} P_{\mathrm{UL},j}(t)\right)$$
$$\text{s.t.} \quad \text{A3, A4, A5, A6.} \tag{7.13}$$

The difficulty in solving (7.13) lies in convexifying the concave components $r_{\mathrm{DL},k}(t)$ and $r_{\mathrm{UL},j}(t)$. To proceed, suppose that the values of $\mathbf{W}_k$ and $P_{\mathrm{UL},j}$ at the i-th iteration are denoted by $\mathbf{W}_k^{(i)}$ and $P_{\mathrm{UL},j}^{(i)}$. Since $r_{\mathrm{DL},k}(t)$ and $r_{\mathrm{UL},j}(t)$ are differentiable, thus, we can express their first order affine approximations as shown below, respectively.

$$r_{\mathrm{DL},k}^{(i)}(t) = r_{\mathrm{DL},k}\left(\mathbf{W}_k^{(i)}, P_{\mathrm{UL},j}^{(i)}\right) + \sum_{j=1}^{J}\left[\left(\Psi_{\mathrm{DL},k}^{(i)}\right)^{-1}\left(P_{\mathrm{UL},j} - P_{\mathrm{UL},j}^{(i)}\right)\left|\ell_{j,k}\right|^2\right] + \sum_{i\neq k}^{K}\left[\left(\Psi_{\mathrm{DL},k}^{(i)}\right)^{-1}\mathbf{h}_k^H\left(\mathbf{W}_i - \mathbf{W}_k^{(i)}\right)\mathbf{h}_k\right], \tag{7.14}$$

$$r_{\mathrm{UL},j}^{(i)}(t) = r_{\mathrm{UL},j}\left(\mathbf{W}_k^{(i)}\right) + \sum_{k=1}^{K}\left[\frac{\rho\mathbf{u}_j^H\mathbf{H}_{\mathrm{SI}}\left(\mathbf{W}_k - \mathbf{W}_k^{(i)}\right)\mathbf{H}_{\mathrm{SI}}^H\mathbf{u}_j}{\rho\mathbf{u}_j^H\mathbf{H}_{\mathrm{SI}}\left(\sum_{l=1}^{K}\mathbf{W}_l^{(i)}\right)\mathbf{H}_{\mathrm{SI}}^H\mathbf{u}_j + \sigma_j^2\left\|\mathbf{u}_j\right\|^2}\right], \tag{7.15}$$

where

$$\Psi_{\mathrm{DL},k}^{(i)} = \sum_{m\neq k}^{K}\mathbf{h}_k^H\mathbf{W}_m^{(i)}\mathbf{h}_k + \sum_{j=1}^{J}P_{\mathrm{UL},j}^{(i)}\left|\ell_{j,k}\right|^2 + \sigma_k^2.$$

Here, we have used the fact that $\nabla_{\mathbf{X}}\log_2\left(\mathbf{I}+\mathbf{ZXZ}^H\right) = \mathbf{X}^H\left(\mathbf{I}+\mathbf{ZXZ}^H\right)^{-1}\mathbf{X}$ and $\nabla_x\log_2(1+zx) = x(1+zx)^{-1}$. Therefore, the transformed optimization problem

Algorithm 7.4 Optimal Algorithm to solve (7.7) or (7.17)

Input: $T =$ the maximum number of time slots
Initialise: $t = 0, Q_{\mathrm{DL},k}(t) = 0, Q_{\mathrm{UL},j}(t) = 0$
Repeat
  Set i = 0,
  Generate initial feasible points for all $\mathbf{W}_k^{(i)}$ and $P_{\mathrm{UL},j}^{(i)}$
  Repeat
    Solve (7.16) or (7.18) to obtain all $\mathbf{W}_k^*$ and $P_{\mathrm{UL},j}^*$
    Update $i = i+1$
    Update all $\mathbf{W}_k^{(i)} = \mathbf{W}_k^*$ and $P_{\mathrm{UL},j}^{(i)} = P_{\mathrm{UL},j}^*$
  Until Convergence
  $t = t+1$,
  Update all queues $Q_{\mathrm{DL},k}(t), Q_{\mathrm{UL},j}(t)$, accordingly.
Until $t = T$
Output: $\mathbf{W}_k^*, \forall k$, and $P_{\mathrm{UL},j}^*, \forall j$.

(7.13) can be expressed as

$$\mathscr{P}7.3: \max_{\substack{\{\mathbf{W}_k \succeq 0\} \\ \{P_{\mathrm{UL},j}\}}} \sum_{k=1}^{K} Q_{\mathrm{DL},k}(t)\left(f_{\mathrm{DL},k}(t) - r_{\mathrm{DL},k}^{(i)}(t)\right) + \sum_{j=1}^{J} Q_{\mathrm{UL},j}(t)\left(f_{\mathrm{UL},j}(t) - r_{\mathrm{UL},j}^{(i)}(t)\right) - V \cdot \left(c_1 \sum_{k=1}^{K} P_{\mathrm{DL},k}(t) + c_2 \sum_{j=1}^{J} P_{\mathrm{UL},j}(t)\right)$$
$$\text{s.t.} \quad \text{A3, A4, A5, A6.} \tag{7.16}$$

Problem (7.16) is convex with respect to the optimization variables and can be solved efficiently using standard convex solvers. Please note that the formulation in (7.16) is a relaxed problem where the rank 1 constraint on $\mathbf{W}_k$ has been dropped. If the resulting solution $\mathbf{W}_k$ after solving (7.16) is rank 1, the optimal $\mathbf{w}_k$ can be obtained by applying eigenvalue-decomposition (EVD), otherwise, randomization technique can be used to retrieve $\mathbf{w}_k$.

After obtaining the beamforming vectors and the transmit powers from (7.16) for slot t, the queues $Q_{\mathrm{DL},k}(t), Q_{\mathrm{UL},j}(t)$ are updated accordingly. The overall procedure to solve the optimization problem (7.7) is summarized in Algorithm 7.4.

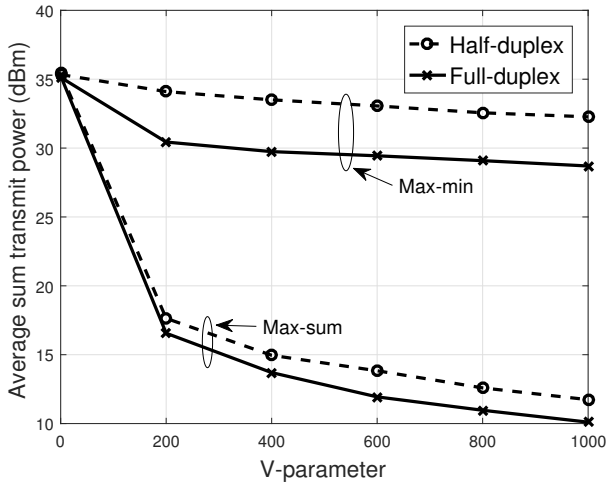

Figure 7.1: Average sum transmit power versus V-parameter with $\Gamma_{\mathrm{DL}} = 8$dB, $\Gamma_{\mathrm{UL}} = 6$dB and $\overline{A}_{\mathrm{DL}} = \overline{A}_{\mathrm{UL}} = 2$ bit/slot/Hz

7.4 Delay Fairness Optimization

Building upon the simplified problem formulation (7.16) in Section 7.3, in this section, we propose a resource allocation algorithm based on delay fairness. By close examination of the simplified convex optimization problem (7.16), it can be observed that (7.16) basically aims at maximizing the sum rate of the uplink and downlink users while minimizing the sum transmit power. Resource allocation that focuses solely on sum rate maximization usually results in an unfair resource allocation, since the system resources are consumed by the users with good channel conditions [169]. In essence, the resource allocation based on (7.16) results in starvation of users with poor channel conditions, which is unfair. As such, we formulate a fair beamforming optimization and resource allocation problem that aims at maximizing the minimum transmission rate for the downlink and uplink users, respectively. This problem is often referred to as the max-min problem and can be mathematically expressed as

$$\begin{aligned}\mathscr{P}7.4: \quad \max_{\substack{\{\mathbf{W}_k \succeq 0\} \\ \{P_{\mathrm{UL},j}\}}} \quad & \min_k \left(Q_{\mathrm{DL},k}(t) \left(f_{\mathrm{DL},k}(t) - r^{(i)}_{\mathrm{DL},k}(t) \right) \right) \\ & + \min_j \left(Q_{\mathrm{UL},j}(t) \left(f_{\mathrm{UL},j}(t) - r^{(i)}_{\mathrm{UL},j}(t) \right) \right) \\ & - V \cdot \left(c_1 \sum_{k=1}^{K} P_{\mathrm{DL},k}(t) + c_2 \sum_{j=1}^{J} P_{\mathrm{UL},j}(t) \right) \\ \text{s.t.} \quad & \text{A3, A4, A5, A6.}\end{aligned} \tag{7.17}$$

The max-min problem (7.17) can not be solved directly in its current form, however, (7.17) can be simplified by introducing auxilary variables [84], $t_{\mathrm{DL}}(t)$ and $t_{\mathrm{UL}}(t)$, respectively. Thus, the simplified convex problem is given by

$$\begin{aligned}\widetilde{\mathscr{P}7.4}: \max_{\substack{\{\mathbf{W}_k \succeq 0\} \\ \{P_{\mathrm{UL},j}\}}} \quad & t_{DL}(t) + t_{UL}(t) - V \cdot \left(c_1 \sum_{k=1}^{K} P_{\mathrm{DL},k}(t) + c_2 \sum_{j=1}^{J} P_{\mathrm{UL},j}(t) \right) \\ \text{s.t.} \quad & Q_{\mathrm{DL},k}(t) \left(f_{\mathrm{DL},k}(t) - r^{(i)}_{\mathrm{DL},k}(t) \right) \geq t_{\mathrm{DL}}(t), \forall k, \\ & Q_{\mathrm{UL},j}(t) \left(f_{\mathrm{UL},j}(t) - r^{(i)}_{\mathrm{UL},j}(t) \right) \geq t_{\mathrm{UL}}(t), \forall j, \\ & \text{A3, A4, A5, A6.}\end{aligned} \tag{7.18}$$

The problem (7.18) is convex and can be efficiently solved using standard solvers. Similar to (7.16), the formulation (7.18) is a relaxed problem. If the resulting solution $\mathbf{W}_k$ after solving (7.16) is rank 1, the optimal $\mathbf{w}_k$ can be obtained by applying eigenvalue-decomposition (EVD), otherwise, randomization technique can be used to retrieve $\mathbf{w}_k$. The procedure for solving (7.17) is summarized in Algorithm 7.4.

7.5 Simulation Results

We consider the system with the FD BS at the centre of a cell with $N = 3$ antennas, each for transmitting and receiving. We assume $K = J = 2$ downlink and uplink users, are randomly and uniformly distributed between the distance of 10m and 50m. We model the channels to the downlink and uplink users as Rayleigh fading. The SI channel is modelled as Rician fading channel with Rician factor 6dB. Furthermore, we consider a similar system set-up as in [116] with $\sigma_i = \sigma_j = -60\text{dBm}, P^{\mathrm{UL}}_{\max} = 23\text{dBm}, P^{\mathrm{DL}}_{\max} = 35\text{dBm}, \rho = -80\text{dB}$ and $c_1 = c_2 = 1$.

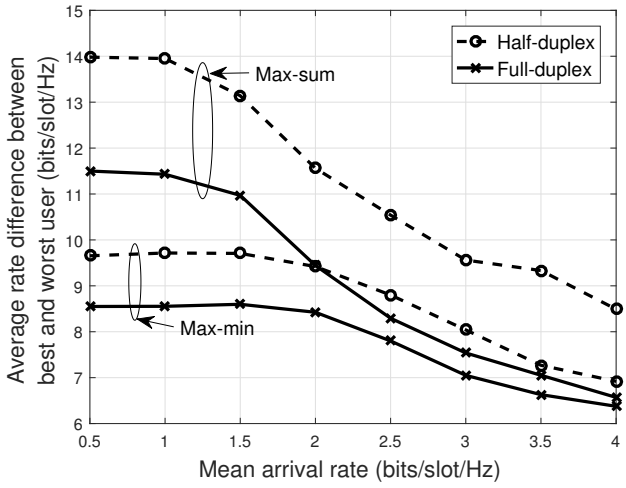

Figure 7.2: Average rate difference between the best and worst user with $\Gamma_{\mathrm{DL}} = 8$dB, $\Gamma_{\mathrm{UL}} = 6$dB and $V = 4$

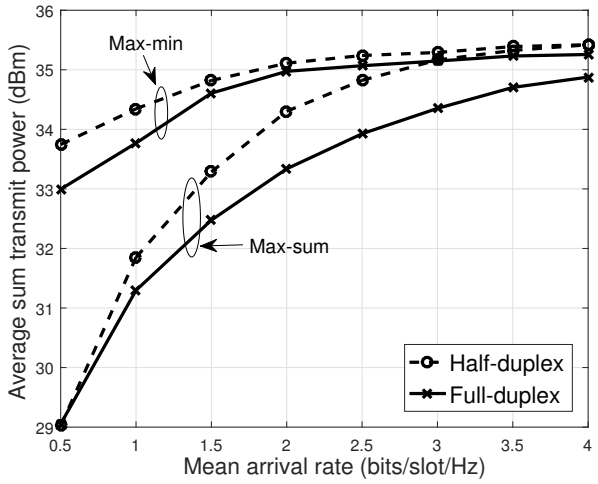

Figure 7.3: Average sum transmit power versus mean arrival rate with $\Gamma_{\mathrm{DL}} = 8$dB, $\Gamma_{\mathrm{UL}} = 6$dB and $V = 4$

Our baseline is the HD scheme as in [163–165]. For fair comparison, here, the overall data rate of HD is set equal to the one for FD which requires that the individual data rate of the downlink and uplink users are double the ones for the FD case, due to the slotted HD transmission. Besides, the CCI and SI are avoided with HD. In the figures, we refer to the results obtained from the problem formulations in (7.7) and (7.17) as max-sum and max-min, respectively.

In Fig. 7.1, we show the average sum transmit power versus the objective weight parameter V. This plot shows the effect of the control parameter V in the

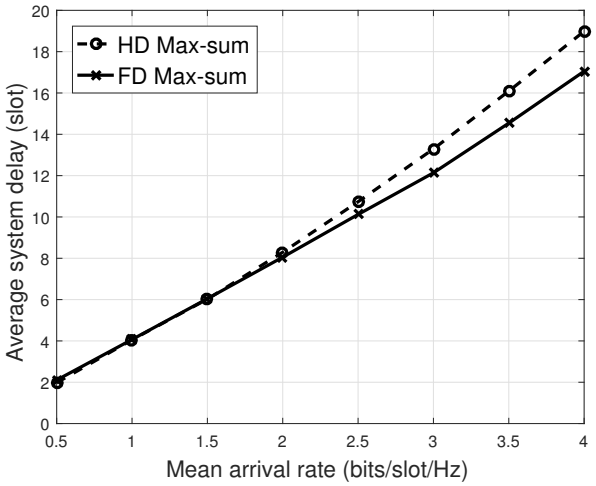

Figure 7.4: Average system delay versus mean arrival rate with $\Gamma_{\mathrm{DL}} = 8\mathrm{dB}$, $\Gamma_{\mathrm{UL}} = 6\mathrm{dB}$ and $V = 4$

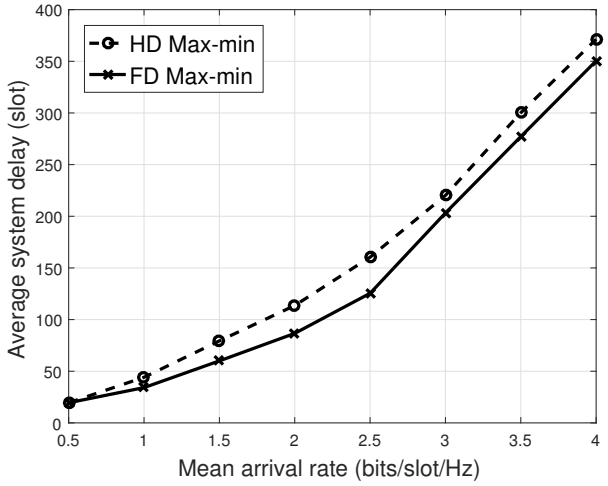

Figure 7.5: Average system delay versus mean arrival rate with $\Gamma_{\mathrm{DL}} = 8\mathrm{dB}$, $\Gamma_{\mathrm{UL}} = 6\mathrm{dB}$ and $V = 4$

optimization problems. As V increases, more emphasis is given to the system objective i.e., minimizing the sum transmit power, as can be seen from the curves in the figure. In addition, the proposed max-sum optimization achieves the minimum sum transmit power compared with the proposed max-min optimization. This is because the proposed max-min optimization tries to balance the power allocation among all users, since some users perform poorer than others. As a result the proposed max-min optimization provides a fairer power allocation for all user than the max-sum schemes where the users with good channel conditions overshadow the

users with poor channel conditions. This is further illustrated in Fig. 7.2, where the average rate difference between the best and worst user is plotted against the mean arrival rate. It can be seen that the proposed max-min optimization has a lower rate difference since it gives no preference in the power allocation between all users. Moreover, the figure also shows that the proposed FD schemes out perform the baseline HD schemes for both max-sum and max-min resource allocation.

Furthermore, in Fig. 7.3 we show the average sum transmit power for varying mean arrival rate. It can be seen that the average sum transmit power increases as the mean arrival rate increases for both the proposed FD max-sum and max-min schemes, since an increase in arrival rate implies more data to be transmitted which requires an increase in the transmit power. However, it can be seen that at the sum transmit power saturates with large arrival rates for all the schemes when the maximum allowable power is reached. Besides, the proposed FD schemes perform better than the HD schemes. This further shows the superiority of the proposed FD schemes over their HD counterpart.

In Figs. 7.4 and 7.5, we show the average system delay in slots with varying mean arrival rate for the proposed FD max-sum and max-min resource allocation schemes, respectively. As can be observed, the system delay is proportional to increase in arrival rates. The proposed max-sum scheme achieves lower delay because it exploits users with good channel conditions to improve the system delay, while the proposed max-min ensures fairness to all users at the expense of higher system delay.

7.6 Summary

In this chapter, we studied the delay-constrained BF and resource allocation problem in a multiuser FD system. We minimized the long-term sum transmit power while satisfying the long-term stability constraints on the queue buffers. By adopting the classic drift-plus-penalty function, the optimization problem was transformed and simplified to a convex problem which aims at maximing the sum rate of the uplink and downlink users while minimizing the sum transmit power which

guarantees system stability. We further proposed a FD max-min resource allocation problem that ensures fairness among all users. Simulation analysis show that the proposed FD schemes show promising improvement compared to their HD schemes.

Chapter 8

Conclusion and Future Work

Beamforming and resource allocation techniques are essential in materializing the goals of the 5G of wireless communication networks. Employing FD in wireless communication systems give the opportunity to serve variety of services to different users since FD has the ability to transmit and receive at the same time and frequency. Therefore, integrating FD with SWIPT is necessary to improve the provision of information and power to users as well as for efficient use of the radio spectrum. Furthermore, as the popularity of smart phones, tablets and other wearable devices is rapidly increasing, the use of computation intensive applications has drastically increased, thus, integrating FD with MEC presents a promising solution. Accordingly, this thesis has studied and proposed a number of design strategies for realistic and efficient communication in multi-user FD systems.

8.1 Conclusion

Chapter 2 of this thesis provides an overview of MIMO communication systems. We reviewed the various precoding schemes in the literature for downlink transmission, both the linear and non-linear schemes, as well as some simulation results highlighting their advantages and disadvantages. Also, the chapter presents a review of the various optimization based beamforming techniques and strategies in the literature. These techniques were categorized into two. The conventional optimization based beamforming that is based on the traditional approach that treats interference as a detrimental phenomenon; and the constructive interference based

beamforming, where the knowledge of the data symbols at the BS is used to exploit interference constructively rather than suppress it for PSK and QAM modulated signals.

In Chapter 3, a review of some of the new and promising technologies that are expected to be employed in 5G systems and even beyond is presented. First, FD communication that allows simultaneous transmission and reception was presented, where the various SI cancellation schemes including passive and active schemes were reviewed. In addition, the chapter discussed the EH technology that provides a promising solution for prolonging the battery life of wireless communication networks. This is then followed by an overview of MEC technology that provides a means for devices to offload their intensive and latency-critical tasks to nearby servers for remote execution. Chapter 3 also presents a review the technologies that support URLLC in 5G systems.

After the two introductory chapters above that discussed the literature review of the technical contributions and focus of this thesis, Chapter 4 - 7 presents the main contributions of this thesis, respectively. Specifically,

- Chapter 4 studied the application of the interference exploitation concept to a MU-MIMO system with a FD BS. We proposed novel MOOP designs to study the trade-off between the total uplink and downlink transmit power for PSK and QAM modulated signals. The main observations in this chapter are:

    1. The significant power gains of the CI technique is extended to multi-user FD systems, where FD gives the opportunity to jointly optimize the uplink and downlink variables i.e., the uplink transmit power and the downlink beamforming vectors. This coexistence of uplink and downlink warrants the MOOP designs, such that, the MOOP designs allow for the power saved in the downlink transmission to be traded-off for both downlink and uplink power savings. Compared to the conventional interference suppression techniques and HD schemes, the proposed FD MOOP schemes show tremendous power gains with low computational complexity.

2. The existence of uplink and downlink transmission brings about the joint optimization of the transmit and receive beamforming vectors, and the uplink transmit power. Hence, we proposed an iterative algorithm that jointly optimizes these variables for both IS and CI schemes. The proposed algorithms show increase in power savings compared to the ZF approaches for both IS and CI schemes at the expense of a scalable complexity increase.

- Chapter 5 focused on exploring FD communications with SWIPT, where robust designs were explored to jointly minimize the total uplink and downlink transmit power, and maximize the total harvested energy with imperfect CSI. By making the practical assumption that the CSI for all the channel links are not perfectly known, two optimization problem formulations were proposed. One based on the classic MUI suppression and the other based on MUI exploitation. It was observed that based on the average harvested energy in terms of the BS transmit power, the minimum harvested energy threshold and CCI level between the uplink and downlink users, the proposed CI scheme harvests more energy than the proposed IS scheme. This is because more power is available to be harvested since less power is required to satisfy the downlink and uplink QoS constraints for the CI scheme compared to the IS scheme. Additionally, the proposed CI scheme proved to be less sensitive to the minimum harvested energy threshold compared to the more sensitive IS scheme. Most importantly, it was observed that for the same data rate requirements the proposed FD schemes show improved performance compared to HD scheme.

- In Chapter 6, we proposed novel algorithms to study the offloading energy and latency trade-off based on MOOP designs in a multiuser FD system that performs both data transmission and MEC in the downlink and uplink, respectively. The following key point were observed

  1. By decomposing the complex optimization formulations into two sub-

problems and employing Lagrangian method, closed form solutions to the transmit power were derived that satisfy the KKT conditions of the original problem. As a result, an the optimal transmit beamforming vectors and power allocation for the mobile devices are obtained via the proposed algorithm, which was shown to converge within few iteration with low computational complexity in terms of the average algorithm runtime in seconds.

2. The proposed MOOP designs show promising performance improvement compared to the baseline HD schemes in terms of the offloading energy and latency. In addition, the proposed MOOP designs allow for a scalable optimization technique, where before one could only optimize either the offloading energy with a fixed latency constraint, or the latency with a fixed energy constraint. This observation further highlights the flexibility provided by the proposed FD schemes.

3. The dependency between the optimization variables and objectives is further proven, where increasing the transmit power of the mobile devices in order to minimize the offloading latency increases the CCI to the downlink users. Similarly, increasing the downlink transmit power to accommodate the increase in CCI increases the SI and offloading energy. This further shows the trade-offs involved in the proposed optimization designs.

- In chapter 7, we proposed a delay-constrained beamforming and resource allocation algorithm for a multiuser FD system to minimize the long-term sum transmit power while satisfying the long-term stability constraints on the queue buffers. The central remarks of this chapter are:

  1. We exploited the classic drift-plus-penalty function to transform the proposed formulation into two different optimization problems. One based on the max-sum, that exploits users with good channel conditions for efficient resource allocation and the other based on the max-min, that

ensures delay-fairness among all users.

2. The proposed max-sum optimization achieves lower transmit power and delay compared to the proposed max-min optimization because the max-sum optimization exploits users with good channel conditions for efficient power allocation as well as to improve the system delay. However, the max-min optimization provides a fairer approach as was shown that the average sum-rate difference between the best and worst user is lower for the proposed max-min optimization compared to the proposed max-sum optimization.

8.2 Future Work

Throughout this thesis, we have developed algorithms that study the trade-off between important and conflicting objectives, for both the system operator and users, based on MOO formulations for multi-user FD systems. Thus, the proposed techniques in this thesis have prompted further investigations in some research directions which are summarized below:

- **URLLC in multiuser FD systems:** URLLC is a generic service that enables mission critical applications such as vehicular communications, industrial automation, cloud computing and augmented reality. URLLC has strict requirement for latency and reliability for the next generation 5G systems in delivering both data and control information. Therefore, depending on just system stability constraints may not be enough to meet the latency and reliability requirement of some applications. Thus, as an extension to the work in Chapter 7, where we used the fact that the system delay is directly dependent on the queue length and stability to design a delay-constrained optimization by ensuring system stability, we consider imposing probability constraints on the queue length to directly constraint the latency. According to Little's law, the queue length is proportional to the average queue latency. To this end, us-

ing $Q_{\mathrm{DL},k}(t)/\overline{A}_{\mathrm{DL},k}$ as the latency measure, we have the following constraint

$$\Pr\left\{\frac{Q_{\mathrm{DL},k}(t)}{\overline{A}_{\mathrm{DL},k}} \geq L_{\mathrm{DL},k}\right\} \leq \varepsilon_k, \forall t, k, \tag{8.1}$$

where $L_{\mathrm{DL},k}$ is the allowable queue length requirement and $\varepsilon_k \ll 1$ is the target probability, for low latency and reliable communication for downlink transmission.

- **Energy efficiency maximization in MEC systems:** In Chapter 6, we have considered the minimization of offloading energy and latency in a multiuser FD MEC system. As a future work, it will be of particular interest to consider the energy efficiency maximization problem of the FD MEC system. Energy efficiency is one of the main aims of the future wireless communication systems due to the high rate of power consumption of mobile devices as well as base stations in the offloading, computation and downloading processes. Another interesting solution to the high power consumption of the mobile devices is to consider wireless power transfer. In particular, it will be interesting to consider the joint optimization of the transmit beamformer, the transmit power of the mobile devices and power splitting or time switching ratio, where the mobile devices can harvest energy from the BS for use in the next phase of communication during the downloading process through power splitting or time switching.

Finally, this thesis has presented key strategies, solutions and results in the study of multiuser FD systems. The author hopes the solutions, the results and conclusions derived in this thesis will help explore the potentials and motivate new novel designs for the 5G wireless communication systems and beyond.

Bibliography

[1] C. B. Peel, B. M. Hochwald, and A. L. Swindlehurst, "A vector-perturbation technique for near-capacity multiantenna multiuser communication-part i: channel inversion and regularization," *IEEE Transactions on Communications*, vol. 53, no. 1, pp. 195–202, 2005.

[2] V. W. Wong, R. Schober, D. W. K. Ng, and L.-C. Wang, *Key technologies for 5G wireless systems*. Cambridge university press, 2017.

[3] A. Goldsmith, *Wireless communications*. Cambridge university press, 2005.

[4] D. Bharadia, E. McMilin, and S. Katti, "Full duplex radios," in *ACM SIGCOMM Computer Communication Review*, vol. 43, pp. 375–386, ACM, 2013.

[5] J. I. Choi, M. Jain, K. Srinivasan, P. Levis, and S. Katti, "Achieving single channel, full duplex wireless communication," in *Proceedings of the sixteenth annual international conference on Mobile computing and networking*, pp. 1–12, ACM, 2010.

[6] B. P. Day, A. R. Margetts, D. W. Bliss, and P. Schniter, "Full-duplex mimo relaying: Achievable rates under limited dynamic range," *IEEE Journal on Selected Areas in Communications*, vol. 30, no. 8, pp. 1541–1553, 2012.

[7] D. Bharadia and S. Katti, "Full duplex mimo radios," *Self*, vol. 1, no. A2, p. A3, 2014.

[8] T. Riihonen, S. Werner, and R. Wichman, "Mitigation of loopback self-interference in full-duplex mimo relays," *IEEE Transactions on Signal Processing*, vol. 59, no. 12, pp. 5983–5993, 2011.

[9] M. Duarte, C. Dick, and A. Sabharwal, "Experiment-driven characterization of full-duplex wireless systems," *IEEE Transactions on Wireless Communications*, vol. 11, no. 12, pp. 4296–4307, 2012.

[10] E. Ahmed and A. M. Eltawil, "All-digital self-interference cancellation technique for full-duplex systems," *IEEE Transactions on Wireless Communications*, vol. 14, no. 7, pp. 3519–3532, 2015.

[11] L. C. Godara, *Handbook of antennas in wireless communications*. CRC press, 2001.

[12] D. W. K. Ng, Y. Wu, and R. Schober, "Power efficient resource allocation for full-duplex radio distributed antenna networks," *IEEE Transactions on Wireless Communications*, vol. 15, no. 4, pp. 2896–2911, 2016.

[13] C. Masouros and G. Zheng, "Exploiting known interference as green signal power for downlink beamforming optimization," *IEEE Transactions on Signal processing*, vol. 63, no. 14, pp. 3628–3640, 2015.

[14] S. Barbarossa, S. Sardellitti, and P. Di Lorenzo, "Communicating while computing: Distributed mobile cloud computing over 5G heterogeneous networks," *IEEE Signal Processing Magazine*, vol. 31, no. 6, pp. 45–55, 2014.

[15] A. Sabharwal, P. Schniter, D. Guo, D. W. Bliss, S. Rangarajan, and R. Wichman, "In-band full-duplex wireless: Challenges and opportunities," *IEEE Journal on Selected Areas in Communications*, vol. 32, no. 9, pp. 1637–1652, 2014.

[16] E. Everett, M. Duarte, C. Dick, and A. Sabharwal, "Empowering full-duplex wireless communication by exploiting directional diversity," in *Signals, Sys-*

tems and Computers (ASILOMAR), 2011 Conference Record of the Forty Fifth Asilomar Conference on, pp. 2002–2006, IEEE, 2011.

[17] E. Everett, A. Sahai, and A. Sabharwal, "Passive self-interference suppression for full-duplex infrastructure nodes," *IEEE Transactions on Wireless Communications*, vol. 13, no. 2, pp. 680–694, 2014.

[18] E. Ahmed, A. M. Eltawil, Z. Li, and B. A. Cetiner, "Full-duplex systems using multireconfigurable antennas," *IEEE Transactions on Wireless Communications*, vol. 14, no. 11, pp. 5971–5983, 2015.

[19] A. Balatsoukas-Stimming, P. Belanovic, K. Alexandris, and A. Burg, "On self-interference suppression methods for low-complexity full-duplex mimo," in *Signals, Systems and Computers, 2013 Asilomar Conference on*, pp. 992–997, IEEE, 2013.

[20] M. Duarte and A. Sabharwal, "Full-duplex wireless communications using off-the-shelf radios: Feasibility and first results," in *Signals, Systems and Computers (ASILOMAR), 2010 Conference Record of the Forty Fourth Asilomar Conference on*, pp. 1558–1562, IEEE, 2010.

[21] E. Ahmed, A. M. Eltawil, and A. Sabharwal, "Self-interference cancellation with nonlinear distortion suppression for full-duplex systems," in *Signals, Systems and Computers, 2013 Asilomar Conference on*, pp. 1199–1203, IEEE, 2013.

[22] Y. Alsaba, S. K. A. Rahim, and C. Y. Leow, "Beamforming in wireless energy harvesting communications systems: A survey," *IEEE Communications Surveys & Tutorials*, vol. 20, no. 2, pp. 1329–1360, 2018.

[23] V. Raghunathan, S. Ganeriwal, and M. Srivastava, "Emerging techniques for long lived wireless sensor networks," *IEEE Communications Magazine*, vol. 44, no. 4, pp. 108–114, 2006.

[24] K. Pentikousis, "In search of energy-efficient mobile networking," *IEEE Communications Magazine*, vol. 48, no. 1, pp. 95–103, 2010.

[25] T. Chen, Y. Yang, H. Zhang, H. Kim, and K. Horneman, "Network energy saving technologies for green wireless access networks," *IEEE Wireless Communications*, vol. 18, no. 5, pp. 30–38, 2011.

[26] P. Grover and A. Sahai, "Shannon meets tesla: Wireless information and power transfer," in *2010 IEEE international symposium on information theory*, pp. 2363–2367, IEEE, 2010.

[27] S. Bi, C. K. Ho, and R. Zhang, "Wireless powered communication: Opportunities and challenges," *IEEE Communications Magazine*, vol. 53, no. 4, pp. 117–125, 2015.

[28] H. Ju and R. Zhang, "Throughput maximization in wireless powered communication networks," *IEEE Transactions on Wireless Communications*, vol. 13, no. 1, pp. 418–428, 2014.

[29] H. Ju and R. Zhang, "User cooperation in wireless powered communication networks," in *2014 IEEE Global Communications Conference*, pp. 1430–1435, IEEE, 2014.

[30] H. Lee, K.-J. Lee, H.-B. Kong, and I. Lee, "Sum-rate maximization for multiuser mimo wireless powered communication networks," *IEEE Transactions on Vehicular Technology*, vol. 65, no. 11, pp. 9420–9424, 2016.

[31] Q. Wu, M. Tao, D. W. K. Ng, W. Chen, and R. Schober, "Energy-efficient resource allocation for wireless powered communication networks," *IEEE Transactions on Wireless Communications*, vol. 15, no. 3, pp. 2312–2327, 2016.

[32] R. Zhang and C. K. Ho, "Mimo broadcasting for simultaneous wireless information and power transfer," *IEEE Transactions on Wireless Communications*, vol. 12, no. 5, pp. 1989–2001, 2013.

[33] X. Chen, X. Wang, and X. Chen, "Energy-efficient optimization for wireless information and power transfer in large-scale mimo systems employing energy beamforming," *IEEE Wireless Communications Letters*, vol. 2, no. 6, pp. 667–670, 2013.

[34] D. W. K. Ng, E. S. Lo, and R. Schober, "Robust beamforming for secure communication in systems with wireless information and power transfer," *IEEE Transactions on Wireless Communications*, vol. 13, no. 8, pp. 4599–4615, 2014.

[35] D. W. K. Ng, E. S. Lo, and R. Schober, "Multiobjective resource allocation for secure communication in cognitive radio networks with wireless information and power transfer," *IEEE Transactions on Vehicular Technology*, vol. 65, no. 5, pp. 3166–3184, 2016.

[36] Y. Liu and X. Wang, "Information and energy cooperation in ofdm relaying: Protocols and optimization," *IEEE Transactions on Vehicular Technology*, vol. 65, no. 7, pp. 5088–5098, 2016.

[37] Y. Mao, C. You, J. Zhang, K. Huang, and K. B. Letaief, "A survey on mobile edge computing: The communication perspective," *IEEE Communications Surveys & Tutorials*, vol. 19, no. 4, pp. 2322–2358, 2017.

[38] J. Flinn, S. Park, and M. Satyanarayanan, "Balancing performance, energy, and quality in pervasive computing," in *Proceedings 22nd International Conference on Distributed Computing Systems*, pp. 217–226, IEEE, 2002.

[39] R. K. Balan, M. Satyanarayanan, S. Y. Park, and T. Okoshi, "Tactics-based remote execution for mobile computing," in *Proceedings of the 1st international conference on Mobile systems, applications and services*, pp. 273–286, ACM, 2003.

[40] J. Flinn, D. Narayanan, and M. Satyanarayanan, "Self-tuned remote execution for pervasive computing," in *hotos*, p. 0061, IEEE, 2001.

[41] K. Kumar and Y.-H. Lu, "Cloud computing for mobile users: Can offloading computation save energy?," *Computer*, no. 4, pp. 51–56, 2010.

[42] D. Huang, P. Wang, and D. Niyato, "A dynamic offloading algorithm for mobile computing," *IEEE Transactions on Wireless Communications*, vol. 11, no. 6, pp. 1991–1995, 2012.

[43] G. Chen, B.-T. Kang, M. Kandemir, N. Vijaykrishnan, M. J. Irwin, and R. Chandramouli, "Studying energy trade offs in offloading computation/compilation in java-enabled mobile devices," *IEEE Transactions on Parallel and Distributed Systems*, vol. 15, no. 9, pp. 795–809, 2004.

[44] Z. Q. Jaber and M. I. Younis, "Design and implementation of real time face recognition system (rtfrs)," *International Journal of Computer Applications*, vol. 94, no. 12, 2014.

[45] W. Zhang, Y. Wen, K. Guan, D. Kilper, H. Luo, and D. O. Wu, "Energy-optimal mobile cloud computing under stochastic wireless channel," *IEEE Transactions on Wireless Communications*, vol. 12, no. 9, pp. 4569–4581, 2013.

[46] C. You, K. Huang, and H. Chae, "Energy efficient mobile cloud computing powered by wireless energy transfer," *IEEE Journal on Selected Areas in Communications*, vol. 34, no. 5, pp. 1757–1771, 2016.

[47] Y. Wang, M. Sheng, X. Wang, L. Wang, and J. Li, "Mobile-edge computing: Partial computation offloading using dynamic voltage scaling," *IEEE Transactions on Communications*, vol. 64, no. 10, pp. 4268–4282, 2016.

[48] S. E. Mahmoodi, R. Uma, and K. Subbalakshmi, "Optimal joint scheduling and cloud offloading for mobile applications," *IEEE Transactions on Cloud Computing*, 2016.

[49] J. Liu, Y. Mao, J. Zhang, and K. B. Letaief, "Delay-optimal computation task scheduling for mobile-edge computing systems," in *2016 IEEE International Symposium on Information Theory (ISIT)*, pp. 1451–1455, IEEE, 2016.

[50] Z. Jiang and S. Mao, "Energy delay tradeoff in cloud offloading for multi-core mobile devices," *IEEE Access*, vol. 3, pp. 2306–2316, 2015.

[51] G. J. Sutton, J. Zeng, R. P. Liu, W. Ni, D. N. Nguyen, B. A. Jayawickrama, X. Huang, M. Abolhasan, Z. Zhang, E. Dutkiewicz, *et al.*, "Enabling technologies for ultra-reliable and low latency communications: From phy and mac layer perspectives," *IEEE Communications Surveys & Tutorials*, 2019.

[52] A. Aijaz, "Towards 5g-enabled tactile internet: Radio resource allocation for haptic communications," in *2016 IEEE Wireless Communications and Networking Conference Workshops (WCNCW)*, pp. 145–150, IEEE, 2016.

[53] M. Simsek, A. Aijaz, M. Dohler, J. Sachs, and G. Fettweis, "The 5g-enabled tactile internet: Applications, requirements, and architecture," in *2016 IEEE Wireless Communications and Networking Conference*, pp. 1–6, IEEE, 2016.

[54] X. Yang, L. Liu, N. H. Vaidya, and F. Zhao, "A vehicle-to-vehicle communication protocol for cooperative collision warning," in *The First Annual International Conference on Mobile and Ubiquitous Systems: Networking and Services, 2004. MOBIQUITOUS 2004.*, pp. 114–123, IEEE, 2004.

[55] G. Pocovi, M. Lauridsen, B. Soret, K. I. Pedersen, and P. Mogensen, "Automation for on-road vehicles: Use cases and requirements for radio design," in *2015 IEEE 82nd Vehicular Technology Conference (VTC2015-Fall)*, pp. 1–5, IEEE, 2015.

[56] P. Schulz, M. Matthe, H. Klessig, M. Simsek, G. Fettweis, J. Ansari, S. A. Ashraf, B. Almeroth, J. Voigt, I. Riedel, *et al.*, "Latency critical iot applications in 5g: Perspective on the design of radio interface and network architecture," *IEEE Communications Magazine*, vol. 55, no. 2, pp. 70–78, 2017.

[57] O. Yilmaz, "Ultra-reliable and low-latency 5g communication," in *Proceedings of the European Conference on Networks and Communications (EuCNC?16)*, 2016.

[58] Y.-M. Huang, M.-Y. Hsieh, H.-C. Chao, S.-H. Hung, and J. H. Park, "Pervasive, secure access to a hierarchical sensor-based healthcare monitoring architecture in wireless heterogeneous networks," *IEEE journal on selected areas in communications*, vol. 27, no. 4, pp. 400–411, 2009.

[59] M. M. Razlighi and N. Zlatanov, "Buffer-aided relaying for the two-hop full-duplex relay channel with self-interference," *IEEE Transactions on Wireless Communications*, vol. 17, no. 1, pp. 477–491, 2018.

[60] M. S. Elbamby, M. Bennis, W. Saad, M. Debbah, and M. Latva-Aho, "Resource optimization and power allocation in in-band full duplex-enabled non-orthogonal multiple access networks," *IEEE Journal on Selected Areas in Communications*, vol. 35, no. 12, pp. 2860–2873, 2017.

[61] M. Sheng, Y. Li, X. Wang, J. Li, and Y. Shi, "Energy efficiency and delay tradeoff in device-to-device communications underlaying cellular networks," *IEEE Journal on Selected Areas in Communications*, vol. 34, no. 1, pp. 92–106, 2016.

[62] Y. Li, M. Sheng, C.-X. Wang, X. Wang, Y. Shi, and J. Li, "Throughput–delay tradeoff in interference-free wireless networks with guaranteed energy efficiency," *IEEE Transactions on Wireless Communications*, vol. 14, no. 3, pp. 1608–1621, 2015.

[63] A. J. Paulraj, D. A. Gore, R. U. Nabar, and H. Bolcskei, "An overview of mimo communications-a key to gigabit wireless," *Proceedings of the IEEE*, vol. 92, no. 2, pp. 198–218, 2004.

[64] E. Viterbo and J. Boutros, "A universal lattice code decoder for fading channels," *IEEE Transactions on Information theory*, vol. 45, no. 5, pp. 1639–1642, 1999.

[65] G. J. Foschini, "Layered space-time architecture for wireless communication in a fading environment when using multi-element antennas," *Bell labs technical journal*, vol. 1, no. 2, pp. 41–59, 1996.

[66] O. Damen, A. Chkeif, and J.-C. Belfiore, "Lattice code decoder for space-time codes," *IEEE Communications letters*, vol. 4, no. 5, pp. 161–163, 2000.

[67] P. W. Wolniansky, G. J. Foschini, G. Golden, and R. A. Valenzuela, "V-blast: An architecture for realizing very high data rates over the rich-scattering wireless channel," in *Signals, Systems, and Electronics, 1998. ISSSE 98. 1998 URSI International Symposium on*, pp. 295–300, IEEE, 1998.

[68] M. Costa, "Writing on dirty paper," *IEEE transactions on information theory*, vol. 29, no. 3, pp. 439–441, 1983.

[69] M. Tomlinson, "New automatic equaliser employing modulo arithmetic," *Electronics letters*, vol. 7, no. 5, pp. 138–139, 1971.

[70] H. Harashima and H. Miyakawa, "Matched-transmission technique for channels with intersymbol interference," *IEEE Transactions on Communications*, vol. 20, no. 4, pp. 774–780, 1972.

[71] B. M. Hochwald, C. B. Peel, and A. L. Swindlehurst, "A vector-perturbation technique for near-capacity multiantenna multiuser communication-part ii: Perturbation," *IEEE Transactions on Communications*, vol. 53, no. 3, pp. 537–544, 2005.

[72] U. Erez, S. Shamai, and R. Zamir, "Capacity and lattice strategies for canceling known interference," *IEEE Transactions on Information Theory*, vol. 51, no. 11, pp. 3820–3833, 2005.

[73] C. Masouros, M. Sellathurai, and T. Ratnarajah, "Interference optimization for transmit power reduction in tomlinson-harashima precoded mimo downlinks," *IEEE Transactions on Signal Processing*, vol. 60, no. 5, pp. 2470–2481, 2012.

[74] A. Garcia-Rodriguez and C. Masouros, "Power-efficient tomlinson-harashima precoding for the downlink of multi-user miso systems," *IEEE Transactions on Communications*, vol. 62, no. 6, pp. 1884–1896, 2014.

[75] C. Windpassinger, R. F. Fischer, T. Vencel, and J. B. Huber, "Precoding in multiantenna and multiuser communications," *IEEE Transactions on Wireless Communications*, vol. 3, no. 4, pp. 1305–1316, 2004.

[76] C. Masouros and E. Alsusa, "Dynamic linear precoding for the exploitation of known interference in mimo broadcast systems," *IEEE Transactions on Wireless Communications*, vol. 8, no. 3, pp. 1396–1404, 2009.

[77] C. Masouros, "Correlation rotation linear precoding for mimo broadcast communications," *IEEE Transactions on Signal Processing*, vol. 59, no. 1, pp. 252–262, 2011.

[78] E. Alsusa and C. Masouros, "Adaptive code allocation for interference management on the downlink of ds-cdma systems," *IEEE transactions on Wireless communications*, vol. 7, no. 7, 2008.

[79] M. Bengtsson and B. Ottersten, "Handbook of antennas in wireless communications," *Optimal and Suboptimal Transmit Beamforming: Boco Raton, FL: CRC*, 2001.

[80] M. Bengtsson and B. Ottersten, "Optimal downlink beamforming using semidefinite optimization," in *37th Annual Allerton Conference on Communication, Control, and Computing*, pp. 987–996, 1999.

[81] M. Alodeh, S. Chatzinotas, and B. Ottersten, "Constructive interference through symbol level precoding for multi-level modulation," in *Global Communications Conference (GLOBECOM), 2015 IEEE*, pp. 1–6, IEEE, 2015.

[82] T. Haustein, C. Von Helmolt, E. Jorswieck, V. Jungnickel, and V. Pohl, "Performance of mimo systems with channel inversion," in *Vehicular Technology*

Conference, 2002. VTC Spring 2002. IEEE 55th, vol. 1, pp. 35–39, IEEE, 2002.

[83] H. El Gamal, G. Caire, and M. O. Damen, "Lattice coding and decoding achieve the optimal diversity-multiplexing tradeoff of mimo channels," *IEEE Transactions on Information Theory*, vol. 50, no. 6, pp. 968–985, 2004.

[84] S. Boyd and L. Vandenberghe, *Convex optimization*. Cambridge university press, 2004.

[85] A. B. Gershman, N. D. Sidiropoulos, S. Shahbazpanahi, M. Bengtsson, and B. Ottersten, "Convex optimization-based beamforming," *IEEE Signal Processing Magazine*, vol. 27, no. 3, pp. 62–75, 2010.

[86] F. Rashid-Farrokhi, K. R. Liu, and L. Tassiulas, "Transmit beamforming and power control for cellular wireless systems," *IEEE Journal on Selected Areas in Communications*, vol. 16, no. 8, pp. 1437–1450, 1998.

[87] E. Visotsky and U. Madhow, "Optimum beamforming using transmit antenna arrays," in *Vehicular Technology Conference, 1999 IEEE 49th*, vol. 1, pp. 851–856, IEEE, 1999.

[88] G. Zheng, K.-K. Wong, and T.-S. Ng, "Robust linear mimo in the downlink: A worst-case optimization with ellipsoidal uncertainty regions," *EURASIP Journal on Advances in Signal Processing*, vol. 2008, p. 154, 2008.

[89] N. Vucic and H. Boche, "Robust qos-constrained optimization of downlink multiuser miso systems," *IEEE Transactions on Signal Processing*, vol. 57, no. 2, pp. 714–725, 2009.

[90] B. K. Chalise, S. Shahbazpanahi, A. Czylwik, and A. B. Gershman, "Robust downlink beamforming based on outage probability specifications," *IEEE Transactions on Wireless Communications*, vol. 6, no. 10, 2007.

[91] A. Pascual-Iserte, D. P. Palomar, A. I. Pérez-Neira, and M. Á. Lagunas, "A robust maximin approach for mimo communications with imperfect channel state information based on convex optimization," *IEEE Transactions on Signal Processing*, vol. 54, no. 1, pp. 346–360, 2006.

[92] M. Schubert and H. Boche, "Solution of the multiuser downlink beamforming problem with individual sinr constraints," *IEEE Transactions on Vehicular Technology*, vol. 53, no. 1, pp. 18–28, 2004.

[93] E. Visotsky and U. Madhow, "Space-time transmit precoding with imperfect feedback," *IEEE transactions on Information Theory*, vol. 47, no. 6, pp. 2632–2639, 2001.

[94] A. Wiesel, Y. C. Eldar, and S. S. Shitz, "Optimization of the mimo compound capacity," *IEEE Transactions on Wireless Communications*, vol. 6, no. 3, 2007.

[95] Q. Shi, M. Razaviyayn, Z.-Q. Luo, and C. He, "An iteratively weighted mmse approach to distributed sum-utility maximization for a mimo interfering broadcast channel," *IEEE Transactions on Signal Processing*, vol. 59, no. 9, pp. 4331–4340, 2011.

[96] K. R. Kumar and F. Xue, "An iterative algorithm for joint signal and interference alignment," in *Information Theory Proceedings (ISIT), 2010 IEEE International Symposium on*, pp. 2293–2297, IEEE, 2010.

[97] T. Elkourdi, O. Simeone, O. Sahin, and S. Shamai, "Signal and interference leakage minimization in mimo uplink-downlink cellular networks," *arXiv preprint arXiv:1408.5204*, 2014.

[98] C. Masouros and G. Zheng, "Power efficient downlink beamforming optimization by exploiting interference," in *Global Communications Conference (GLOBECOM), 2015 IEEE*, pp. 1–6, IEEE, 2015.

[99] M. Alodeh, S. Chatzinotas, and B. Ottersten, "Data aware user selection in cognitive downlink miso precoding systems," in *Signal Processing and Information Technology (ISSPIT), 2013 IEEE International Symposium on*, pp. 000356–000361, IEEE, 2013.

[100] M. Alodeh, S. Chatzinotas, and B. Ottersten, "A multicast approach for constructive interference precoding in miso downlink channel," in *Information Theory (ISIT), 2014 IEEE International Symposium on*, pp. 2534–2538, IEEE, 2014.

[101] M. Alodeh, S. Chatzinotas, and B. Ottersten, "Constructive multiuser interference in symbol level precoding for the miso downlink channel," *IEEE Transactions on Signal processing*, vol. 63, no. 9, pp. 2239–2252, 2015.

[102] M. Alodeh, S. Chatzinotas, and B. Ottersten, "Energy-efficient symbol-level precoding in multiuser miso based on relaxed detection region," *IEEE transactions on Wireless Communications*, vol. 15, no. 5, pp. 3755–3767, 2016.

[103] M. Alodeh, S. Chatzinotas, and B. Ottersten, "Energy efficient symbol-level precoding in multiuser miso channels," in *Signal Processing Advances in Wireless Communications (SPAWC), 2015 IEEE 16th International Workshop on*, pp. 36–40, IEEE, 2015.

[104] K. L. Law and C. Masouros, "Constructive interference exploitation for downlink beamforming based on noise robustness and outage probability," in *Acoustics, Speech and Signal Processing (ICASSP), 2016 IEEE International Conference on*, pp. 3291–3295, IEEE, 2016.

[105] A. Li and C. Masouros, "Exploiting constructive mutual coupling in p2p mimo by analog-digital phase alignment," *IEEE Transactions on Wireless Communications*, vol. 16, no. 3, pp. 1948–1962, 2017.

[106] P. V. Amadori and C. Masouros, "Constant envelope precoding by interference exploitation in phase shift keying-modulated multiuser transmission,"

IEEE Transactions on Wireless Communications, vol. 16, no. 1, pp. 538–550, 2017.

[107] K. L. Law, C. Masouros, and M. Pesavento, "Transmit precoding for interference exploitation in the underlay cognitive radio z-channel," *IEEE Transactions on Signal Processing*, vol. 65, no. 14, pp. 3617–3631, 2017.

[108] V. R. Cadambe and S. A. Jafar, "Interference alignment and spatial degrees of freedom for the k user interference channel," in *2008 IEEE International Conference on Communications*, pp. 971–975, IEEE, 2008.

[109] D. Nguyen, L.-N. Tran, P. Pirinen, and M. Latva-aho, "Precoding for full duplex multiuser mimo systems: Spectral and energy efficiency maximization," *IEEE Transactions on Signal Processing*, vol. 61, no. 16, pp. 4038–4050, 2013.

[110] D. Nguyen, L.-N. Tran, P. Pirinen, and M. Latva-aho, "On the spectral efficiency of full-duplex small cell wireless systems," *IEEE Transactions on wireless communications*, vol. 13, no. 9, pp. 4896–4910, 2014.

[111] L. Song, Y. Li, and Z. Han, "Resource allocation in full-duplex communications for future wireless networks," *IEEE Wireless Communications*, vol. 22, no. 4, pp. 88–96, 2015.

[112] H. Ju and R. Zhang, "Optimal resource allocation in full-duplex wireless-powered communication network," *IEEE Transactions on Communications*, vol. 62, no. 10, pp. 3528–3540, 2014.

[113] D. W. K. Ng, E. S. Lo, and R. Schober, "Dynamic resource allocation in mimo-ofdma systems with full-duplex and hybrid relaying," *IEEE Transactions on Communications*, vol. 60, no. 5, pp. 1291–1304, 2012.

[114] H. Q. Ngo, H. A. Suraweera, M. Matthaiou, and E. G. Larsson, "Multipair full-duplex relaying with massive arrays and linear processing," *IEEE Jour-*

nal on Selected Areas in Communications, vol. 32, no. 9, pp. 1721–1737, 2014.

[115] Y. Sun, D. W. K. Ng, and R. Schober, "Multi-objective optimization for power efficient full-duplex wireless communication systems," in *Global Communications Conference (GLOBECOM), 2015 IEEE*, pp. 1–6, IEEE, 2015.

[116] Y. Sun, D. W. K. Ng, J. Zhu, and R. Schober, "Multi-objective optimization for robust power efficient and secure full-duplex wireless communication systems," *IEEE Transactions on Wireless Communications*, vol. 15, no. 8, pp. 5511–5526, 2016.

[117] S. Leng, D. W. K. Ng, N. Zlatanov, and R. Schober, "Multi-objective resource allocation in full-duplex swipt systems," in *Communications (ICC), 2016 IEEE International Conference on*, pp. 1–7, IEEE, 2016.

[118] R. T. Marler and J. S. Arora, "Survey of multi-objective optimization methods for engineering," *Structural and multidisciplinary optimization*, vol. 26, no. 6, pp. 369–395, 2004.

[119] M. Alodeh, S. Chatzinotas, and B. Ottersten, "Symbol-level multiuser MISO precoding for multi-level adaptive modulation," *IEEE Transactions on Wireless Communications*, vol. 16, no. 8, pp. 5511–5524, 2017.

[120] P. V. Amadori and C. Masouros, "Interference-driven antenna selection for massive multiuser MIMO," *IEEE Transactions on Vehicular Technology*, vol. 65, no. 8, pp. 5944–5958, 2016.

[121] P. V. Amadori and C. Masouros, "Large scale antenna selection and precoding for interference exploitation," *IEEE Transactions on Communications*, vol. 65, no. 10, pp. 4529–4542, 2017.

[122] S. Timotheou, G. Zheng, C. Masouros, and I. Krikidis, "Exploiting constructive interference for simultaneous wireless information and power transfer in

multiuser downlink systems," *IEEE Journal on Selected Areas in Communications*, vol. 34, no. 5, pp. 1772–1784, 2016.

[123] M. R. Khandaker, C. Masouros, and K.-K. Wong, "Constructive interference based secure precoding: A new dimension in physical layer security," *IEEE Transactions on Information Forensics and Security*, 2018.

[124] F. Liu, C. Masouros, A. Li, T. Ratnarajah, and J. Zhou, "Interference exploitation for radar and cellular coexistence-the power-efficient approach," 2017.

[125] A. Li and C. Masouros, "Interference exploitation precoding made practical: Optimal closed-form solutions for psk modulations," *IEEE Transactions on Wireless Communications*, 2018.

[126] A. Li, C. Masouros, F. Liu, and A. L. Swindlehurst, "Massive mimo 1-bit dac transmission: A low-complexity symbol scaling approach," *IEEE Transactions on Wireless Communications*, 2018.

[127] H. Min, J. Lee, S. Park, and D. Hong, "Capacity enhancement using an interference limited area for device-to-device uplink underlaying cellular networks," *IEEE Transactions on Wireless Communications*, vol. 10, no. 12, pp. 3995–4000, 2011.

[128] M. Ni, L. Zheng, F. Tong, J. Pan, and L. Cai, "A geometrical-based throughput bound analysis for device-to-device communications in cellular networks," *IEEE Journal on Selected Areas in Communications*, vol. 33, no. 1, pp. 100–110, 2015.

[129] Y. Feng, X. Shen, R. Zhang, and P. Zhou, "Interference-area-based resource allocation for full-duplex communications," in *Communication Systems (ICCS), 2016 IEEE International Conference on*, pp. 1–5, IEEE, 2016.

[130] H. Zhang, Y. Liao, and L. Song, "D2D-U: Device-to-device communications in unlicensed bands for 5G system," *IEEE Transactions on Wireless Communications*, vol. 16, no. 6, pp. 3507–3519, 2017.

[131] B. Li, H. H. Dam, A. Cantoni, and K. L. Teo, "Some interesting properties for zero-forcing beamforming under per-antenna power constraints in rural areas," *Journal of Global Optimization*, vol. 62, no. 4, pp. 877–886, 2015.

[132] M. Grant, S. Boyd, and Y. Ye, "Cvx: Matlab software for disciplined convex programming," 2008.

[133] W.-K. Ma, J. Pan, A. M.-C. So, and T.-H. Chang, "Unraveling the rank-one solution mystery of robust MISO downlink transmit optimization: A verifiable sufficient condition via a new duality result," *IEEE Transactions on Signal Processing*, vol. 65, no. 7, pp. 1909–1924, 2017.

[134] Z.-Q. Luo, W.-K. Ma, A. M.-C. So, Y. Ye, and S. Zhang, "Semidefinite relaxation of quadratic optimization problems," *IEEE Signal Processing Magazine*, vol. 27, no. 3, pp. 20–34, 2010.

[135] A. Ben-Tal and A. Nemirovski, *Lectures on modern convex optimization: analysis, algorithms, and engineering applications*. SIAM, 2001.

[136] K.-Y. Wang, A. M.-C. So, T.-H. Chang, W.-K. Ma, and C.-Y. Chi, "Outage constrained robust transmit optimization for multiuser miso downlinks: Tractable approximations by conic optimization," *IEEE Transactions on Signal Processing*, vol. 62, no. 21, pp. 5690–5705, 2014.

[137] "Evolved universal terrestrial radio access (e-utra); lte physical layer; general description 3gpp ts 36.201 v11.1.0 release 11,"

[138] A. A. Nasir, X. Zhou, S. Durrani, and R. A. Kennedy, "Relaying protocols for wireless energy harvesting and information processing," *IEEE Trans. Wireless Comms.*, vol. 12, no. 7, pp. 3622–3636, 2013.

[139] Y. Wang, R. Sun, and X. Wang, "Transceiver design to maximize the weighted sum secrecy rate in full-duplex SWIPT systems," *IEEE Sig. Process. Letter*, vol. 23, no. 6, pp. 883–887, 2016.

[140] Z. Hu, C. Yuan, and F. Gao, "Maximizing harvested energy for full-duplex swipt system with power splitting," *IEEE Access*, vol. 5, pp. 24975–24987, 2017.

[141] M.-M. Zhao, Q. Shi, Y. Cai, and M.-J. Zhao, "Joint transceiver design for full-duplex cloud radio access networks with swipt," *IEEE Transactions on Wireless Communications*, vol. 16, no. 9, pp. 5644–5658, 2017.

[142] C. You, K. Huang, H. Chae, and B.-H. Kim, "Energy-efficient resource allocation for mobile-edge computation offloading," *IEEE Transactions on Wireless Communications*, vol. 16, no. 3, pp. 1397–1411, 2017.

[143] L. Yang, J. Cao, H. Cheng, and Y. Ji, "Multi-user computation partitioning for latency sensitive mobile cloud applications," *IEEE Transactions on Computers*, vol. 64, no. 8, pp. 2253–2266, 2015.

[144] F. Wang, J. Xu, X. Wang, and S. Cui, "Joint offloading and computing optimization in wireless powered mobile-edge computing systems," *IEEE Transactions on Wireless Communications*, vol. 17, no. 3, pp. 1784–1797, 2018.

[145] S. Sardellitti, G. Scutari, and S. Barbarossa, "Joint optimization of radio and computational resources for multicell mobile-edge computing," *IEEE Transactions on Signal and Information Processing over Networks*, vol. 1, no. 2, pp. 89–103, 2015.

[146] X. Chen, L. Jiao, W. Li, and X. Fu, "Efficient multi-user computation offloading for mobile-edge cloud computing," *IEEE/ACM Transactions on Networking*, no. 5, pp. 2795–2808, 2016.

[147] T. Q. Dinh, J. Tang, Q. D. La, and T. Q. Quek, "Offloading in mobile edge computing: Task allocation and computational frequency scaling," *IEEE Transactions on Communications*, vol. 65, no. 8, pp. 3571–3584, 2017.

[148] Z. Wen, K. Yang, X. Liu, S. Li, and J. Zou, "Joint offloading and computing design in wireless powered mobile-edge computing systems with full-duplex relaying," *IEEE Access*, vol. 6, pp. 72786–72795, 2018.

[149] S. Mao, S. Leng, K. Yang, X. Huang, and Q. Zhao, "Fair energy-efficient scheduling in wireless powered full-duplex mobile-edge computing systems," in *GLOBECOM 2017-2017 IEEE Global Communications Conference*, pp. 1–6, IEEE, 2017.

[150] Z. Tan, F. R. Yu, X. Li, H. Ji, and V. C. Leung, "Virtual resource allocation for heterogeneous services in full duplex-enabled scns with mobile edge computing and caching," *IEEE Transactions on Vehicular Technology*, vol. 67, no. 2, pp. 1794–1808, 2018.

[151] M. Liu, Y. Mao, S. Leng, and S. Mao, "Full-duplex aided user virtualization for mobile edge computing in 5g networks," *IEEE Access*, vol. 6, pp. 2996–3007, 2018.

[152] M. T. Kabir, M. R. A. Khandaker, and C. Masouros, "Reducing self-interference in full duplex transmission by interference exploitation," *IEEE Global Communications Conference*, pp. 1–6, Dec 2017.

[153] M. T. Kabir, M. R. Khandaker, and C. Masouros, "Robust energy harvesting FD transmission: Interference suppression vs exploitation," *IEEE Communications Letters*, vol. 22, no. 9, pp. 1866–1869, 2018.

[154] M. T. Kabir, M. R. Khandaker, and C. Masouros, "Interference exploitation in full-duplex communications: Trading interference power for both uplink and downlink power savings," *IEEE Transactions on Wireless Communications*, vol. 17, no. 12, pp. 8314–8329, 2018.

[155] H. A. Suraweera, I. Krikidis, G. Zheng, C. Yuen, and P. J. Smith, "Low-complexity end-to-end performance optimization in mimo full-duplex relay systems.," *IEEE Trans. Wireless Communications*, vol. 13, no. 2, pp. 913–927, 2014.

[156] E. Sharma, R. Budhiraja, K. Vasudevan, and L. Hanzo, "Full-duplex massive mimo multi-pair two-way af relaying: Energy efficiency optimization," *IEEE Transactions on Communications*, 2018.

[157] C. Masouros, T. Ratnarajah, M. Sellathurai, C. B. Papadias, and A. K. Shukla, "Known interference in the cellular downlink: A performance limiting factor or a source of green signal power?," *IEEE Communications Magazine*, vol. 51, no. 10, pp. 162–171, 2013.

[158] C. Masouros, M. Sellathurai, and T. Ratnarajah, "Vector perturbation based on symbol scaling for limited feedback miso downlinks," *IEEE Transactions on Signal Processing*, vol. 62, no. 3, pp. 562–571, 2014.

[159] K. L. Law and C. Masouros, "Detection region based beamforming for interference exploitation," *IEEE Transaction on Communications*, in press.

[160] A. Li and C. Masouros, "Interference exploitation precoding made practical: Optimal closed-form solutions for PSK modulations," *IEEE Transaction on Wireless Communications*, in press.

[161] A. Li, C. Masouros, F. Liu, and L. Swindlehurst, "Massive MIMO 1-Bit DAC transmission: A low-complexity symbol scaling approach," *IEEE Transaction on Wireless Communications*, in press.

[162] J. D. Little, "A proof for the queuing formula: L= λ w," *Operations research*, vol. 9, no. 3, pp. 383–387, 1961.

[163] Y. Li, M. Sheng, Y. Shi, X. Ma, and W. Jiao, "Energy efficiency and delay tradeoff for time-varying and interference-free wireless networks," *IEEE*

Transactions on Wireless Communications, vol. 13, no. 11, pp. 5921–5931, 2014.

[164] J. Hajipour, J. M. Niya, and D. W. K. Ng, "Energy-efficient resource allocation in buffer-aided wireless relay networks," *IEEE Transactions on Wireless Communications*, vol. 16, no. 10, pp. 6648–6659, 2017.

[165] H. Ju, B. Liang, J. Li, and X. Yang, "Dynamic joint resource optimization for lte-advanced relay networks," *IEEE Transactions on Wireless Communications*, vol. 12, no. 11, pp. 5668–5678, 2013.

[166] M. I. Ashraf, C.-F. Liu, M. Bennis, and W. Saad, "Towards low-latency and ultra-reliable vehicle-to-vehicle communication," in *Networks and Communications (EuCNC), 2017 European Conference on*, pp. 1–5, IEEE, 2017.

[167] M. J. Neely, "Stochastic network optimization with application to communication and queueing systems," *Synthesis Lectures on Communication Networks*, vol. 3, no. 1, pp. 1–211, 2010.

[168] T. Lipp and S. Boyd, "Variations and extension of the convex–concave procedure," *Optimization and Engineering*, vol. 17, no. 2, pp. 263–287, 2016.

[169] M. A. Abd-Elmagid, T. ElBatt, and K. G. Seddik, "A generalized optimization framework for wireless powered communication networks," *arXiv preprint arXiv:1603.01115*, 2016.